論文 / 著書情報
Article / Book Information

題目(和文)	アゾベンゼン液晶の相構造の光制御
Title(English)	Photochemical Control of Phase Structures of Azobenzene Liquid Crystals
著者(和文)	堤治
Author(English)	Osamu Tsutsumi
出典(和文)	学位:博士（工学）, 学位授与機関:東京工業大学, 報告番号:甲第3839号, 授与年月日:1998年3月26日, 学位の種別:課程博士, 審査員:
Citation(English)	Degree:Doctor of Engineering, Conferring organization: Tokyo Institute of Technology, Report number:甲第3839号, Conferred date:1998/3/26, Degree Type:Course doctor, Examiner:
学位種別(和文)	博士論文
Type(English)	Doctoral Thesis

Photochemical Control of Phase Structures of Azobenzene Liquid Crystals

OSAMU TSUTSUMI

TOKYO INSTITUTE OF TECHNOLOGY

1997

CONTENTS

Abbreviations

AIBN	2,2'-azobis-(isobutyronitrile)
Ch	cholesteric
DCC	dicyclohexylcarbodiimide
ΔH_{NI}	change in enthalpy of N-I phase transition
DMAP	4-dimethylaminopyridine
DMF	*N,N*-dimethylformamide
DMSO	dimethyl sulfoxide
DSC	differential scanning calorimeter
ΔS_{NI}	change in entropy of N-I phase transition
ε	dielectric constant
Φ	quantum yield
G	glass
GPC	gel permeation chromatography
I	isotropic
$k_{c\text{-}t}$	rate constant for the thermal *cis-trans* isomerization
LC	liquid crystal, liquid-crystalline
LCD	liquid crystal display
Mn	number-average molecular weight
Mw	weight-average molecular weight
N	nematic
R	dichroic ratio
S	order parameter
Sm	smectic
TBAF	tetra-*tert*-butylammonium fluoride
TBS	*tert*-butyldimethylsilyl
T_c	liquid-crystalline to isotropic phase transition temperature
TES	triethylsilyl
Tg	glass transition temperature
THF	tetrahydrofuran
T_{red}	reduced temperature

Chapter 1

General Introduction

It is unquestionable that information processing plays an important role in our modern life. Recently, information processing is required to be more rapid and to deal with larger amounts of information. Photon has many parameters: intensity, wavelength, polarization, phase and so on, and this means that photon has much more information than electron.[1-4] Furthermore, photon is a high-speed information carrier; it travels at speed of light, and can be packed close together without interaction, allowing many streams of information to be transmitted together.[3] Hence, photonics, which is information processing systems using photons instead of electrons, has been expected for new information processing technology.[1-3] In fact, many of today's information and messages (telephone calls, facsimiles, e-mails and so on) are converted from electronic signals to pulses of light and communicated through optical fibers.[1-3] The Japanese Government plans to construct a web of optical fibers all over the country until 2005. At present, however, the fiber-optic systems relay the signals to low-speed electronic components at the terminals for switching, sending, and storing the information. To speed up these processes, the signal of light has to be processed without electronic components.

ORGANIC MATERIALS FOR PHOTONICS

The basic concept of photonics is control of light by light as a stimulus; they accept one beam of light as an input and manipulate it according to a stimulus light (Figure 1-1). To control light by another light, the photonic materials need to vary the optical properties on irradiation. Many approaches to manipulate the optical properties of the materials were proposed (Table 1-1).[1-6] These photonic materials are usually based on photochemical and photophysical processes of the substances. The features of the organic materials are:

1) One can design and synthesize the molecules which are expected to show intended function.
2) Structures of molecular assembly can be controlled.
3) Especially in polymer materials, they are workable easily.

These features of the organic materials are advantageous to photonic materials, so that a great many organic materials have been studied to construct photonic devices.

PHOTOCHROMIC MATERIALS

The photochromic compounds change their molecular structures and colors by photochemical reaction. Thus, the photochromic compounds is expected as a candidate for the photonic materials.[2,5-8] Strictly, photochromism is defined as a reversible change of a single chemical species between two states having distinguishably different

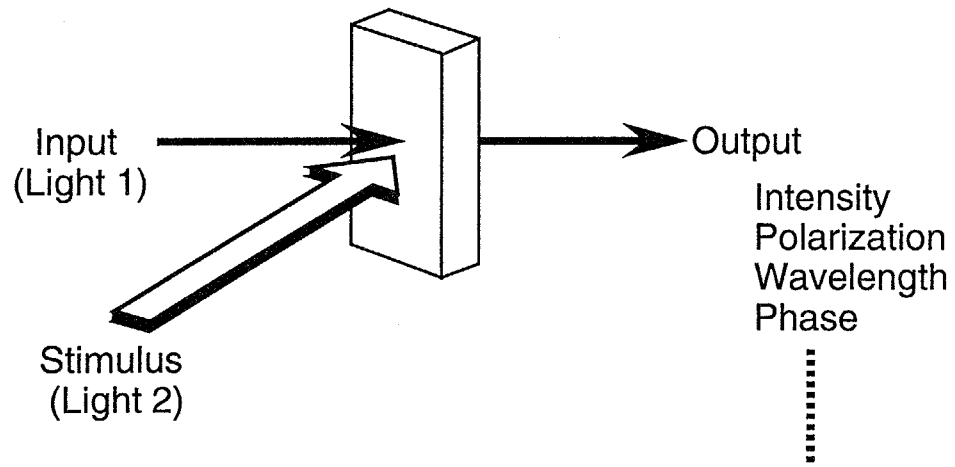

Figure 1-1. Concept of photonic control of light.

Table 1-1. Organic materials for photonics[2,5-8]

process	optical properties	phenomena	materials	properties of light controlled by materials	application
photochemical	absorbance	photochromism	photochromic materials	intensity	optical switch, optical storage
	refractive index, birefringence	photochromism, phase transition	photochromic materials, liquid crystals	phase, polarization	
photophysical	absorbance	nonlinear absorption	NLO materials[a]	intensity	optical limiter
	refractive index, birefringence	photoconductivity	liquid crystals	phase, polarization	SLM[a]
		Pockels effect, optical Kerr effect, photorefractive effect	NLO materials[a]		optical switch
	nonlinear polarization	harmonic generation, optical parametric oscillation	NLO materials[a]	wavelength	wavelength conversion

[a] Abbreviations: NLO, nonlinear optical; SLM, spatial light modulator.

absorption spectra, being induced in at least one direction by the action of a photon.[5] This definition can be represented by the following equation:

$$A\ (\lambda_1) \overset{h\nu}{\rightleftharpoons} B\ (\lambda_2) \qquad (1\text{-}1)$$

In 1956, Hirshberg proposed that the photochromism can be utilized for optical storage.[9] Real images or data can be stored into the photochromic materials with high resolution and erased easily with light or heat. In addition, one can also alter the intensity of light by changing the absorbance of the materials. The photochemical reaction of the photochromic molecules takes place in molecular scale on irradiation, thus one can control the optical properties of the photochromic systems with high spatial resolution. However, a serious problem exists in this type of photonic materials; because there is no threshold of intensity in the photochemical reaction, reading light also induces the photochemical reaction of the photochromic molecules even though the intensity of the reading light is very low, and the data are destroyed through read-out process.[5-8]

The photochemical reaction of the photochromic molecules is accompanied by change in other properties of the system: refractive indices,[10,11] birefringence,[8,12-15] nonlinear optical properties,[16,17] and so on. When one reads out or processes the data with these properties, one can avoid destroying the data.

For instance, the birefringence and dichroism are induced in amorphous polymers containing photochromic azobenzenes with linearly polarized light.[12-15] This arises from the photochemically induced alignment of the azobenzene molecules (Figure 1-2).[8] Azobenzene show *trans*-to-*cis* isomerization by photoirradiation (eq 1-2).

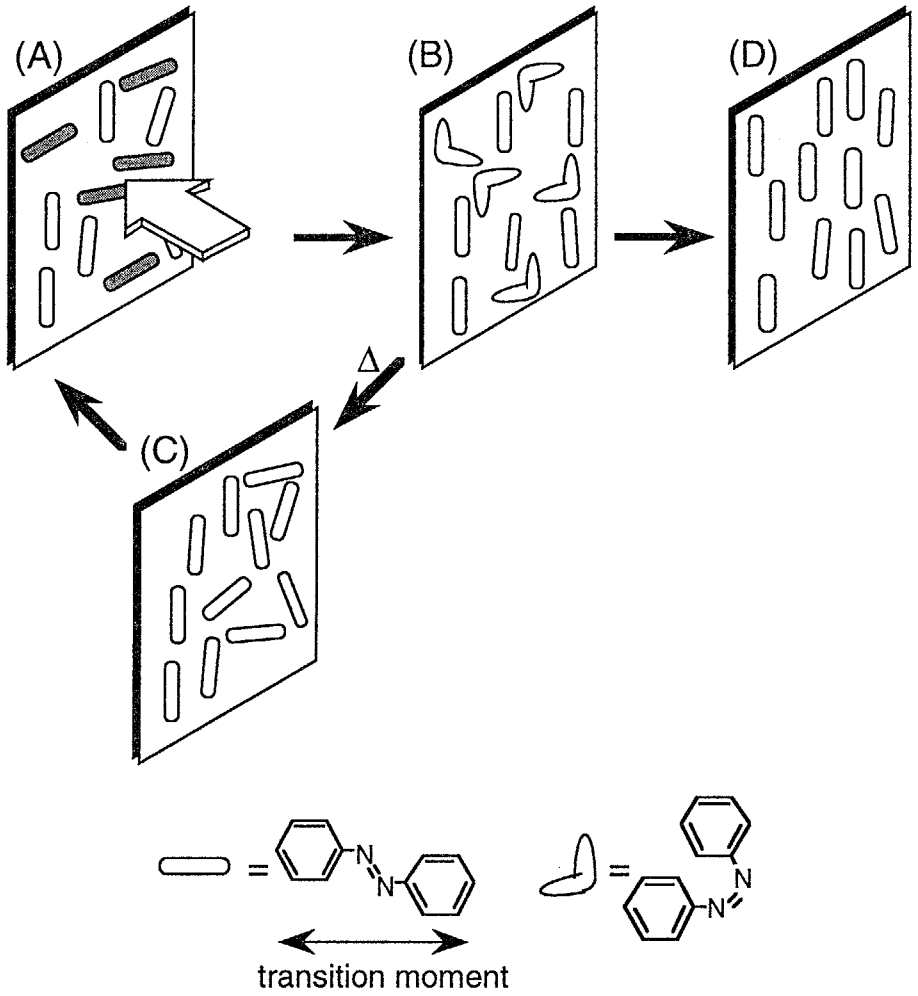

Figure 1-2. Photoinduced alignment of photochromic molecules. With linearly polarized light, azobenzene molecules which are aligned parallel to the polarization direction are excited selectively, (A), and isomerize to *cis*-form, (B). The thermal *cis*-to-*trans* back-isomerization is spontaneous, and the resulting *trans*-azobenzenes may fall in any direction, (C). Azobenzenes with component parallel to the polarization direction of the light continuously repeat this *trans-cis-trans* isomerization cycle. Finally, the materials reach the state with an excess of azobenzenes aligned perpendicular to the polarization direction of the light and show the birefringence, (D).

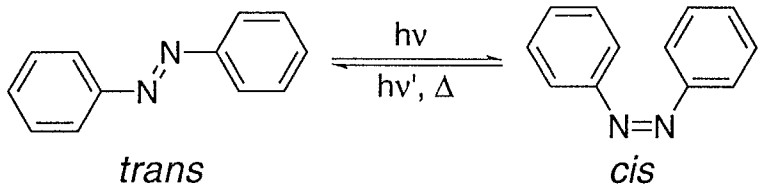

(1-2)

The transition moment of *trans*-azobenzenes is parallel to the molecular long axis. With a polarized light, therefore, the azobenzenes which are aligned parallel to the polarization direction of the light have the highest isomerization probability. On the other hand, the azo group is inert to excitation by polarized light if its alignment is perpendicular to the polarization direction. The thermal *cis*-to-*trans* back-isomerization is spontaneous, and the resulting *trans*-azobenzenes may fall in any direction. Azobenzenes with component parallel to the polarization direction of the light continuously repeat this *trans-cis-trans* isomerization cycle. However, the azobenzenes which are perpendicular to the polarization direction of the light are not excited again and remain in this direction. Finally, the materials reach the state with an excess of azobenzenes aligned perpendicular to the polarization direction of the light and show the birefringence. Namely, the alignment of the azobenzene molecules is induced photochemically with linearly polarized light in the amorphous polymers. Under irradiation with the circular polarized light, however, the orientational order is destroyed because of the random *trans-cis* isomerization. The phenomenon of photoinduced birefringence in amorphous polymers containing photochromic compounds has been investigated in applications such as polarization holography, birefringence diffraction grating, and all-optical switching.[12-15]

Birefringence, refractive indices, and nonlinear optical properties are the *macroscopic nature of molecular assembly* but they are not the microscopic nature of a single molecule. The systems described above,

therefore, can be regarded as the photochemically induced molecular assembly systems, and the macroscopic nature of the systems is varied by photon to control another light. When the structures of assembly of the *self-organizing system* (liquid crystals,[18-25] Langmuir-Blodgett films,[26-28] micelles[29-31] and so on) are changed by photon, the light can be controlled much more effectively because of *cooperative effect* of the molecules.

LIQUID CRYSTAL PHOTONICS

Liquid crystals (LCs) are fluid liquid with optical anisotropy. LCs are supramolecular assembly of rod-shaped molecules. In the LC phase, rod-shaped molecules are assembled with their long axes aligned into a particular direction. For rod-shaped molecules, three types of the LC phases are known: nematic (N), smectic (Sm), and cholesteric (Ch) phase.

LCs are suitable for the photonic materials, because they show a large optical anisotropy and one can control this anisotropy by changing the phase structures of the LCs with external fields applied as a stimulus. LCs, therefore, are well-known materials in electro-optic devices. For example, when an electric field is applied to the LCs placed between a pair of electrodes, the direction of the alignment of the LC molecules are changed, and the intensity of the light transmitted through two crossed polarizers, with the LC cell between them, is altered concomitantly by the change in the molecular alignment. This is a working principle of the liquid crystal display (LCD), thus LCs are now used widely as active media in the LCD devices.

When the phase structures of the LCs are changed with light, the intensity of another light is modulated by irradiation. Namely, the LCs act as optical switch driven by light. An LC Spatial Light Modulator (SLM, usually called an "LC light valve") based on a photoconductive cell is one of such devices, and it is now in a stage of practical use.[32] The LC SLM is driven with electric field in response to stimulus of light.

Linearly polarized light can induce the change in alignment of the LCs with photochromic molecules without electric field.[18-24] In the LC phase, the photoinduced alignment of the photochromic molecules also takes place by irradiation with a linearly polarized light. This phenomenon is based on the same principle as that in the amorphous polymers described above. In LC phase, the isomerization of azobenzenes affects the alignment of the mesogens; the photoinduced alignment of the azobenzenes causes the reorientation of the mesogens. Consequently, the direction of the LC alignment can be manipulated with the linearly polarized light. With the photochemically controlled LC alignment, one can control the refractive index and birefringence of the materials. Thus, this phenomenon has attracted great interest also from practical view point.[18-24] Wendorff et al. demonstrated that the LCs with photochromic compounds are potential for holographic recording materials.[18]

Since LCs are self-organizing materials, the birefringence and refractive index of LCs controlled by light is lager than that of amorphous polymers: they are ~ 10^{-1} in the LCs, while they are 10^{-3} ~ 10^{-2} in the amorphous polymers.[8] This means that one can process and store the data with high sensitivity, high contrast, and high signal-to-noise ratio. Thus, the self-organizing material is advantageous for photonic materials.

PHOTOCHEMICAL PHASE TRANSITION OF LIQUID CRYSTALS

The other approach to manipulate the phase structure of LCs is based on the phenomenon known as *Photochemical Phase Transition.*[33-42] When a small amount of photochromic compounds is dispersed into LCs and irradiated to cause the photochemical reaction of the photochromic guest molecules at temperature just below their LC-to-isotropic (I) phase transition temperature (T_C), the LC-I phase transition is induced photochemically on the time scale of 50 ~ 200 ms.[41,42] This process is reversible: when the back-reaction of the photochromic molecules is induced either photochemically or thermally, the initial LC phase is restored.

The working principle of the photochemical phase transition can be explained in terms of change in the molecular shape of the photochromic guest molecules. For instance, *trans* form of the azobenzene derivatives stabilizes the LC phase, since their molecular shape (rod-like shape) is similar to that of the host LC molecules. On the other hand, the *cis* isomer destabilizes the LC phase because their molecular shape is bent. Consequently, *trans-cis* photoisomerization of the guest azobenzene derivatives lowers the T_C from Tc (*trans*) to Tc (*cis*) (Figure 1-3 (A)). If the system is held at temperature between Tc (*trans*) and Tc (*cis*) and irradiated, T_C is lowered with the accumulation of the *cis* isomer. When T_C falls below the irradiation temperature, the orientational relaxation of the mesogens from the LC state to the I state takes place and the LC-I phase transition is induced isothermally (Figure 1-4 (A)).

In the photochemical phase transition system described above, the photochromic guest molecules act as a *molecular switch* driven by photon. One can consider that the principle of this phenomenon is *change in*

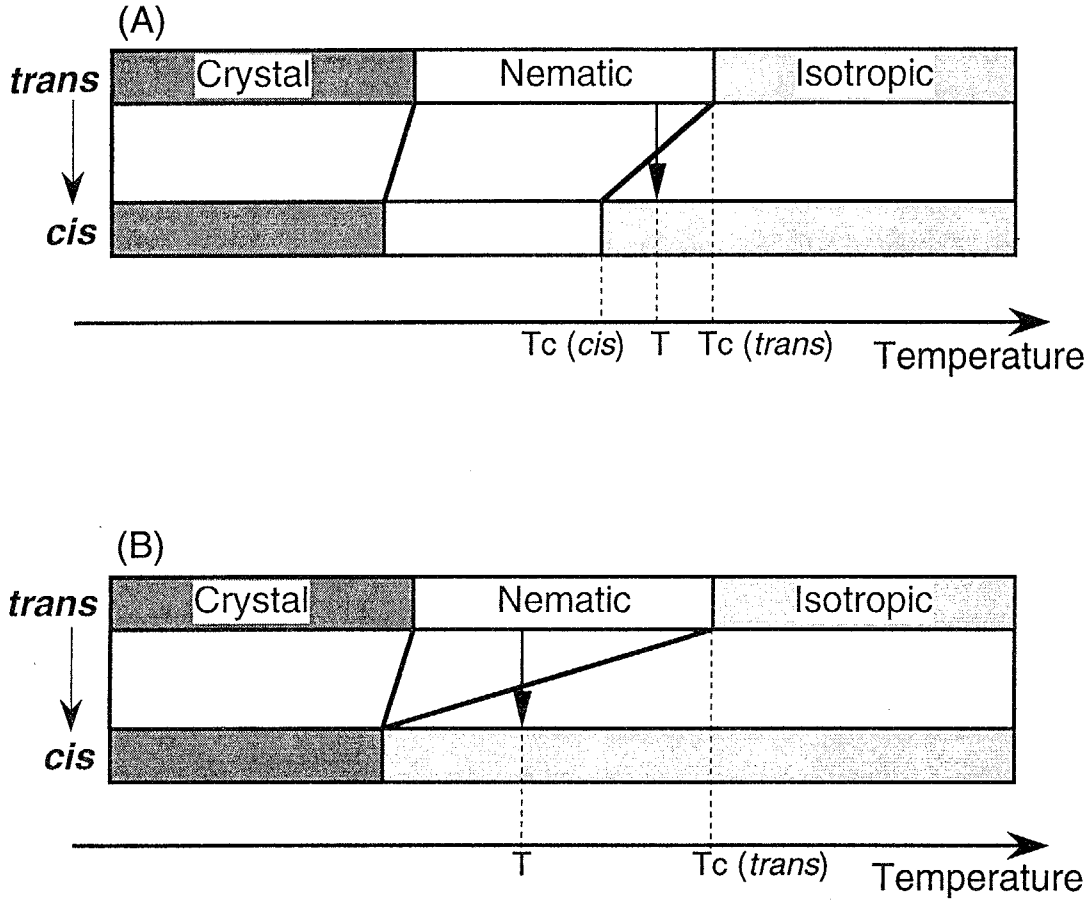

Figure 1-3. Phase diagram before and after isomerization of photochromic molecules: (A), guest/host system; (B), photochromic liquid-crystalline system.

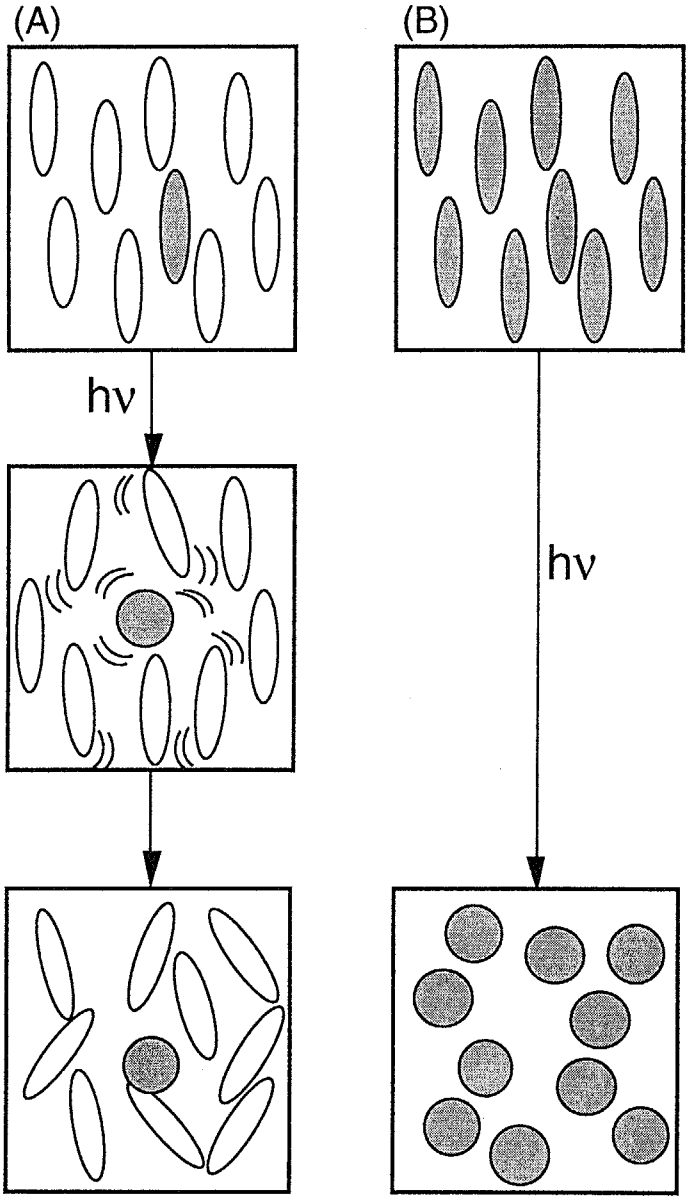

Figure 1-4. Photochemical phase transition of LCs: (A), guest/host system; (B), photochromic liquid-crystalline system.

structures of the whole assembly induced by a small amount of the molecular switch incorporated into the system. When such a molecular switch is attached directly to each mesogen (*photochromic mesogen*), structures of molecular assembly may be controlled more effectively. In the guest/host system, the propagation of the perturbation in the form of the isomerization of a small amount of the molecular switch (photochromic molecule) is required in order to change the structures of the whole assembly (Figure 1-4 (A)). Furthermore, the photochemical phase transition in the guest/host system takes place only at temperature between Tc (*trans*) and Tc (*cis*), because the LC nature still remains even after the photoisomerization below Tc (*cis*). In *photochromic LCs*, however, the propagation of the perturbation may not be needed and LC nature may vanish completely in the whole temperature range of the LC phase, because each mesogen is switched directly by photon (Figure 1-3 (B) and 1-4 (B)).

Some azobenzene derivatives show an N phase in the *trans* form, but the *cis* isomers show no LC phase at any temperature. In this system, the azobenzene moiety plays both roles as a mesogen and a photosensitive moiety. In other words, azobenzene LCs are photochromic LCs, and the mesogenic molecules (*trans* form) are converted into the non-mesogenic molecules (*cis* form) with light. The LC nature of the system may disappear suddenly in whole temperature range of the LC phase on irradiation with a short laser pulse, and one can expect that the photochemical phase transition of the azobenzene LCs is induced principally on the same time scale as the photoisomerization of the azobenzene moiety.

SCOPE OF THE PRESENT THESIS

In the present thesis, various types of low-molecular-weight and polymer azobenzene LCs were prepared as photochromic LCs, and their photochemical phase transition behavior was explored intensively.

In Chapter 2, low-molecular-weight and polymer azobenzene LCs with alkyl or alkoxyl chains at both ends were prepared, and the photochemical phase transition behavior of these LCs was explored under steady light or laser pulse irradiation, in which emphasis was placed on the comparison between the low-molecular-weight and polymer LCs. Furthermore, the author studied photochemical phase transition behavior of the polymer LC below glass transition temperature (Tg) and the mechanism of the thermal recovery of the LC phase.

In Chapter 3, the effect of the position of core units of the mesogens in side chains on the photochemical phase transition behavior of the polymer azobenzene LCs was investigated. The photochemical phase transition behavior was discussed in terms of the mobility of the mesogen and stability of the LC phase.

The thermal recovery of the LC phase took place much slower than the photochemical phase transition. In Chapter 4, in order to accelerate the thermal recovery of the LC phase, azobenzenes with various donor-acceptor pairs were prepared, and the phase transition behavior was studied in the guest/host system. The correlation between the phase transition behavior and the strength of the donor-acceptor pairs was examined.

In Chapter 5, the photochemical phase transition behavior of the polymer LCs with donor-acceptor azobenzenes was studied. Two types of the azobenzene (two- and three-ring type azobenzenes) with strong donor-acceptor pairs were used and introduced into the polymer LCs by

copolymerization. The effects of mole fraction and structure of the azobenzenes on the photochemical and thermal phase transition behavior were discussed.

According to knowledge obtained in Chapters 4 and 5, the donor-acceptor azobenzene LCs were designed and their photochemical phase transition behavior was investigated in Chapter 6. In addition, the author explored the effect of structure of main chain of the polymer on the phase transition behavior of the azobenzene LCs.

In Chapter 7, the effect of the heat generated by photoirradiation on the photochemical phase transition of LCs was discussed. Azobenzene with hydroxyl group, which isomerizes to *cis* form with a very low quantum yield, was prepared, and the phase transition behavior was examined to evaluate the influence of heat on the phenomena.

In Chapter 8, the author summarized the results obtained in this study.

References and Notes

(1) Feitelson, D.G. In *Optical Computing*; The MIT Press: Cambridge, USA, 1988.

(2) Sasabe, H. In *Yuki Fotonikusu*, Agune-Shohusya: Tokyo, Japan, 1995.

(3) Service, R.F. *Science* **1997**, *276*, 1195.

(4) Marder, S.R.; Kippelen, B.; Jen, A.K.-Y.; Peyghambarian, N. *Nature* **1997**, *388*, 845.

(5) Brown, G.H. In *Photochromism*, John Wiley & Sons: New York, USA, 1971.

(6) Irie, M. et al. In *Kikan Kagaku Sousetsu: Yuki Fotokuromizumu no Kagaku (Chemistry of Organic Photochromism)*, Gakkai Shuppan Senta: Tokyo, Japan, 1996.

(7) Kumar, G.; Neckers, D. *Chem. Rev.* **1989**, *89*, 1915.

(8) Xie, S.; Natansohn, A.; Rochon, P. *Chem. Mater.* **1993**, *5*, 403.

(9) Hirshberg, Y. *J. Am. Chem. Soc.* **1956**, *78*, 2304.

(10) Tanio, N.; Irie, M. *Jpn. J. Appl. Phys.* **1993**, *33*, 1550.

(11) (a) Sekkat, Z.; Büchel, H.; Orendi, H.; Menzel, H.; Knoll, W. *Chem. Phys. Lett.* **1994**, *220*, 497. (b) Sekkat, Z.; Kang, C.-S.; Aust, E.F.; Wegner, G.; Knoll, W. *Chem. Mater.* **1995**, *7*, 142.

(12) (a) Todorov, T.; Tomova, N.; Nikolova, L. *Opt. Commun.* **1983**, *47*, 123. (b) Todorov, T.; Nikolova, L.; Tomova, N. *Appl. Opt.* **1984**, *23*, 4309.

(13) Läsker, L.; Fischer, T.; Stumpe, J.; Kostromin, S.; Ivanov, S.; Shibaev, V.; Ruhmann, R. *Mol. Cryst. Liq. Cryst.* **1994**, *246*, 347.

(14) Couture, J.A.; Lessard, R.A. *Appl. Opt.* **1988**, *27*, 3368.

(15) (a) Rochon, P.; Gosselin, J.; Natansohn, A.; Xie, S. *Appl. Phys. Lett.* **1992**, *60*, 4. (b) Natansohn, A.; Rochon, P.; Gosselin, J.; Xie,

S. *Macromolecules* **1992**, *25*, 2268. (c) Natansohn, A.; Xie, S.; Rochon, P. *Macromolecules* **1992**, *25*, 5531. (d) Rochon, P.; Bissonnetto, D.; Natansohn, A.; Xie, S. *Appl. Opt.* **1993**, *32*, 7277. (e) Brown, D.; Natansohn, A.; Rochon, P. *Macromolecules* **1995**, *28*, 6116. (f) Natansohn, A.; Rochon, P.; Ho, M.S.; Barrett, C. *Macromolecules* **1995**, *28*, 4179. (g) Ho, M.S.; Natansohn, A.; Rochon, P. Macromolecules **1995**, *28*, 6124.

(16) Gilat, S.L.; Kawai, S.H.; Lehn, J.-M. *J. Chem. Soc. Chem. Commun.* **1993**, 1439.

(17) Sekkat, Z.; Knoesen, A.; Lee, V.Y.; Miller, R.D. *J. Phys. Chem. B* **1997**, *101*, 4733-4739.

(18) (a) Eich, M.; Wendorff, J.; Ringsdorf, H.; Reck, B. Makromol. Chem., Rapid Commun. **1987**, *8*, 59. (b) Eich, M.; Wendorff, J.; *Makromol. Chem., Rapid Commun.* **1987**, *8*, 467. (c) Eich, M.; Wendorff, J. *J. Opt. Soc. Am. B* **1990**, *7*, 1428. (d) Anderle, K.; Wendorff, J. *ACS Symposium Series* **1994**, *579*, 357.

(19) (a) Wiesner, U.; Antonietti, M.; Boeffel, C.; Spiess, H.W. *Makromol. Chem.* **1990**, *191*, 189. (b) Wiesner, U.; Schmidt-Rohr, K.; Boeffel, C.; Pawelzik, U.; Spiess, H.W. *Adv. Mater.* **1990**, *2*, 484. (c) Wiesner, U.; Reynolds, N.; Boeffel, C.; Spiess, H.W. *Makromol. Chem., Rapid Commun.* **1991**, *12*, 457.

(20) (a) Ivanov, S.; Yakovlev, I.; Kostromin, S.; Shibaev, V.; Läsker, L.; Stumpe, J.; Kreysig, D. *Makromol. Chem., Rapid Commun.* **1991**, *12*, 709. (b) Menzel, H.; Hallensleben, M.L.; Schmidt, A.; Knoll, W.; Fischer, T.; Stumpe, J. *Macromolecules* **1993**, *26*, 3644. (c) Menzel, H.; Weichart, B.; Schmidt, A.; Paul, S.; Knoll, W.; Stumpe, J.; Fischer, T. *Langmuir* **1994**, *10*, 1926. (d) Fischer, T.; Läsker, L.; Stumpe, J.; Kostromin, S. *J. Photochem. Photobiol. A: Chem.*

1994, *80*, 453. (e) Stumpe, J. Fischer, T. Menzel, H. *Macromolecules* **1996**, *29*, 2831.

(21) (a) Petri, A.; Kummer, S.; Anneser, H.; Feiner, F.; Bräuchle, C. *Ber. Bunsenges. Phys. Chem.* **1993**, *97*, 1281. (b) Petri, A.; Kummer, S.; Bräuchle, C. *Liq. Cryst.* **1995**, *19*, 277.

(22) (a) Gibbons, W.M.; Shannon, P.J.; Sun, S.T.; Swetlin, B.J. *Nature* **1991**, *351*, 49. (b) Shannon, P.J.; Gibons, W.M.; Sun, S.T. *Nature* **1994**, *368*, 532. (c) Gibbons, W.M.; Kosa, T.; Palffy-Muhoray, P.; Shannon, P.J.; Sun, S.T. *Nature* **1995**, *377*, 43.

(23) Schadt, M.; Seiberle, H.; Schuster, A.; Kelly, S.M. *Jpn. J. Appl. Phys.* **1995**, *34*, 3240.

(24) (a) Ichimura, K. *ACS Symposium Series* **1994**, *579*, 365. (b) Akiyama, H.; Kudo, K.; Ichimura, K.; Yokoyama, S.; Kakimot, M.; Imai, Y. Langmuir 1995, 11, 1033. (c) Ichimura, K. *Supramol. Sci.* **1996**, *3*, 67-82.

(25) (a) Ikeda, T.; Sasaki, T.; Ichimura, K. *Nature* **1993**, *361*, 428. (b) Sasaki, T.; Ikeda, T.; Ichimura, K. *J. Am. Chem. Soc.* **1994**, *116*, 625. (c) Sasaki, T.; Ikeda, T. *J. Phys. Chem.* **1995**, *99*, 13002. (d) *ibid.*, 13008. (e) *ibid.*, 13013.

(26) (a) Minami, T.; Tamai, N.; Yamazaki, T.; Yamazaki, I. *J. Phys. Chem.* **1991**, *95*, 3988. (b) Yamazaki, I.; Okazaki, S.; Minami, T.; Ohta, N. *Appl. Opt.* **1994**, *33*, 7561.

(27) (a) Maack, J.; Ajuja, R.C.; Tachibana, H. *J. Phys. Chem.* **1995**, *99*, 9210. (b) Ajuja, R.C.; Maack, J.; Tachibana, H. *J. Phys. Chem.* **1995**, *99*, 9221.

(28) Seki, T.; Sakuragi, M.; Kawanishi, Y.; Suzuki, Y.; Tamaki, T.; Fukuda, R.; Ichimura, K. *Langmuir* **1993**, *9*, 211.

(29) Sunamoto, J.; Iwamoto, K.; Akutagawa, M.; Nagase, M.; Kondo, H. *J. Am. Chem. Soc.* **1982**, *104*, 4904.

(30) Tazuke, S.; Kurihara, S.; Yamaguchi, H.; Ikeda, T. *J. Phys. Chem.* **1987**, *91*, 249.

(31) Tomioka, H.; Murata, S.; Inagaki, G. *J. Photopolym. Sci. Technol.* **1989**, *2*, 143.

(32) (a) Bleha, W.P.; Lipton, L.T.; Wiener-Avnear, E.; Grinberg, J.; Relf, P.G.; Casasent, D.; Brown, H.B.; Markevitch, B.V. *Opt. Eng.* **1978**, *17*, 371. (b) Efron, U.; Braatz, P.O.; Little, M.J.; Schwartz, R.N.; Grinberg, J. *Opt. Eng.* **1983**, *22*, 682. (c) Hacker, H.; Kwon, Y.; Lontz, R.; Lefkowitz, I. *Appl. Opt.* **1980**, *19*, 1278.

(33) Sackmann, E. *J. Am. Chem. Soc.* **1971**, *93*, 7088.

(34) Hass, W.E.; Nelson, K.F.; Adams, J.E.; Dir, G.A. *J. Electrochem. Soc.* **1974**, *121*, 1667.

(35) Ogura, K.; Hirabayashi, H.; Uejima, A.; Nakamura, K. *Jpn. J. Appl. Phys.* **1982**, *21*, 969.

(36) (a) Tazuke, S.; Kurihara, S.; Ikeda, T. *Chem. Lett.* **1987**, 911. (b) Ikeda, T.; Horiuchi, S.; Karanjit, D.B.; Kurihara, S.; Tazuke, S. *Chem. Lett.* **1988**, 1679.

(37) Kurihara, S.; Ikeda, T.; Sasaki, S.; Kim, H.B.; Tazuke, S. *J. Chem. Soc. Chem. Commun.* **1990**, 1751.

(38) (a) Ikeda, T.; Horiuchi, S.; Karanjit, D.B.; Kurihara, S.; Tazuke, S. *Macromolecules* **1990**, *23*, 36. (b) *ibid.*, 42. (c) Ikeda, T.; Kurihara, S.; Karanjit, D.B.; Tazuke, S. *Macromolecules* **1990**, *23*, 3938.

(39) (a) Ikeda, T.; Miyamoto, T.; Sasaki, T.; Kurihara, S.; Tazuke, S. *Mol. Cryst. Liq. Cryst.* **1990**, *182B*, 357. (b) Ikeda, T.; Miyamoto, T.; Kurihara, S.; Tsukada, M.; Tazuke, S. *Mol. Cryst. Liq. Cryst.* **1990**, *182B*, 373. (c) Ikeda, T.; Miyamoto, T.; Kurihara, S.; Tazuke, S. *Mol. Cryst. Liq. Cryst.* **1990**, *188*, 207. (d) Ikeda, T. Miyamoto, T. Kurihara, S. Tazuke, S. *Mol. Cryst. Liq. Cryst.*

1990, *188*, 223. (e) Ikeda, T.; Miyamoto, T.; Sasaki, T.; Kurihara, S.; Tazuke, S. *Mol. Cryst. Liq. Cryst.* **1990**, *188*, 235.

(40) Kurihara, S.; Ikeda, T.; Tazuke, S.; Seto, J. *J. Chem. Soc. Faraday Trans.* **1991**, *87*, 3251.

(41) Ikeda, T.; Sasaki, T.; Kim, H.B. *J. Phys. Chem.* **1991**, *95*, 509.

(42) Sasaki, T.; Ikeda, T.; Ichimura, K. *Macromolecules* **1992**, *25*, 3807.

Chapter 2

Photochemical Phase Transition Behavior of Azobenzene Liquid Crystals

INTRODUCTION

As described in General Introduction (Chapter 1), it was demonstrated that introduction of photochromic molecules (azobenzene, spiropyran, and so on) is a powerful method to control the phase structure of the LC phase. At temperature just below Tc, the isothermal phase transition of LCs is brought about reversibly by a photochemical reaction of the photochromic guest molecules. The photochemical N-to-I phase transition takes place on a timescale of 50 ~ 200 ms for the N hosts of low-molecular-weight and polymer LCs.[1,2]

Photoisomerization of the photochromic molecules is a fast process. When the photochromic moiety is introduced into each mesogen, one can transform the mesogenic molecules to non-mesogenic molecules by photochemical reaction of the photochromic moiety, expecting that disappearance of the LC phase may be induced in principle on the same timescale as the *trans-cis* photoisomerization with the laser pulse.

In this chapter, the author investigated the photochemical phase transition behavior of photochromic LCs. The *trans* form of some

azobenzene derivatives shows the N phase while the *cis* form shows no LC phase at any temperature, and the *trans*-azobenzene can be isomerized to the *cis* form instantaneously with the aid of a short laser pulse. Thus, low-molecular-weight and polymer NLCs composed of photosensitive azobenzenes which also act as mesogens in the *trans* form were used as the photochromic LCs.

EXPERIMENTAL

1. Materials.

Structures of the LCs used in this chapter are shown in Figure 2-1. 4-Butyl-4'-methoxyazobenzene (**BMAB**) and 4,4'-dioctyloxyazobenzene (**8AB8**) were synthesized and purified as reported previously.[3,4] Poly[6-[4-(4'-ethoxyphenylazo)phenoxy]hexyl acrylate] (**PA6AB2**) was prepared by the method reported by Angeloni et al (Scheme 2-1).[4]

General Method of Preparation. Unless otherwise noted, materials and solvents were purchased from commercial suppliers and were used without further purification. ^{1}H-NMR and ^{13}C-NMR spectra were recorded in $CDCl_3$ on a Brucker AC-200 NMR spectrometer at 200.4 MHz (^{1}H) or 50.3 MHz (^{13}C), respectively. IR spectra were determined on a Hitachi 260-10 IR spectrometer.

4-Ethoxy-4'-hydroxyazobenzene (2-1). *p*-Ethoxyaniline (10 g, 73 mmol) was dissolved in 300 mL of hydrochloric acid (2 M) and the resulting solution was cooled at 0 °C. With stirring, 5.0 g (73 mmol) of sodium nitrite in water (150 mL) was added dropwise into the solution to

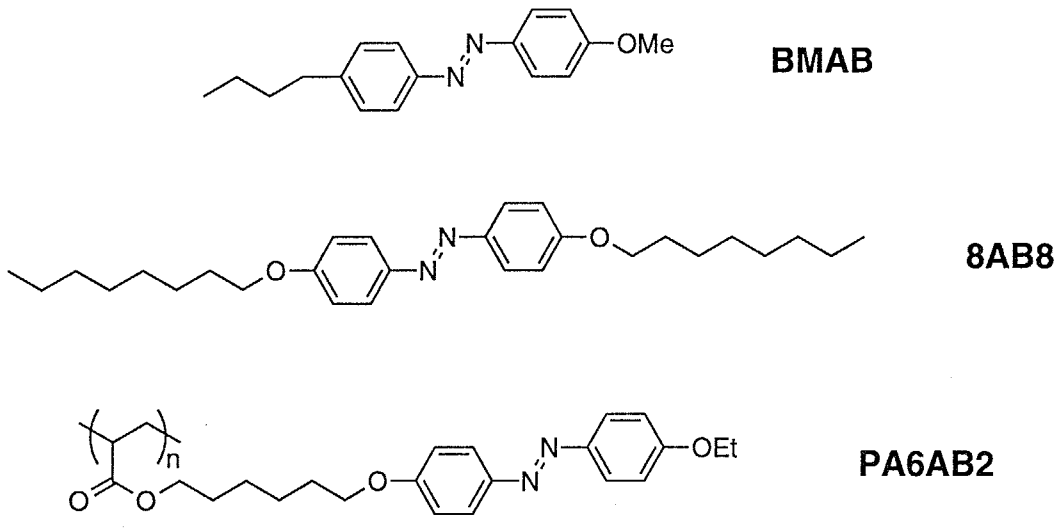

Figure 2-1. Structures of LCs used in this chapter and their abbreviations.

Schem 2-1. Synthetic route for **PA6AB2**

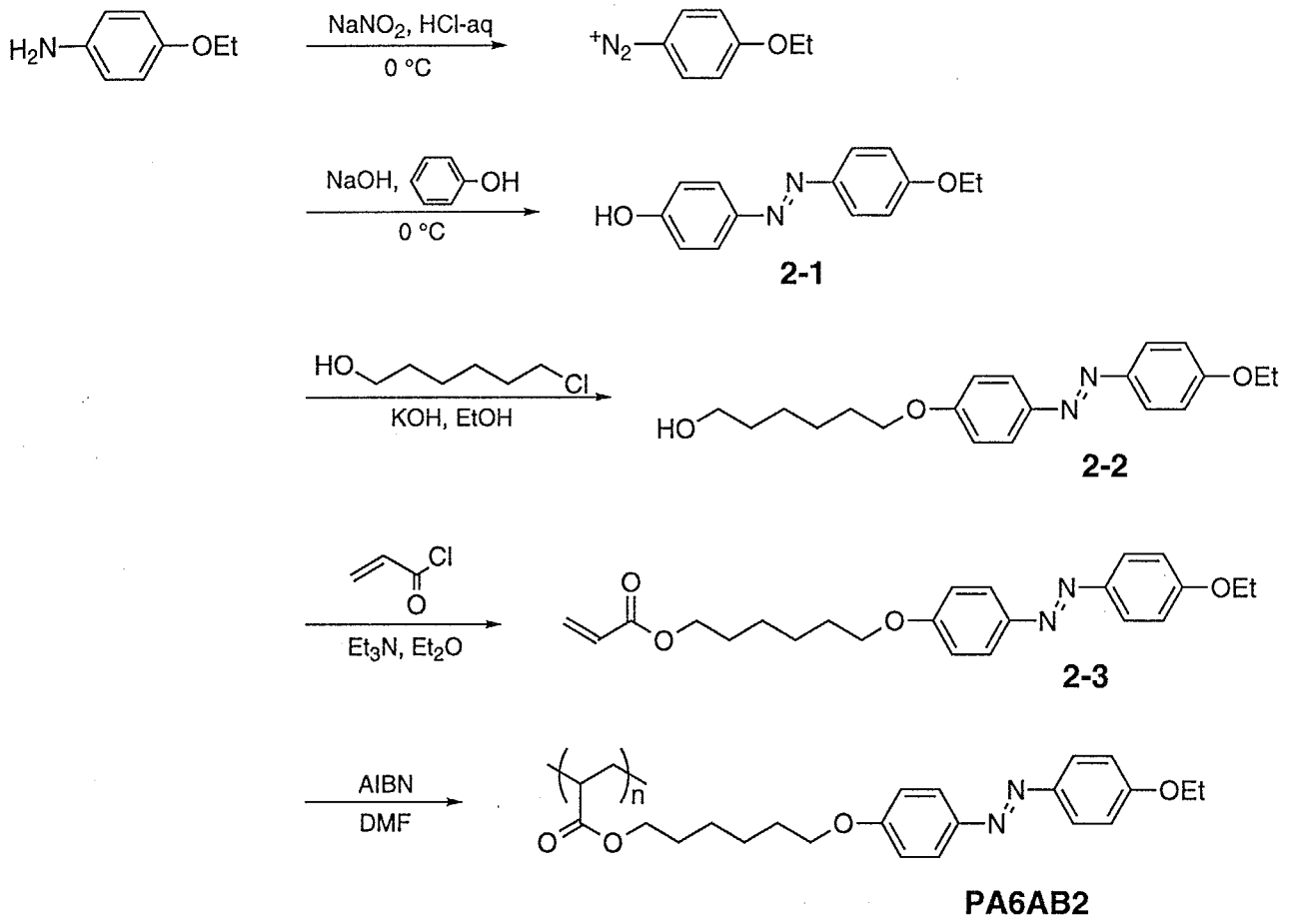

produce diazonium salt. A mixture of phenol (6.9 g, 73 mmol) and sodium hydroxide (8.8 g, 220 mmol) in water (200 mL) was added slowly at 0 °C, and then yellow solid precipitated. The reaction mixture was stirred at room temperature for 2 h. After the reaction mixture was neutralized with acetic acid, the precipitated solid was collected and washed with water. The crude product was purified by recrystallization from a mixture of *n*-hexane and benzene (7/2) to give **2-1** (7.5 g, 31 mmol) in 43 % yield. mp: 127-129 °C. ^{1}H-NMR ($CDCl_3$): δ 1.5 (t, J = 7 Hz; 3H; *CH*$_3$), 4.1 (q, J = 7 Hz; 2H; *OCH*$_2$), 5.8 (s; 1H; *OH*), 6.9 (m; 4H; *CH* in aromatic), 7.8 (m, 4H, *CH* in aromatic). IR (KBr, cm^{-1}): 3530, 1600, 1590, 1260, 850, 810.

4-Ethoxy-4'-(6-hydroxyhexyloxy)azobenzene (**2-2**). A mixture of **2-1** (4.0 g, 16 mmol) and 6-chlorohexanol (3.3 g, 24 mmol) was dissolved in 50 mL of ethanol, and potassium hydroxide (1.4 g, 24 mmol) in water was added to the solution. The resulting solution was refluxed for 12 h. After evaporation, the solid obtained was dissolved in dichloromethane (200 mL) and washed with water. After the solvent was removed, the crude product was recrystallized from *n*-hexane, and **2-2** (3.1 g, 9.0 mmol) was obtained in 51 % yield. mp: 108-109 °C. ^{1}H-NMR ($CDCl_3$): δ 1.3-1.9 (m; 11H; *CH*$_2$, *CH*$_3$), 3.7 (t, J = 7 Hz; 2H; *CH*$_2$OH), 4.2 (m; 4H; *OCH*$_2$), 5.6 (s; 1H; *OH*), 6.9-7.1 (m; 4H; *CH* in aromatic), 7.8-8.0 (m; 4H; *CH* in aromatic). IR (KBr, cm^{-1}): 3290, 1600, 1580, 1230, 840, 800. Anal. Calcd for $C_{20}H_{26}N_2O_3$: C, 70.15; H, 7.65; N, 8.18. Found: C, 69.84; H, 7.66; N, 8.18.

6-[4-(4'-Ethoxyphenylazo)phenoxy]hexyl acrylate (**2-3**). **2-2** (3.0 g, 8.8 mmol), triethylamine (1.8 g, 18 mmol), and trace amount of hydroquinone were dissolved in distilled benzene (50 mL), and the resulting solution was cooled at 0 °C. With stirring under a nitrogen

atmosphere, 1.6 g (18 mmol) of acryloyl chloride was added dropwise to the solution, and the reaction mixture was stirred at room temperature for 12 h. The reaction mixture was poured into water, and the product was extracted with ether. The ether layer was dried with sodium sulfate. After the solvent was removed, yellow solid obtained was recrystallized from ethanol, and **2-3** (1.1 g, 2.8 mmol) was obtained in 32 % yield. mp: 93-95 °C. ^{1}H-NMR ($CDCl_3$): δ 1.5-1.9 (m; 11H; *CH_2*, *CH_3*), 3.9-4.2 (m; 6H; *OCH_2*), 5.8 (dd, *J* = 10, 2 Hz; 1H; *cis-CH_2*=CH), 6.1 (dd, *J* = 18, 10 Hz; 1H; CH_2=*CH*), 6.4 (dd, *J* = 18, 2 Hz; 1H; *trans-CH_2*=CH), 7.0 (m; 4H; *CH* in aromatic), 7.8 (m; 4H; *CH* in aromatic). ^{13}C-NMR ($CDCl_3$, δ): 14.8, 25.8, 28.6, 29.1, 63.8, 64.5, 68.1, 114.7, 124.3, 128.6, 130.5, 147.1, 161.0, 161.1, 166.3. IR (KBr, cm^{-1}): 2940, 1710, 1630, 1600, 1500, 1470, 1250, 1200, 1000. Anal. Calcd for $C_{23}H_{28}N_2O_4$: C, 69.67; H, 7.12; N, 7.07. Found: C, 69.66; H, 7.14; N, 7.00.

Poly[6-[4-(4'-ethoxyphenylazo)phenoxy]hexyl acrylate] (PA6AB2). A solution of **2-3** (1.0 g, 2.5 mmol) and 2,2'-azobis-(isobutyronitrile) (AIBN; 5.0 mg, 20 μmol) in distilled dimethylformamide (DMF, 10 mL) was degassed by several freeze-pump-thaw cycles, and stirred in a sealed tube at 60 °C for 48 h. The resulting solution was cooled to room temperature and poured into 300 mL of methanol with vigorously stirring to precipitate the polymer. The polymer obtained was purified by repeated reprecipitation from chloroform into a large excess of ethyl acetate and dried under vacuum for 48 h to yield 0.32 g of **PA6AB2** in 32 % conversion.

2. Characterization of LCs.

Molecular weight of the polymer was determined by gel permeation chromatography (GPC; Toyo Soda HLC-802; column, GMH6 X 2 + G4000H8 + G500H8; eluent, chloroform) calibrated with standard polystyrenes. Liquid-crystalline behavior and phase transition behavior were examined on an Olympus Model BH-2 polarizing microscope equipped with Mettler hot-stage models FP-90 and FP-82. Thermotropic properties of LCs were determined with a differential scanning calorimeter (Seiko I&E SSC-5200 and DSC220C) at a heating rate of 10 °C/min. At least three scans were performed for each sample to check reproducibility. The thermodynamic properties of the LCs and molecular weight of the polymer are given in Table 2-1.

Table 2-1. Thermodynamic Properties of LCs and Molecular Weight of Polymer Used in This Chapter[a]

	Mn	M_W/Mn	phase transition temperature, °C	ΔH_{NI}, kJ/mol	ΔS_{NI}, J/mol·K
BMAB	-	-	K 35 N 48 I	0.35	1.1
8AB8	-	-	K 99 N 113 I	1.6	4.2
PA6AB2	9,100	1.3	G 45 N 155 I	0.84	2.0

[a] Abbreviations: *Mn*, number-average molecular weight; *Mw*, weight-average molecular weight; K, crystal; N, nematic; I, isotropic; G, glass; ΔH_{NI}, change in enthalpy of N-I phase transition; ΔS_{NI}, change in entropy of N-I phase transition.

3. Photochemical Phase Transition.

Azobenzene derivatives were dissolved in chloroform (spectroscopic grade) at a low concentration (~ 10^{-3} mol/L) and a small portion of the resultant solution was cast on a glass plate which had been coated with poly(vinyl alcohol) (PVA; Tokyo Kasei; degree of polymerization: 1750 ± 50; degree of saponification: ~ 100%) and rubbed to align mesogens. The solvent was removed under reduced pressure at room temperature. After the solvent was removed, the LC film was annealed at a temperature just below Tc to yield a monodomain of a well-aligned N phase. Thickness of the LC films was estimated as ~ 200 nm by absorption spectroscopy on the basis of molar extinction coefficients of the azobenzene moieties. The LC films thus prepared were placed in a thermostated block and photochemical phase transition behavior of the LC films was followed by means of an apparatus shown in Figure 2-2. The films were irradiated at 366 nm from a 500 W high-pressure mercury lamp through glass filters (Toshiba, UV-D36A + UV-35 + IRA-25), and the intensity of the linearly polarized light at 830 nm from a diode laser transmitted through a pair of crossed polarizers, with the sample film between them, was measured with a photodiode.

Figure 2-3 shows the optical setup for time-resolved measurements of the photochemical phase transition of the azobenzene films. The LC film was thermostated and set between two crossed polarizers. The sample was irradiated with a single pulse of a Nd:YAG laser (Spectron, SL805 laser system; the third harmonic, 355 nm; 40 mJ/cm^2; 10 ns, fwhm), and the transmittance of the probe light (NEC, GLG5370 He-Ne laser; 633 nm; 1 mW) through crossed polarizers was measured with a Hamamatsu R-928 photomultiplier as a function of time and recorded with a storage scope (Iwatsu, DS-8631).

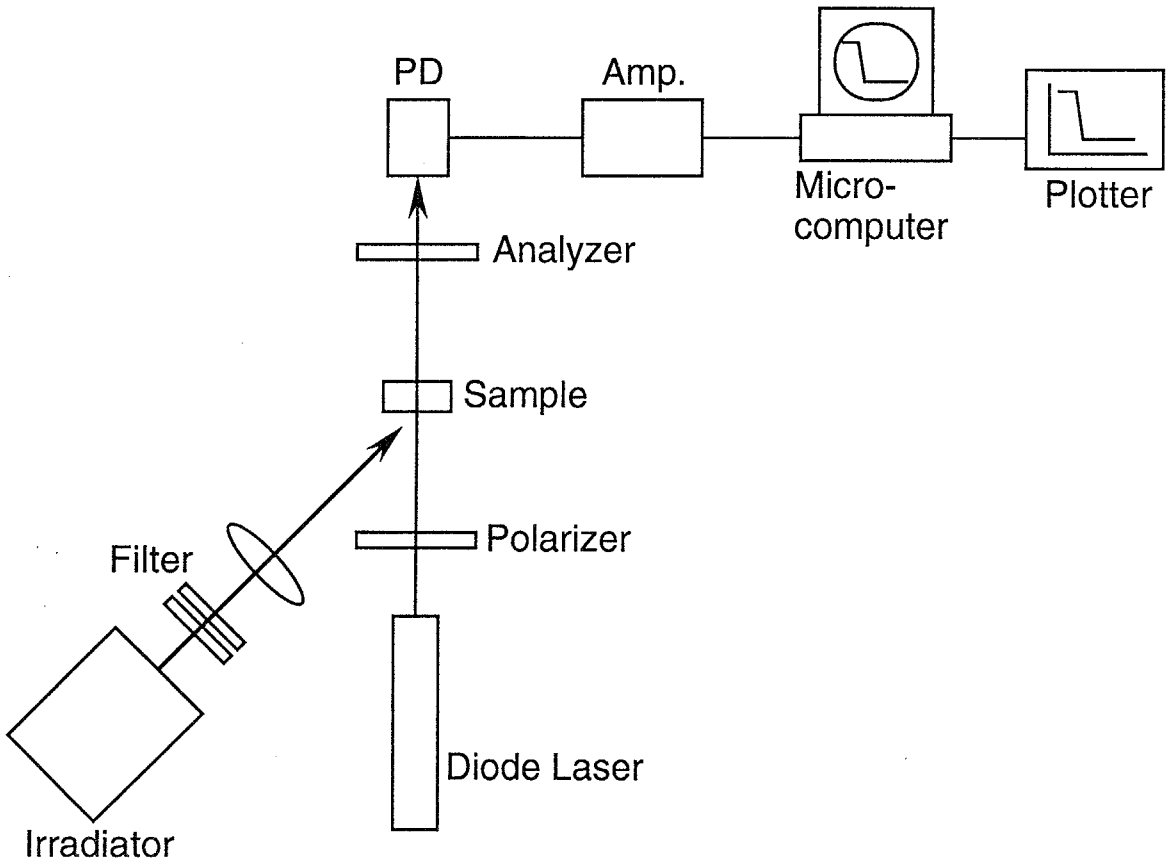

Figure 2-2. Schematic diagram for the measurement of photochemical N-I and thermal I-N phase transition behavior.

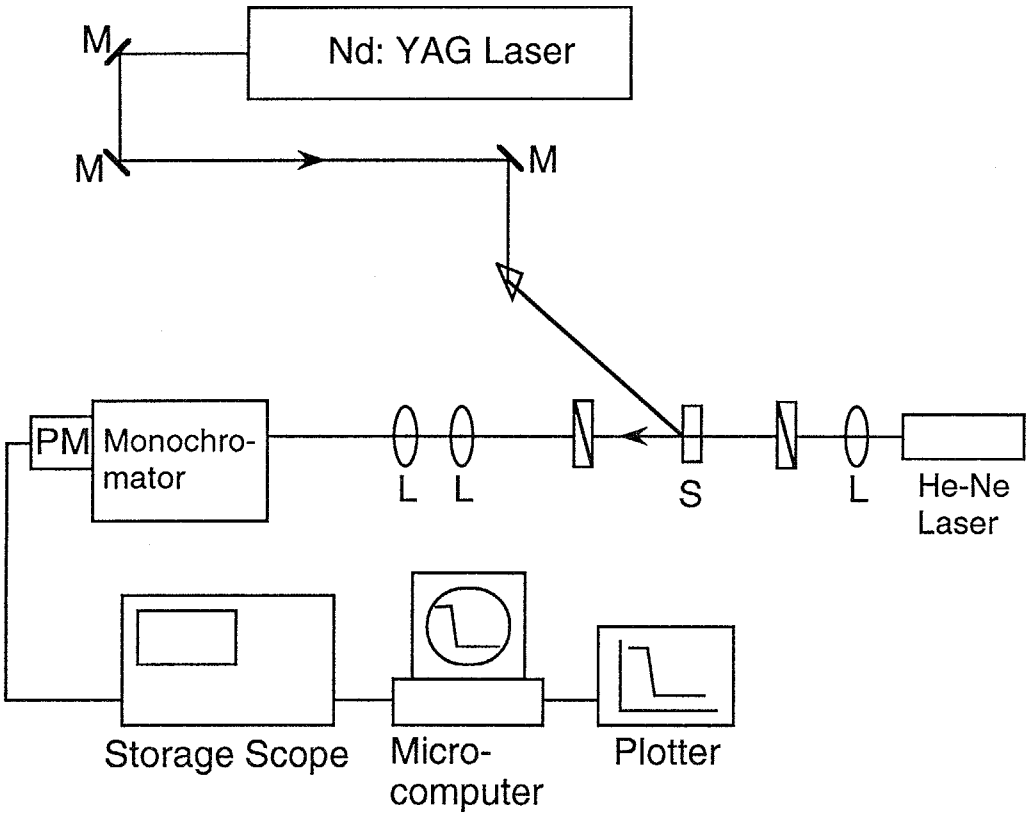

Figure 2-3. Schematic diagram for the time-resolved measurement of photochemical N-I phase transition behavior: M, mirror; L, lens; S, sample film.

4. Isomerization Behavior of Azobenzene

The change in absorption spectra was observed to determine photo- and thermal isomerization behavior of the azobenzene moieties. Absorption spectra were recorded with a Shimadzu UV-200S absorption spectrometer.

For the time-resolved observation of the *trans-cis* photoisomerization of azobenzene derivatives, the laser pulse at 355 nm was also used as an excitation source. The analyzing light from a Xe flash-lamp was irradiated synchronously on the LC film. The analyzing light passed through the LC film was collimated on a Jobin-Ybon HR-320 monochromator. Intensity of the analyzing light at 360 nm was measured with a photomultiplier and recorded with the storage scope.

RESULTS AND DISCUSSION

1. *trans-cis* Photoisomerization Behavior of Azobenzene LCs.

trans-Azobenzenes exhibit their absorption maxima at around 350 nm due to a π–π^* transition and at around 450 nm due to an n-π^* transition. It was observed that irradiation at 366 nm induced *trans-cis* isomerization of the azobenzene moiety in N phase as shown in Figure 2-4 for **BMAB**. Time-resolved measurement of change in absorbance at 360 nm showed that the *trans-cis* photoisomerization occurred within 20 ns in the N phase (Figure 2-4, inset). The absorbance at 360 nm decreased abruptly on laser pulse irradiation and then increased slightly. This increase in absorbance at later stage may be interpreted in terms of rise in temperature due to the laser pulse irradiation. The rise in temperature caused change in density of **BMAB** with concomitant variation of

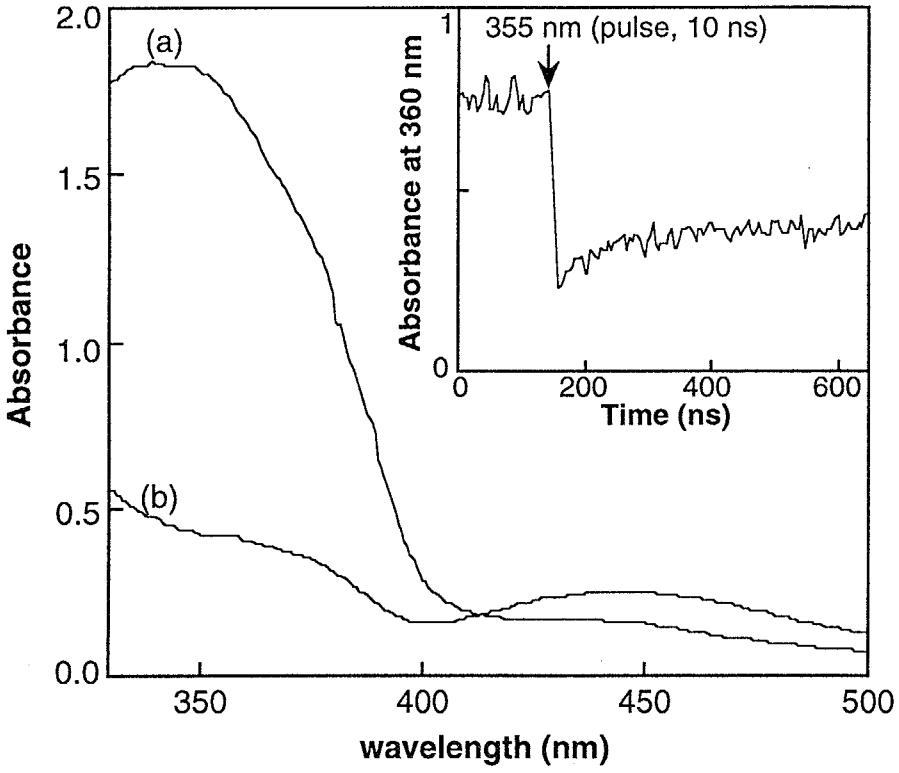

Figure 2-4. Absorption spectra of **BMAB** film: (a), before irradiation; (b), after irradiation at 366 nm from mercury lamp. The inset contains time-resolved measurement of change in absorbance of the **BMAB** film at 360 nm by laser pulse irradiation (355 nm; 10 ns fwhm).
Measurement was performed at 35 °C where **BMAB** showed the N phase.

refractive index. The change in the refractive index altered the transmittance of the analyzing light and could be observed as the change in absorbance. Consequently, absorbance at 360 nm increased slightly.

2. Phase Transition Behavior of Low-Molecular-Weight LCs.

It was observed with a polarizing microscope that the *trans* form of all the azobenzene derivatives used in this study showed the N phase, while the *cis* form showed no LC phase. Linearly polarized light at 830 nm from a diode laser could transmit through a pair of crossed polarizers, with the azobenzene film between them, because of birefringence of the liquid-crystalline azobenzene. Transmittance of the probe light decayed immediately upon irradiation at 366 nm in the N phase as shown in Figure 2-5 for **8AB8**. This was caused by the disappearance of the LC phase due to the photoisomerization of the azobenzene with concomitant loss of birefringence. The transmittance of the probe light recovered approximately in 30 s when photoirradiation was ceased. At a temperature above 100 °C, the thermal *cis-trans* back-isomerization took place effectively, followed by reorientation of mesogens, so that the initial N phase was recovered rapidly when the LC film was kept in dark. The photochemical N-I phase transition and the thermal I-N phase transition occurred repeatedly in **8AB8**. The N-I phase transition was also induced in **BMAB** at 35 °C on the same timescale as **8AB8**. The thermal recovery of the N phase, however, required several hours. **BMAB** shows the N phase at a lower temperature than that of **8AB8**. At 35 °C, the thermal *cis-trans* back-isomerization occurs very slowly, so that the thermal recovery of the N phase needed a much longer time.

Figure 2-6 shows time-resolved measurements of the photochemical

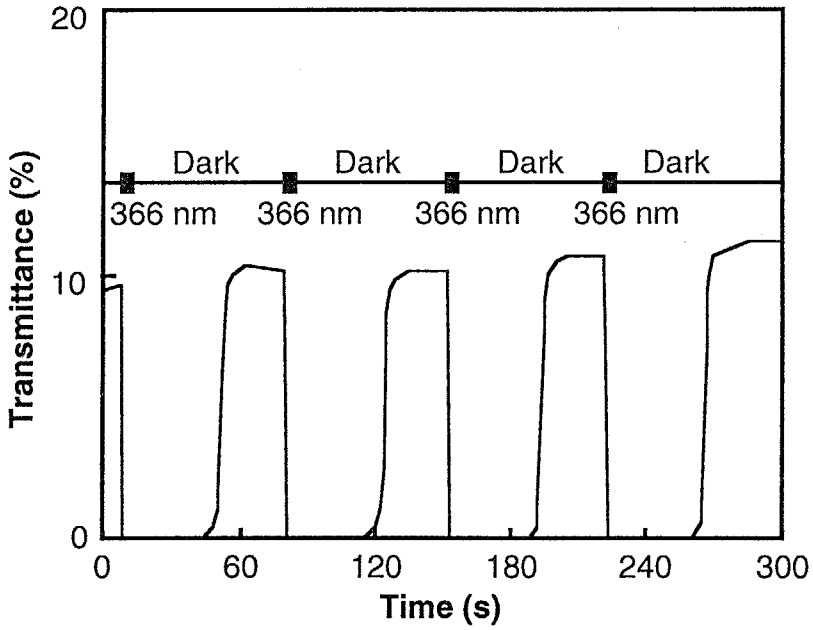

Figure 2-5. Photochemical N-I phase transition and thermal I-N transition of **8AB8**.
Photoirradiation was performed at 110 °C.

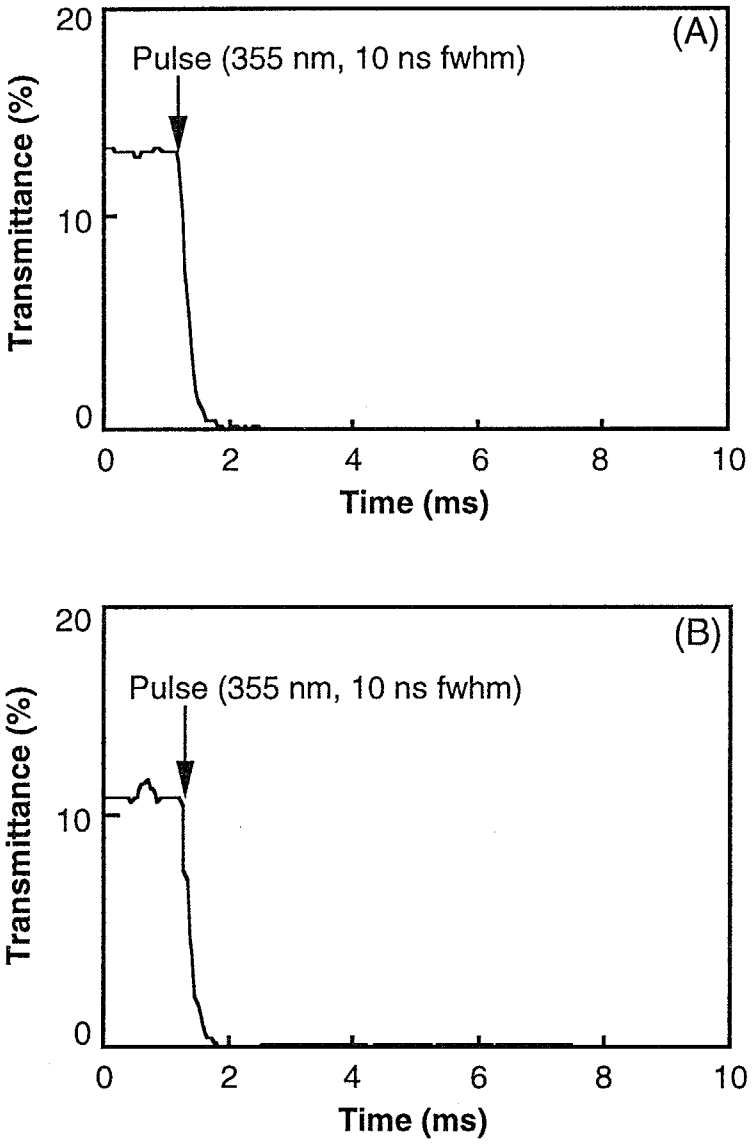

Figure 2-6. Time-resolved measurements of the photochemical N-I phase transition induced by pulse irradiation (355 nm; 10 ns fwhm): (A), **BMAB** at 35 °C; (B), **8AB8** at 110 °C.

N-I phase transition in **BMAB** and **8AB8**. To discuss the phase transition behavior quantitatively, the response time of the N-I phase transition was defined as the time necessary to reduce the transmittance of the probe light to 10 % of the maximum value. Similarly, the response time of the I-N phase transition was defined as the time required to restore the transmittance to 90 % of the maximum value. It became apparent that the response time of the N-I phase transition was 200 μs in both **BMAB** (Figure 2-6(A)) and **8AB8** (Figure 2-6(B)). This response was faster by 1 ~ 2 orders of magnitude than the response of NLCs reported so far.[1,2] To examine if heat-mode process was involved in the phase transition, the LC films were irradiated with a high-power infrared laser pulse at 1064 nm using a Nd:YAG laser (fundamental; 1 J/cm^2; 10 ns, fwhm) but no phase transition was induced in any sample.

Under the present experimental set-up, the photochemical N-I phase transition was observed only in the thin films (~ 200 nm) in all samples. In thick films, the pumping light was absorbed entirely at the surface of the films, since molar extinction coefficients of the azobenzenes are very large (~ 2 X 10^4 L/mol·cm) at 366 nm and 355 nm, and the photochemical reaction was induced only in the surface area. Consequently, the N-I phase transition occurred only in the surface of the films, leaving the remaining part of the films intact as the N phase. The present optical set-up allows us to detect the N-I phase transition solely when it takes place completely across the films.

3. Photochemical Phase Transition Behavior of Polymeric LC.

The photochemical N-I phase transition and the thermal I-N phase transition also occurred repeatedly in **PA6AB2** at 140 °C as shown in Figure 2-7. At this temperature, the thermal *cis-trans* back-isomerization

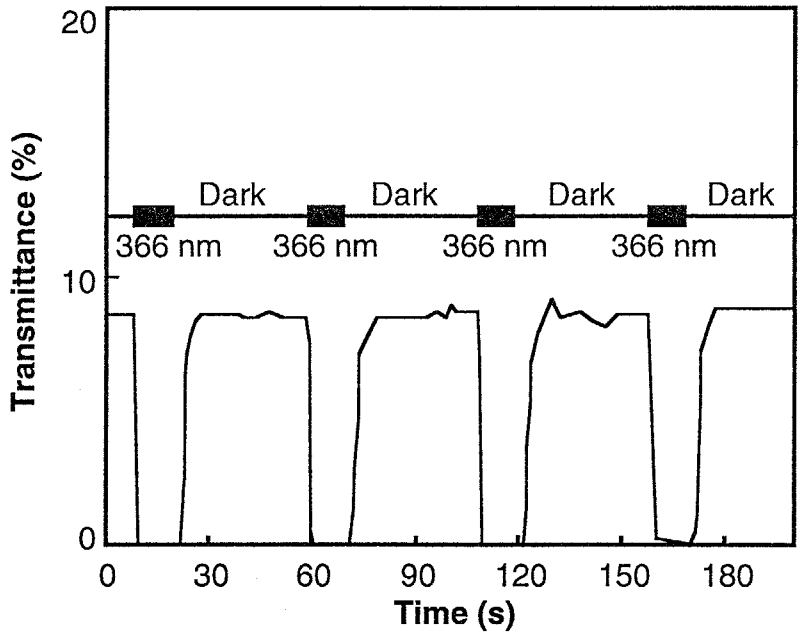

Figure 2-7. Photochemical N-I phase transition and thermal I-N transition of **PA6AB2**.
Photoirradiation was performed at 140 °C.

of the azobenzene moiety took place more effectively than that at 110 °C (Figure 2-5), and it took only 7 ~ 8 s for the recovery of the N phase. In the temperature range between Tg and 140 °C, the thermal I-N phase transition was also observed because the *cis-trans* back-isomerization of the azobenzene and the reorientation of the mesogens occurred thermally.

Time-resolved measurements revealed that the photochemical N-I phase transition was induced in 200 μs even in the polymer LC as shown in Figure 2-8. In general, the response time of the polymer LCs is longer than that of the low-molecular-weight LCs, since in the polymer LCs the mobility of mesogens is highly restricted by main chain of the polymer.

In a system where the center of gravity of each molecule is aligned regularly like in crystals, optical anisotropy is observed even after the anisotropy in shape of each molecule is eliminated (Figure 2-9(A)). On the other hand, in NLCs optical anisotropy originates only from the anisotropy in molecular shape (rod-like shape) and the center of gravity of each molecule is distributed randomly. While the molecular shape is anisotropic even in the *cis* form, the optic axis of the molecule is distributed randomly. Therefore, in the NLCs the optical anisotropy disappears if the anisotropy in shape of each molecule vanishes through *trans-cis* isomerization as shown in Figure 2-9(B). Note that phase transition of this type does not require lateral movement of LC molecules; the center of gravity of each molecule remains almost unchanged. Then it is possible that the phase transition takes place similarly in low-molecular-weight LCs as well as in polymer LCs. The polymer azobenzene LCs show a much wider temperature range in general for the N phase, so that they are advantageous in view of a wide temperature range available for the optical switching.

It is worth noting that the photochemical N-I phase transition was also induced in 200 μs even below Tg (at room temperature, 23 °C) as

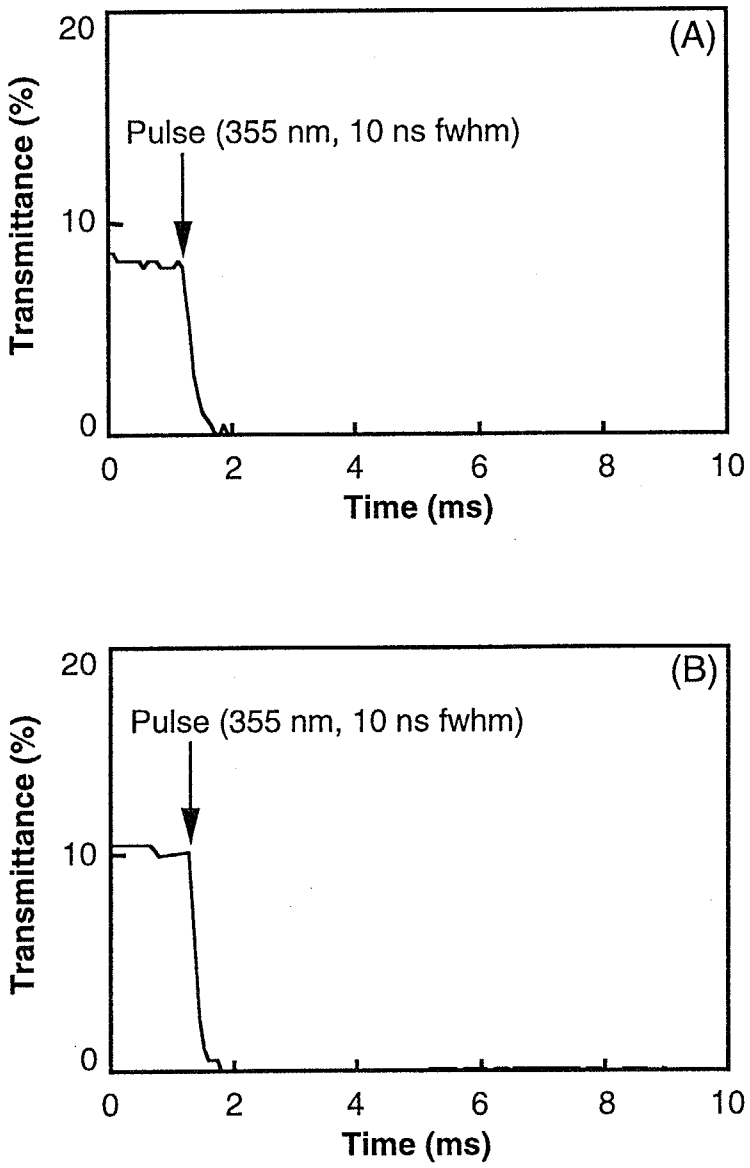

Figure 2-8. Time-resolved measurements of the photochemical N-I phase transition induced by pulse irradiation (355 nm; 10 ns fwhm) in **PA6AB2**: (A), at 140 °C; (B), at room temperature (below Tg).

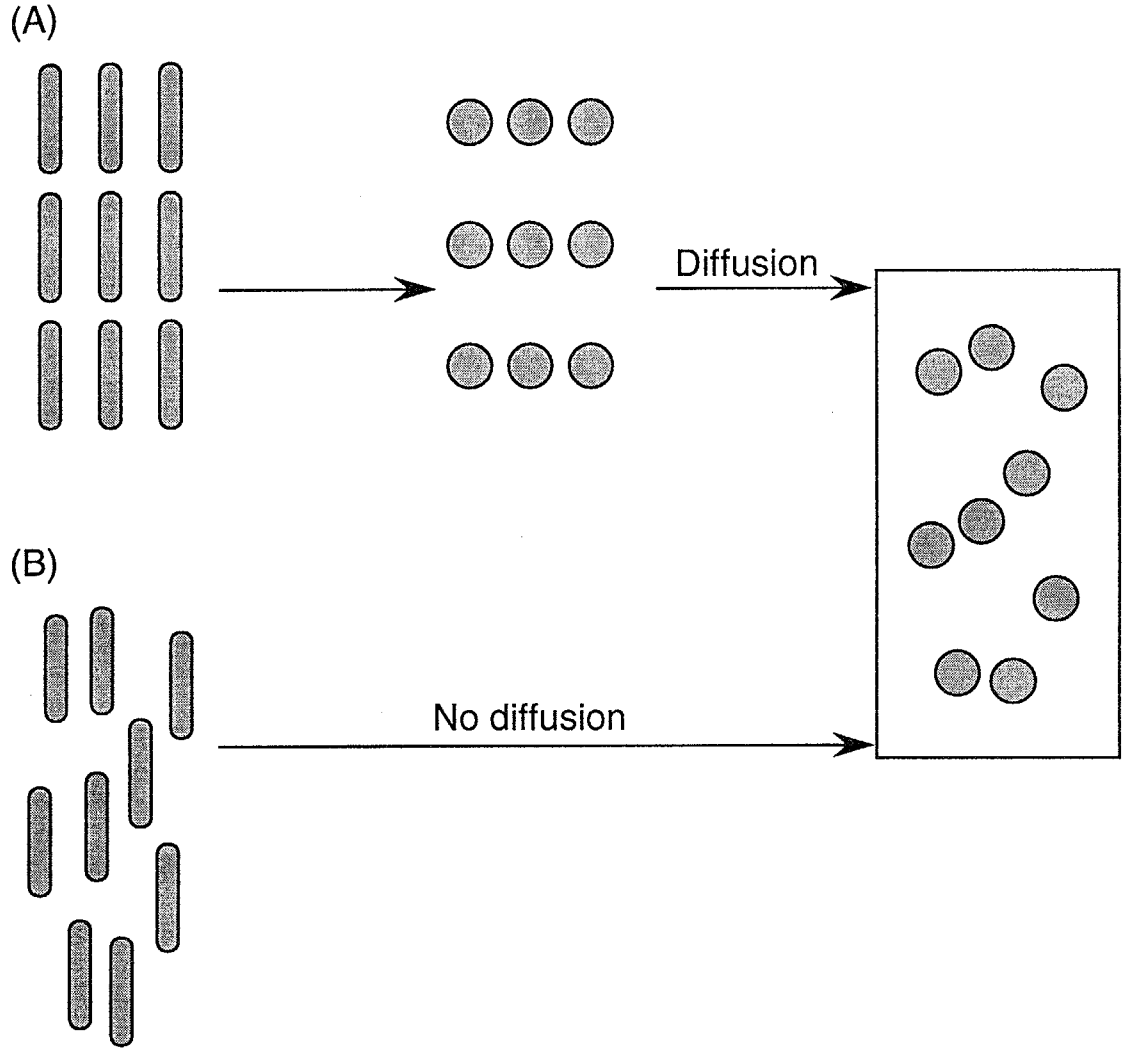

Figure 2-9. Schematic illustration for loss of optical anisotropy. In crystal, diffusion is required for the loss of optical anisotropy, (A). In N phase, however, phase transition dose not require lateral movement of LC molecules, (B).

demonstrated in Figure 2-8(B). There has been a significant amount of studies on the mechanism of photoisomerization of azobenzene derivatives, concerned with an inversion mechanism or a rotation mechanism. It is now accepted that the photoisomerization of azobenzenes occurs mainly through the inversion mechanism.[5,6] This mechanism requires much smaller sweep volume for the isomerization than the rotation mechanism. In addition, while segmental movement of main chains of the polymer is frozen below Tg, movement of side chains is allowed to some extent. Thus the azobenzene derivatives can isomerize in relatively rigid matrices like polymer matrices below Tg, depending on the spatial and temporal distribution in size of free volume in the polymer.[7-9]

When the thin film of **PA6AB2** was covered with a photomask (Figure 2-10(A)) and irradiated with a single pulse of the laser at 355 nm below Tg (at room temperature), the image was stored into the film with spatial resolution of 2 μm (Figure 2-10(B)). The stored image remained unchanged after 2 years when the irradiated film was kept at room temperature (< Tg) in the dark. However, when the irradiated film was heated above Tg, the stored image disappeared and the initial N phase was recovered.

In **PA6AB2**, it was observed that the thermal *cis* to *trans* back-isomerization took place in 24 h at room temperature (23 °C). As mentioned above, although the *trans* form was recovered nearly completely, the isotropic glass (glassy state in which the mesogenic *trans*-azobenzenes are randomly aligned) induced at the irradiated site below Tg still remained unchanged at room temperature even after 2 years. To explore this strange behavior of **PA6AB2**, the order parameter (S), which indicates degree of orientation of the mesogens, was measured before and after photoirradiation at room temperature.

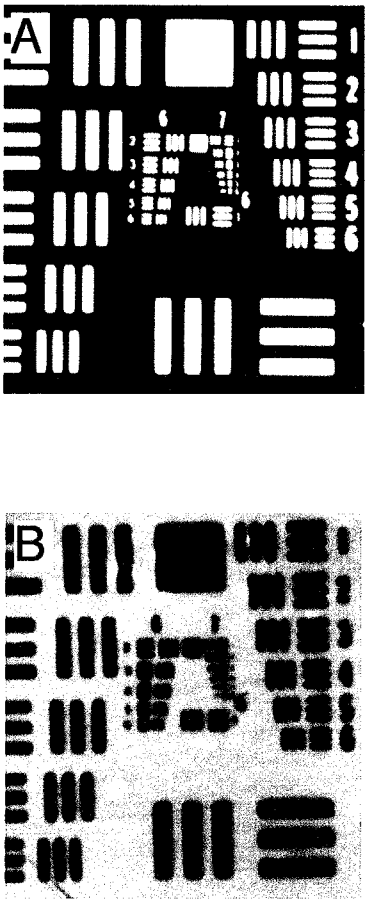

Figure 2-10. Stored image in **PA6AB2** film by irradiation with a laser pulse at 355 nm at room temperature: (A), photomask; (B), image after storage fo 2 years.

For a symmetrical system, the dichroic ratio, R, can be given by eq 2-1,[10]

$$R = \frac{A_{\parallel}}{A_{\perp}} = \frac{4\cos^2\alpha\langle\cos^2\theta\rangle + 2\sin^2\alpha\langle\sin^2\theta\rangle}{2\cos^2\alpha\langle\sin^2\theta\rangle + \sin^2\alpha\langle 1+\cos^2\theta\rangle} \qquad (2\text{-}1)$$

where $A_{\parallel}$ and $A_{\perp}$ are the absorbance measured with the UV beam polarized parallel and perpendicular to the optic axis of the molecule, respectively. θ is the angle between the direction of the molecular long axis and the optic axis of the uniformly oriented NLCs, and α is the angle between the molecular long axis and the direction of the transition moment. In the case where the transition moment is oriented parallel to the molecular long axis, the S can be written in the form of eq 2-2.[10]

$$S = \frac{R-1}{R+2} \qquad (2\text{-}2)$$

Figure 2-11 shows the polarized absorption spectra of **PA6AB2** measured before and after irradiation at room temperature. Absorption at 360 nm is due to the π–π^* transition of the *trans*-azobenzene moiety, and this peak was used for the determination of the order parameter of **PA6AB2**. Before irradiation, the value of S was 0.45, indicating that the mesogens were aligned well in the N phase. After irradiation, when the *trans*-forms were thermally restored, the S value decreased to 0.05, indicating that the mesogenic *trans*-azobenzenes were not aligned, forming no N phase. These results lead to the conclusion that orientation of the mesogenic *trans*-azobenzenes became disordered through the process of thermal *cis-trans* back-isomerization. Even though the *trans* form was recovered thermally, orientation of the mesogens could be hardly attained

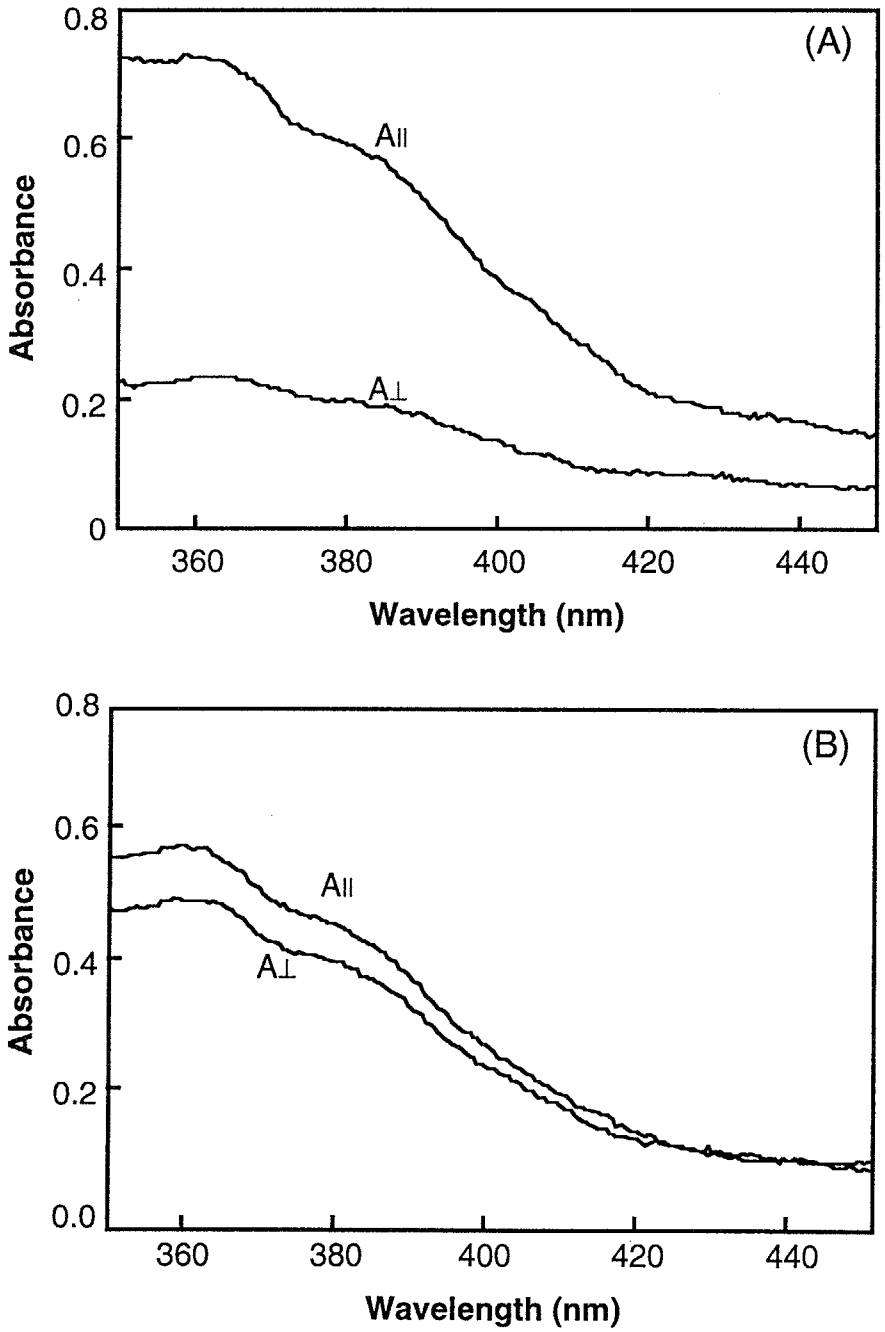

Figure 2-11. Polarized absorption spectra of **PA6AB2**: (A), before irradiation; (B), after irradiation.

in the absence of segmental motion of the main chain of the polymer below Tg (Figure 2-12).

4. Thermal I-N Phase Transition Behavior of Polymeric LC.

The thermal I-N phase transition consists of two processes: thermal *cis-trans* isomerization and reorientation of mesogenic *trans*-azobenzenes. The author investigated the thermal *cis-trans* isomerization process in detail. For the thermal *cis-trans* isomerization,

$$\ln \frac{[cis]}{[cis]_0} = - k_{c\text{-}t}\, t \qquad (2\text{-}3)$$

where [*cis*] and $[cis]_0$ are the concentrations of the *cis*-azobenzene at time t and time zero, respectively, and $k_{c\text{-}t}$ is the rate constant for the thermal *cis-trans* isomerization. The first-order rate constant was determined by fitting the experimental data to the equation,

$$\ln \frac{A_\infty - A_t}{A_\infty - A_0} = - k_{c\text{-}t}\, t \qquad (2\text{-}4)$$

where A_t, A_0 and A_∞ are the absorbance at 360 nm at time t, time zero and infinite time, respectively.[11] Examples of the first-order plots according to eq 2-4 for the *cis-trans* thermal isomerization of **PA6AB2** film are shown in Figure 2-13. From the slope of the Arrhenius plot, a value of 19 kcal/mol was obtained as an activation energy for the *cis-trans* isomerization (Figure 2-14).

Figure 2-14 also shows the Arrhenius plot for the thermal I-N phase transition of **PA6AB2** film. The rate constant of the I-N phase transition was defined as a reciprocal of the response time. As can be seen from Figure 2-14, the slope of the Arrhenius plot for the thermal I-N phase

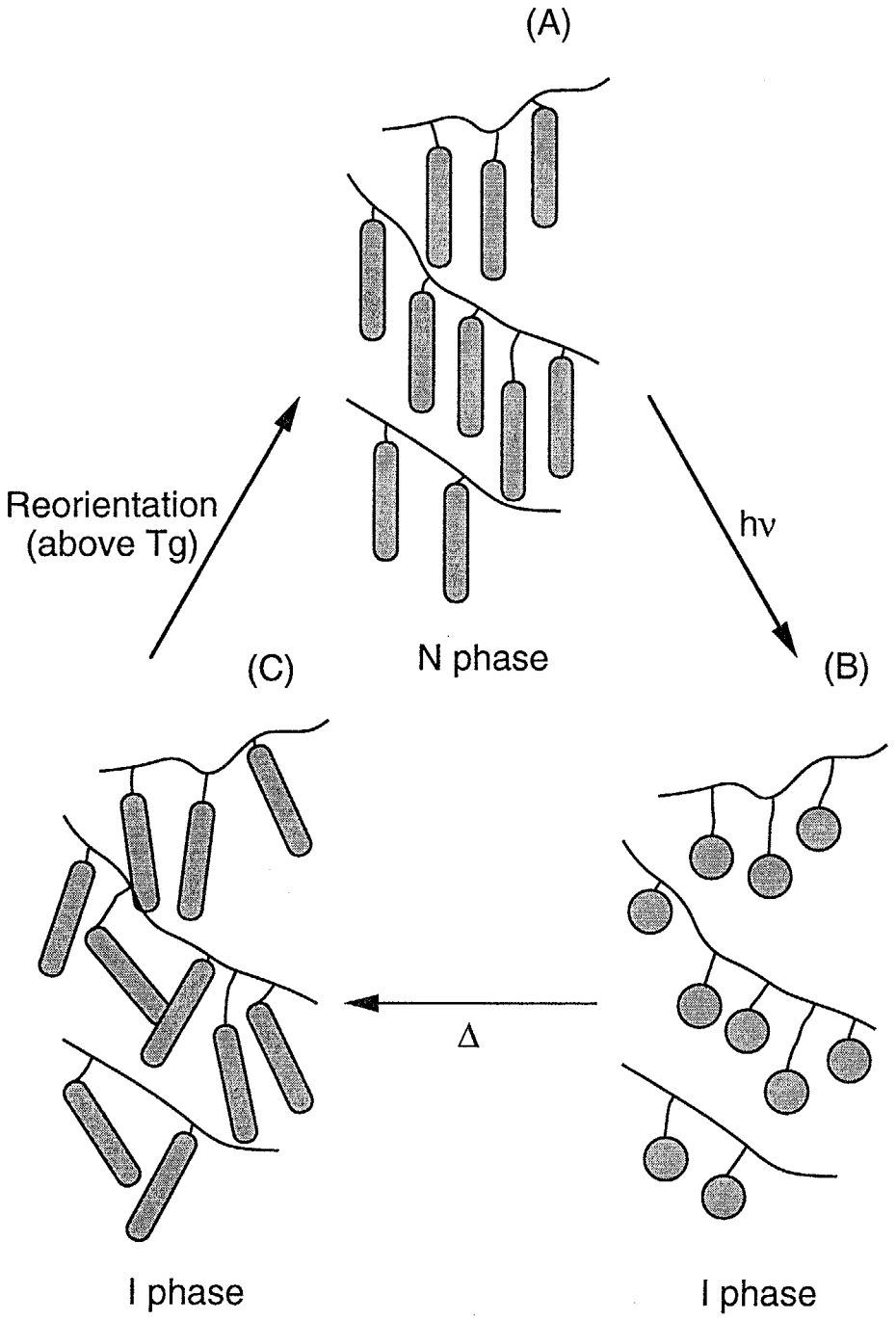

Figure 2-12. Schematic illustration for orientation of *trans*-azobenzene mesogens.
Before irradiation, mesogens are aligned and form N phase, (A). Immediately after irradiation, the N phase disappears because of *trans* to *cis* photoisomerization of the azobenzene, (B). After thermal *cis* to *trans* back-isomerization of the azobenzene moieties, the mesogens (*trans* form) no longer form the N phase since the molecular long axis of each *trans* form is random, (C).

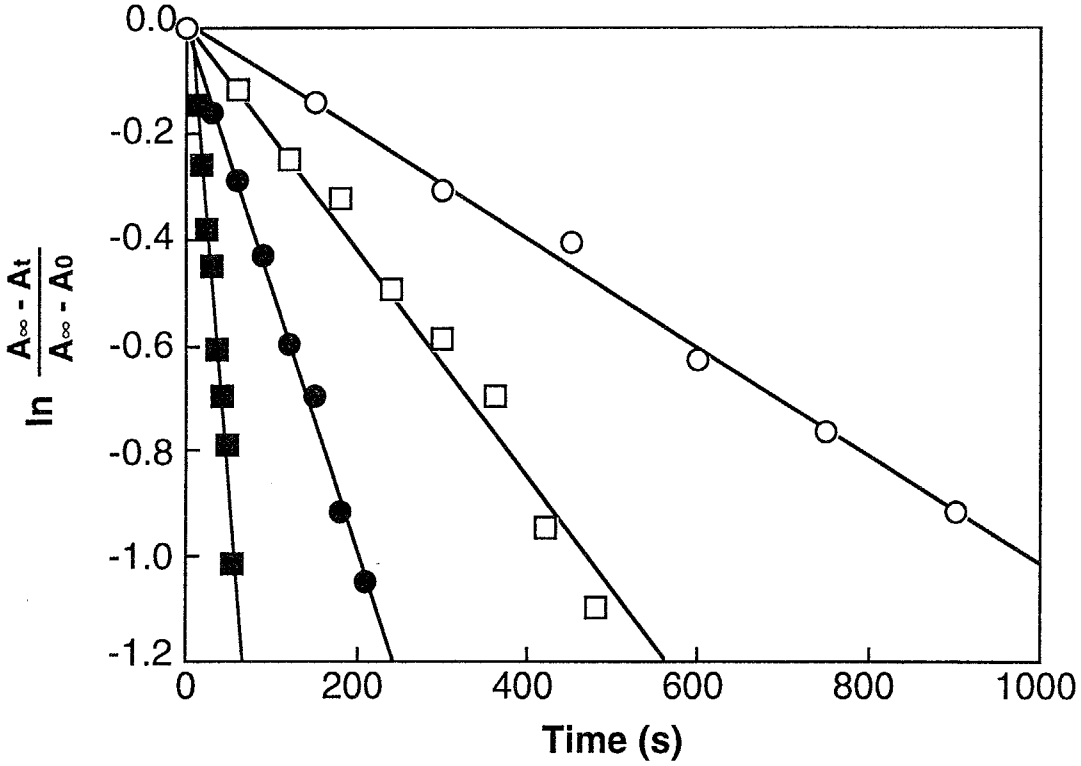

Figure 2-13. First-order plots for *cis* to *trans* thermal isomerization in **PA6AB2**: ○, at 49 °C; □, at 58 °C; ●, at 67 °C; ■, at 85 °C.

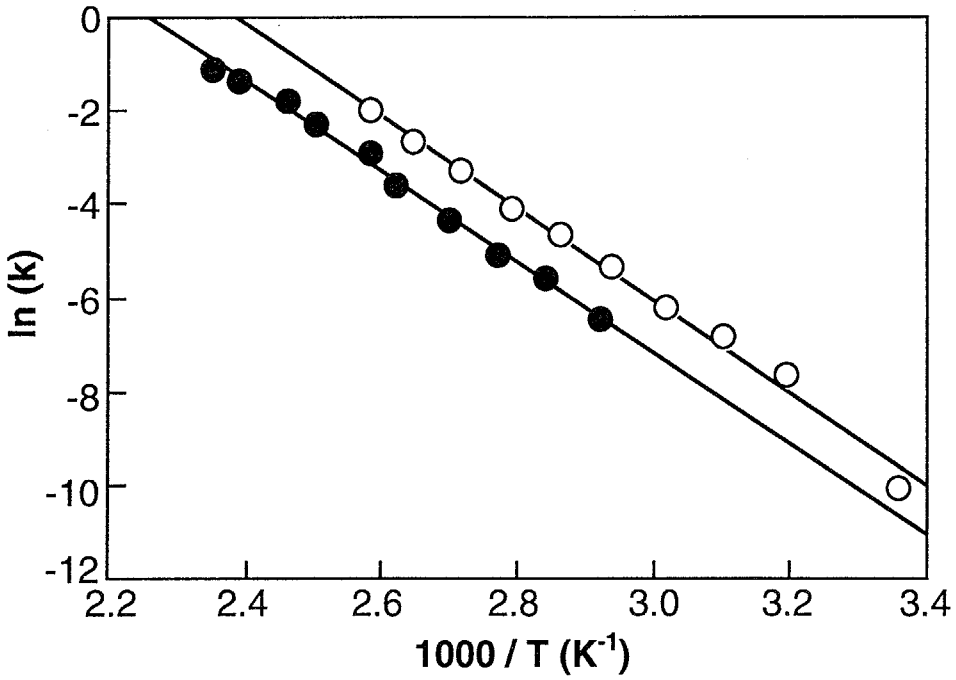

Figure 2-14. Arrhenius plots for *cis-trans* thermal isomerization of azobenzene moiety and for I-N thermal phase transition in **PA6AB2**: ○, for *cis-trans* isomerization; ●, for I-N phase transition.

transition is the same as that for the thermal *cis-trans* isomerization. Thus the activation energy for the I-N phase transition is identical with that for the *cis-trans* isomerization. This result indicates that the rate-determining step of the thermal I-N phase transition is the *cis-trans* isomerization process.

CONCLUSION

Quick photoresponse has been obtained in nematic azobenzene LCs in which the azobenzene moiety plays a dual role of a mesogen and a photosensitive chromophore. In these azobenzene LCs, only the *trans* form showed the N phase while the *cis* form did not show LC phase at any temperature. The N-I phase transition took place when the *trans-cis* isomerization was caused by photoirradiation. Since the *trans-cis* photoisomerization of the azobenzene moieties is a very fast process, the N-I phase transition was induced in 200 μs for the low-molecular-weight LCs and the polymer LC by the use of a short laser pulse to bring about the isomerization. The polymer LC showed quite a different behavior from those of the low-molecular-weight LCs because of the glass transition. At temperatures above Tg, the I phase induced at the irradiated site disappeared after some time, depending on the temperature; at high temperatures the I phase disappeared quickly because of effective thermal *cis-trans* back-isomerization, and at temperatures just above Tg, it disappeared very slowly. On the other hand, at temperatures below Tg, the I glass induced at the irradiated site remained very stable (more than 2 years) even though the *trans* form was restored thermally. This high stability of the I glass arises from the fact that after the *trans-cis-trans*

cycles the orientation of the *trans* form became random and this random orientation was frozen in the absence of segmental motion of main chain of the polymer below Tg.

References and Notes

(1) Kurihara, S.; Ikeda, T.; Sasaki, T.; Kim, H.-B.; Tazuke, S. *J. Chem. Soc. Chem. Commun.* **1990**, 1751.

(2) Ikeda, T.; Sasaki, T.; Kim, H.-B. *J. Phys. Chem.* **1991**, *95*, 509.

(3) Weygand, C.; Gabler, R. *J. Prakt. Chem.* **1940**, *155*, 322.

(4) Angeloni, A.S.; Caretti, D.; Carlini, C.; Chiellini, G.; Galli, G.; Altomare, A.; Solaro, R. *Liq. Cryst.* **1989**, *4*, 513.

(5) Rau, H.; Luddecke, E.J. *J. Am. Chem. Soc.* **1982**, *104*, 1616.

(6) Naito, T.; Horie, K.; Mita, I. *Macromolecules* **1991**, *24*, 2907.

(7) Sung, C.S.P.; Gould, I.R.; Turro, N.J. *Macromolecules* **1984**, *17*, 1447.

(8) Victor, J.G.; Torkelson, J.M. *Macromolecules* **1987**, *20*, 2241.

(9) Mita, I.; Horie, K.; Hirao, K. *Macromolecules* **1989**, *22*, 558.

(10) Neff, V.D. In *Liquid Crystals and Plastic Crystals*; Gray, G.W., Winsor, P.A., Eds.; Ellis Horwood: Chichester, U.K., 1974; Vol. 2, pp 231-253.

(11) Sasaki, T.; Ikeda, T.; Ichimura, K. *Macromolecules* **1993**, *26*, 151.

Chapter 3

Effect of Position of Rigid Core on Photochemical Phase Transition of Polymer Azobenzene Liquid Crystals

INTRODUCTION

In Chapter 2, it became apparent that the photochemical N-I phase transition of the low-molecular-weight and polymer azobenzene LCs was induced in 200 μs by irradiation with a single pulse of laser. It was known that the mesomorphic properties and the photochemical phase transition behavior of polymer LCs were influenced by the length[1-3] and the structure[4,5] of the spacer unit. Furthermore, these LC behavior was also influenced by the length of the alkoxyl-end group.[6] Therefore, when the polymers have side-chain mesogen with the same total length, the LC properties and the photochemical phase transition behavior may be affected by the position of the core group of the mesogen. In this chapter, the author used four types of the polymer azobenzene LCs and investigated the photochemical and the thermal phase transition behavior of these LCs. Special attention was paid to the effect of position of the azobenzene moiety as the core group of the side-chain mesogen on the phase transition behavior of the polymer LCs.

EXPERIMENTAL

1. Materials.

Figure 3-1 shows the structures of the polymer azobenzene LCs, in which the 4'-alkoxyazobenzene moiety is attached to main chain of poly(acrylate) through various length of methylene spacer units, and their abbreviations used in this chapter. In **PAxABy**, x indicates the number of carbon atoms in the spacer between the azobenzene moiety and the main chain of the polymer, and y indicates the number of carbon atoms in the alkoxyl end-group. These polymers have the side chains of approximately the same total length, while the azobenzene moieties were introduced at a deferent position as a rigid core of mesogens. The polymers were prepared by the method described in Chapter 2. Polymerization was conducted in DMF with AIBN as an initiator.

2. Characterization of LCs.

Molecular weight of the polymers was determined by GPC and thermotropic properties of the LCs were determined with DSC as described in Chapter 2. The thermodynamic properties and molecular weight of the polymer LCs are given in Table 3-1.

3. Transmission-Mode Analysis of Photochemical Phase Transition.

The photochemical phase transition behavior of the polymer LCs was investigated by the transmission-mode analysis described in Chapter 2. Sample films were prepared in the same manner as described in the preceding chapter.

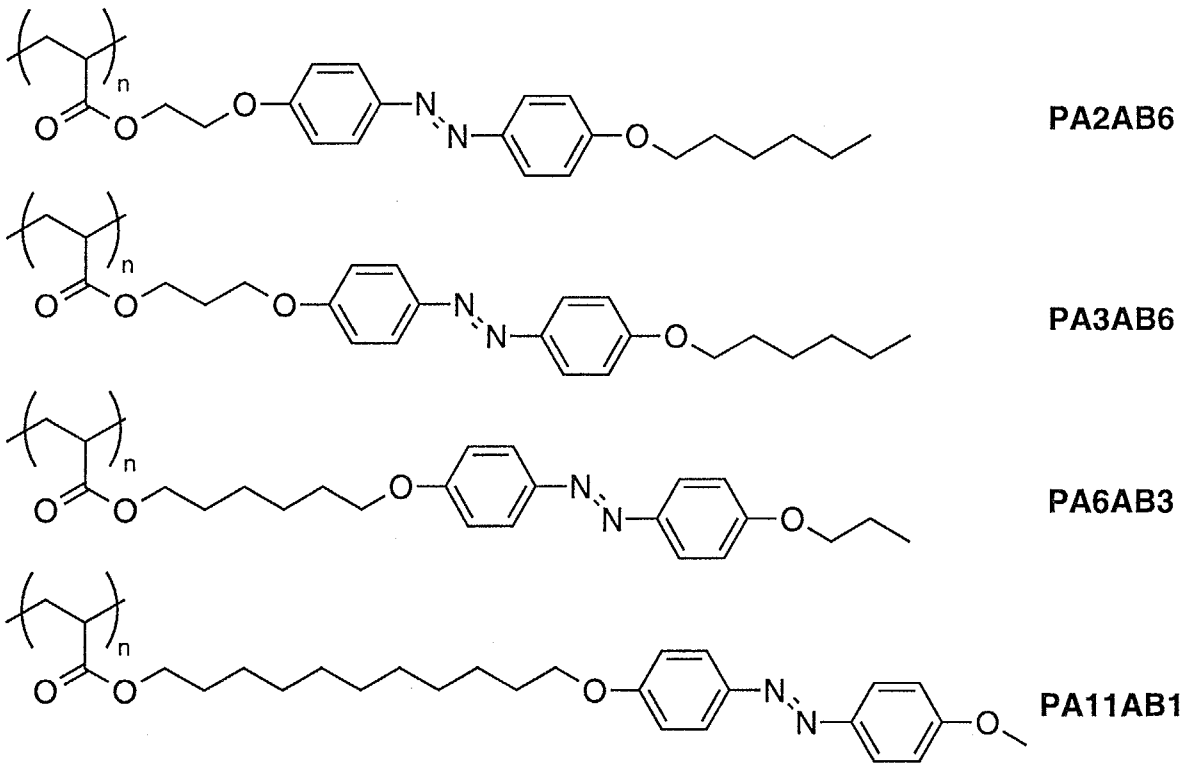

Figure 3-1. Structures of polymer azobenzene liquid crystals used in this chapter and their abbreviations.

4. Reflection-Mode Analysis of Photochemical Phase Transition.

In reflection-mode analysis, the intensity of the reflected light from the interface between the sample and the substrate was measured to investigate the photochemical phase transition behavior of the azobenzene LCs. Samples were prepared by casting the chloroform solution of the polymers onto the quartz block substrate and the photochemical phase transition behavior of the LC films was followed by means of an apparatus already reported (Figure 3-2).[7,8] The quartz substrate had been rubbed to align mesogens uniaxially in homogeneous manner, or it had been treated with lecithin to align mesogens in homeotropic manner. The laser pulse at 355 nm (30 mJ/cm^2; 10 ns, fwhm) was used as an excitation light and the linearly polarized light at 633 nm was used as the probe light. The incident angle of the probe light (θ_i) was 78 °. The intensity of the probe light reflected at the interface between the azobenzene LC and the quartz substrate was measured with a photomultiplier as a function of time.

RESULTS AND DISCUSSION

1. Characterization of Polymer Azobenzene LCs.

It became apparent with the polarizing microscope and the DSC that all the azobenzene polymers used in this chapter showed the LC phases in the *trans* form, while they showed no LC phase at any temperature in the *cis* form. It was also observed that the polymers with azobenzenes in the neighborhood of the main chain (**PA2AB6** and **PA3AB6**) showed high values of Tc and Tg and were highly viscous in the LC phase. In polymer LCs with side-chain phenyl benzoate or cyanobiphenyl mesogens, polymers with spacer of three methylene units exhibited a low value of

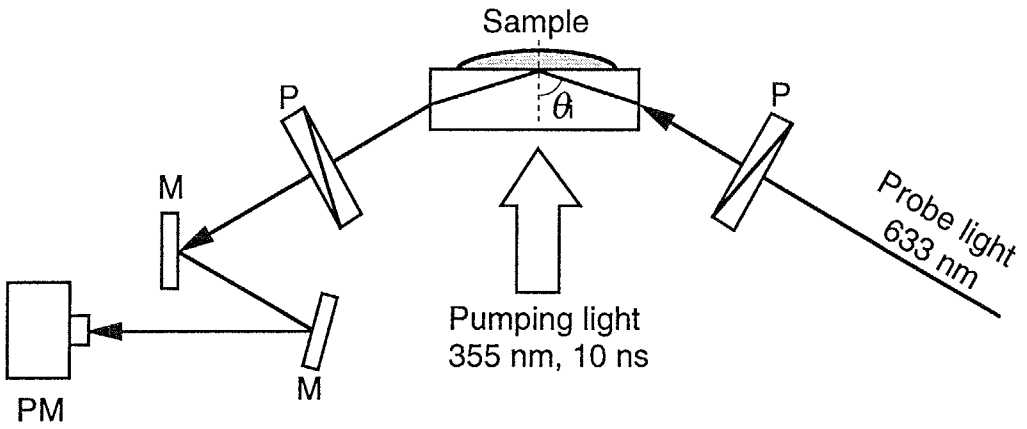

Figure 3-2. Schematic diagram of optical setup for reflection-mode analysis: M, mirror; P, polarizer; PM, photomultiplier; θi, incident angle.

Tc.[1-3] In the present polymer system, **PA3AB6** with three methylene units in the spacer contained a long alkoxyl end-group which stabilized the LC phase,[6] so that the value of Tc in **PA3AB6** would be high. Furthermore, **PA6AB3** and **PA11AB1** were aligned in the homogeneous manner in the LC phase. On the other hand, **PA2AB6** and **PA3AB6** showed homeotropic alignment in the LC phase with no birefringence by observation with the polarizing microscope.

Table 3-1. Molecular Weights and Phase Transition Temperatures of Polymer Azobenzene LCs Used in This Chapter[a]

	Mn	*Mw / Mn*	Phase Transition Temperature,[b] °C
PA2AB6	8,000	1.2	G 107 Sm 154 N 167 I
PA3AB6	17,000	1.7	G 118 Sm 178 I
PA6AB3	13,000	1.6	G 80 N 141 I
PA11AB1	20,000	3.4	G 47 Sm 146 I

[a] Abbreviations: *Mn*, number-average molecular weight; *Mw*, weight-average molecular weight; G, glass; Sm, smectic; N, nematic; I, isotropic.
[b] Determined by DSC.

It was confirmed by absorption spectroscopy that irradiation at 366 nm induced *trans-cis* photoisomerization of the azobenzene moiety. When the irradiated sample was kept in the dark, the *cis-trans* thermal back-isomerization was observed in all polymers.

2. Photochemical Phase Transition Behavior of Polymer Azobenzene LCs.

The linearly polarized light at 830 nm from the diode laser could transmit through a pair of crossed polarizers, with **PA6AB3** aligned in homogeneous manner between them, owing to birefringence of the *trans* form of the azobenzene LC. In **PA6AB3**, the transmittance of the probe light decayed immediately on irradiation at 366 nm in LC phase (Figure 3-3). This is attributable to LC-I phase transition of the azobenzene LCs due to *trans-cis* photoisomerization of the azobenzene moiety. The transmittance of the probe light recovered in 10 s when photoirradiation was ceased. The thermal *cis-trans* back-isomerization took place, followed by the reorientation of the mesogenic *trans*-azobenzene, so that the LC phase was recovered when the film was kept in the dark. Figure 3-4 shows the time-resolved measurement of the photochemical LC-I phase transition for **PA6AB3** evaluated by the transmission-mode analysis. The LC-I phase transition was induced in 200 μs by laser pulse irradiation. This is the same response as the low-molecular-weight and polymer LCs described in Chapter 2.

Figure 3-5 shows the results of the time-resolved measurements of the photochemical LC-I phase transition for **PA6AB3** in homogeneous alignment evaluated by the reflection-mode analysis with *p*-polarized light. In Figure 3-5, the director of the LC was perpendicular to the plane of the polarization of the probe light. The intensity of the reflected light increased in 100 μs due to the photochemical LC-I phase transition. In **PA6AB3** aligned in the homogeneous manner, the same results were obtained both by transmission-mode analysis and by reflection-mode analysis.

When the mesogens were aligned in the homeotropic manner, the reflectivity of the *p*-polarized light decreased in 100 μs (Figure 3-6 (A)).

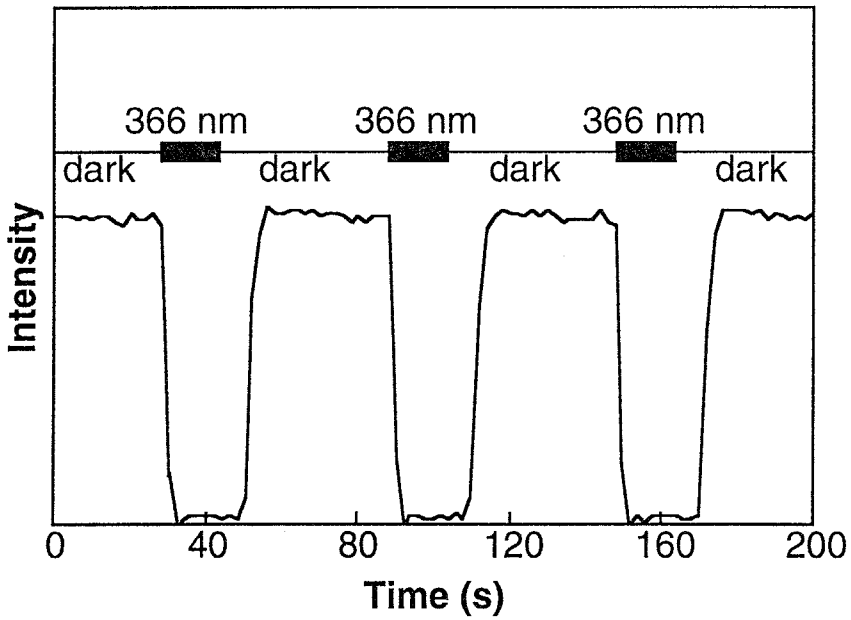

Figure 3-3. Photochemical N-I phase transition and thermal I-N transition of **PA6AB3**.
Photoirradiation was performed at 130 °C.

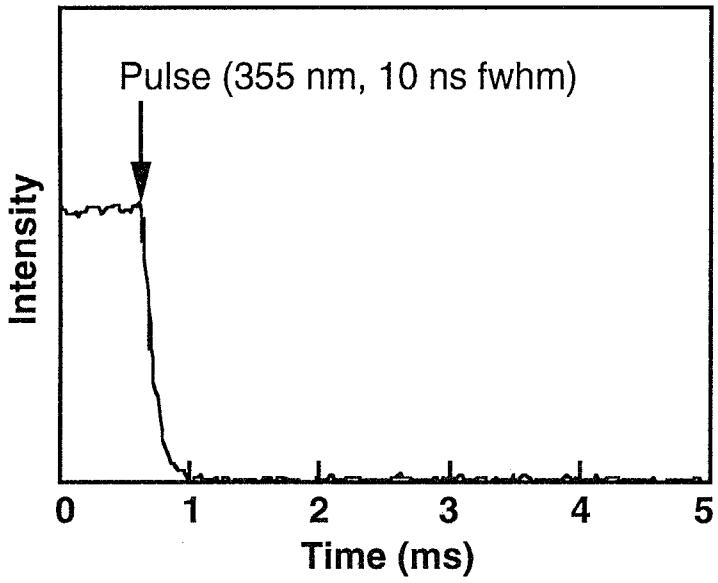

Figure 3-4. Time-resolved measurement of the photochemical LC-I phase transition induced by laser pulse irradiation in **PA6AB3** evaluated by the transmission-mode analysis at 130 °C.

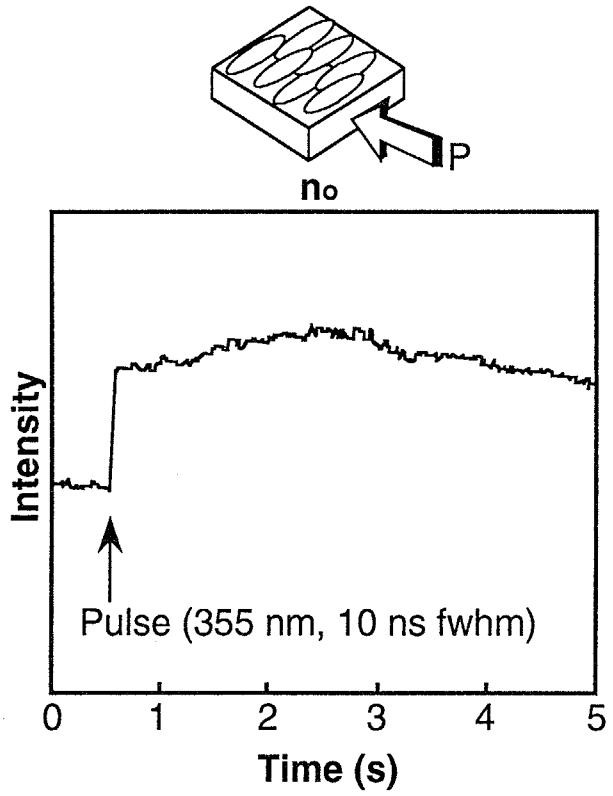

Figure 3-5. Time-resolved measurement of the photochemical phase transition in **PA6AB3** in homogeneous alignment evaluated by the reflection-mode analysis at 130 °C.

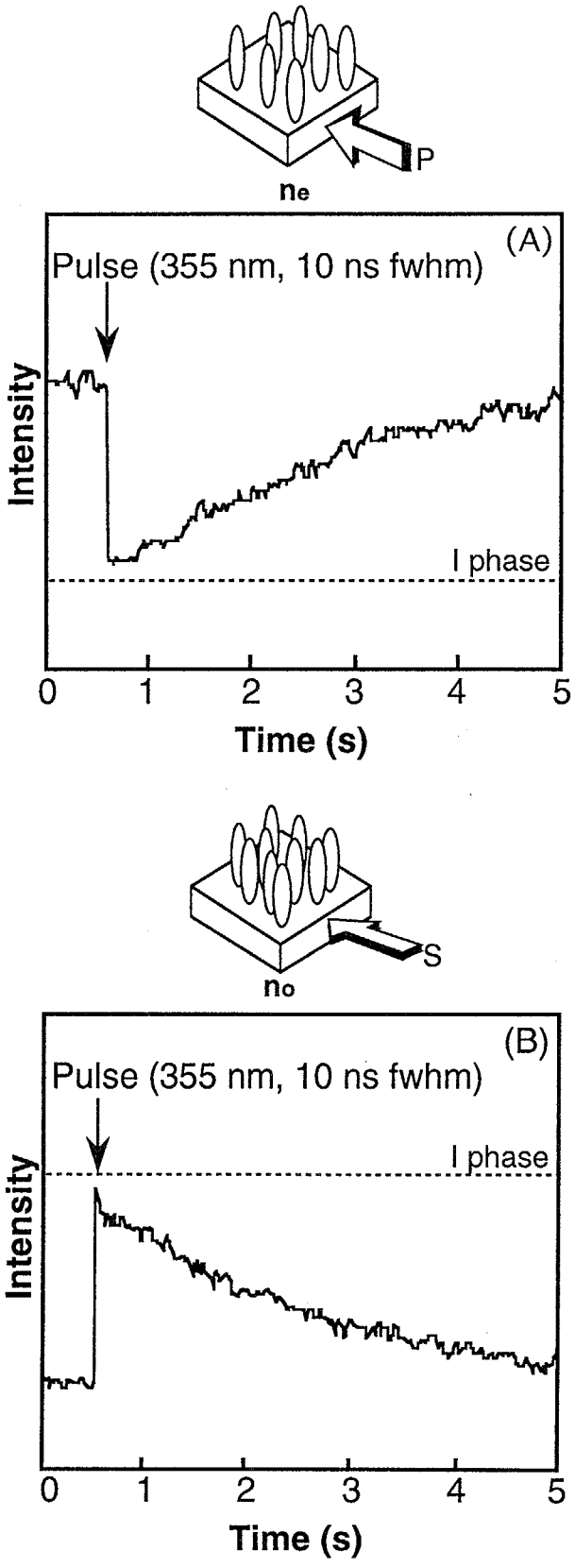

Figure 3-6. Time-resolved measurements of change in the reflectivity of probe light for **PA6AB3** aligned in homeotropic manner at 130 °C. Dashed lines indicate the reflectivity at I phase.
(A), *p*-polarization; (B), *s*-polarization.

However, when *s*-polarized light was used, the intensity of the reflected light increased in the same time (Figure 3-6 (B)). Under the present experimental setup, increase in the intensity of the reflected light means increase in the refractive index of the sample.[7] The LC phase shows birefringence: the refractive index parallel to the long axis of the LC molecules, n_e, is different from that perpendicular to the long axis, n_o. The I phase, however, shows no birefringence, and its refractive index is n. Relationship among n_o, n_e and n is given by eq 3-1,

$$n_o < n < n_e \tag{3-1}$$

For *p*-polarized light, the refractive index of the LC phase was n_o in the homogeneous alignment. The refractive index can be changed to n by the LC-I phase transition. The intensity of the reflected light, therefore, increased for *p*-polarized light in the homogeneous alignment. When the azobenzene LCs are aligned in the homeotropic manner, the refractive indices of the sample are n_e and n_o for the *p*-polarized light and *s*-polarized light, respectively. Consequently, the reflectivity of the probe light decreased for the *p*-polarization and increased for the *s*-polarization on pulse irradiation.

The thermal recovery of the LC phase in the reflection-mode analysis took place faster than that in the transmission-mode analysis. The LC phase recovered in 10 s in the transmission-mode analysis, while the recovery in the reflection-mode analysis proceeded in 8 s in the homogeneous alignment and in 3 s in the homeotropic alignment. This difference in the response time of the thermal recovery results from difference in mechanism of the I-LC phase transition between the transmission-mode analysis and the reflection-mode analysis.[8]

The thermal recovery of the LC phase in the homeotropic alignment occurred more quickly than that in the homogeneous alignment. When the azobenzene LCs were aligned in the homeotropic manner, transition moment of the azobenzenes was parallel to the direction of the pumping light. Therefore, the concentration of the *cis* isomer formed by laser pulse irradiation was very low, and the LC phase recovered quickly in the homeotropic alignment.

3. Effect of Position of Azobenzene Moiety on Photochemical Phase Transition Behavior.

PA2AB6 and **PA3AB6** exhibit no birefringence when viewed in the direction normal to the glass substrate where thin film of the sample was prepared, since they were aligned in the homeotropic manner in the LC phase. One could not, therefore, evaluate the photochemical phase transition behavior by means of the transmission-mode analysis. The author employed the reflection-mode analysis and investigated the effect of the position of azobenzene moiety on the photochemical phase transition behavior in full detail.

Figure 3-7 shows the results of the time-resolved measurements of change in the reflectivity for **PA3AB6** aligned in homeotropic manner. The intensity of the reflected light decreased in 100 μs on laser pulse irradiation for *p*-polarization and it increased in the same time for *s*-polarization. In other samples, the same results were obtained for photochemical LC-I phase transition when evaluated by the reflection-mode analysis. However, the degree of the change in the intensity of the reflected light decreased as the distance between the azobenzene moiety and the polymer main chain decreased. The reflectivity varied nearly to the level at I phase in **PA6AB3** (Figure 3-6). However, the reflectivity in

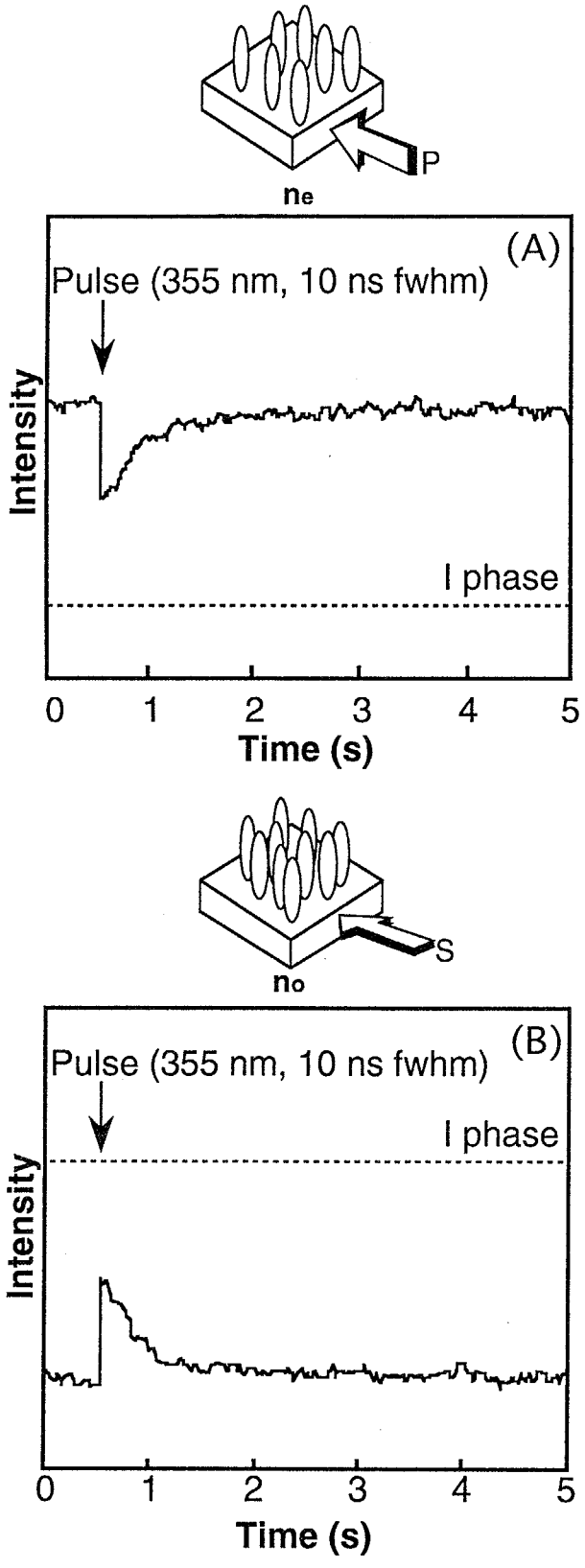

Figure 3-7. Time-resolved measurements of change in the reflectivity of probe light for **PA3AB6** aligned in homeotropic manner at 145 °C. Dashed lines indicate the reflectivity at I phase.
(A), *p*-polarization; (B), *s*-polarization.

PA3AB6 changed to about half of the level at I phase (Figure 3-7). This indicates that the photochemical phase transition in the polymer LCs with a short spacer was induced only in local areas.[8]

Figure 3-8 shows the temperature dependence of the thermal recovery of the LC phase evaluated by the reflection-mode analysis. In all the azobenzene LCs, the response time for the recovery of the LC phase decreased with increasing the temperature. This temperature dependence of the recovery observed in the polymer LCs is quite different from that in the low-molecular-weight LCs.[7,8] In the reflection-mode analysis, the thermal recovery of the LC phase is composed of two processes: diffusion of the *cis* isomer produced in the surface region into the bulk region and reorientation of the mesogenic *trans*-azobenzene.[8] At high temperature, since the diffusion process takes place effectively, the recovery proceeded rapidly. Furthermore, the recovery tends to be faster in the sample with a short spacer. In this temperature range, **PA2AB6**, **PA3AB6** and **PA11AB1** showed Sm phase, while **PA6AB3** showed N phase. All the samples showed the same tendency, while the phase structure was different. Under this experimental condition, phase transition behavior was not affected by the phase structure of the azobenzene LCs.

The rapid recovery of the LC phase in the polymers with a short spacer may be due to the local phase transition. Because of the local LC-I phase transition, alignment of the mesogens after photoirradiation was less disordered, so that the reorientation of the mesogens in **PA2AB6** and **PA3AB6** proceeded more quickly than that in **PA6AB3** and **PA11AB1**. Consequently, the thermal recovery of the LC phase proceeded quickly in **PA2AB6** and **PA3AB6**. By introduction of a flexible spacer between the polymer main chain and the mesogens, the motion of the mesogenic side chains was decoupled from that of the polymer main chain.[9] In the sample with a short spacer (**PA2AB6** and **PA3AB6**), however, the motion of the

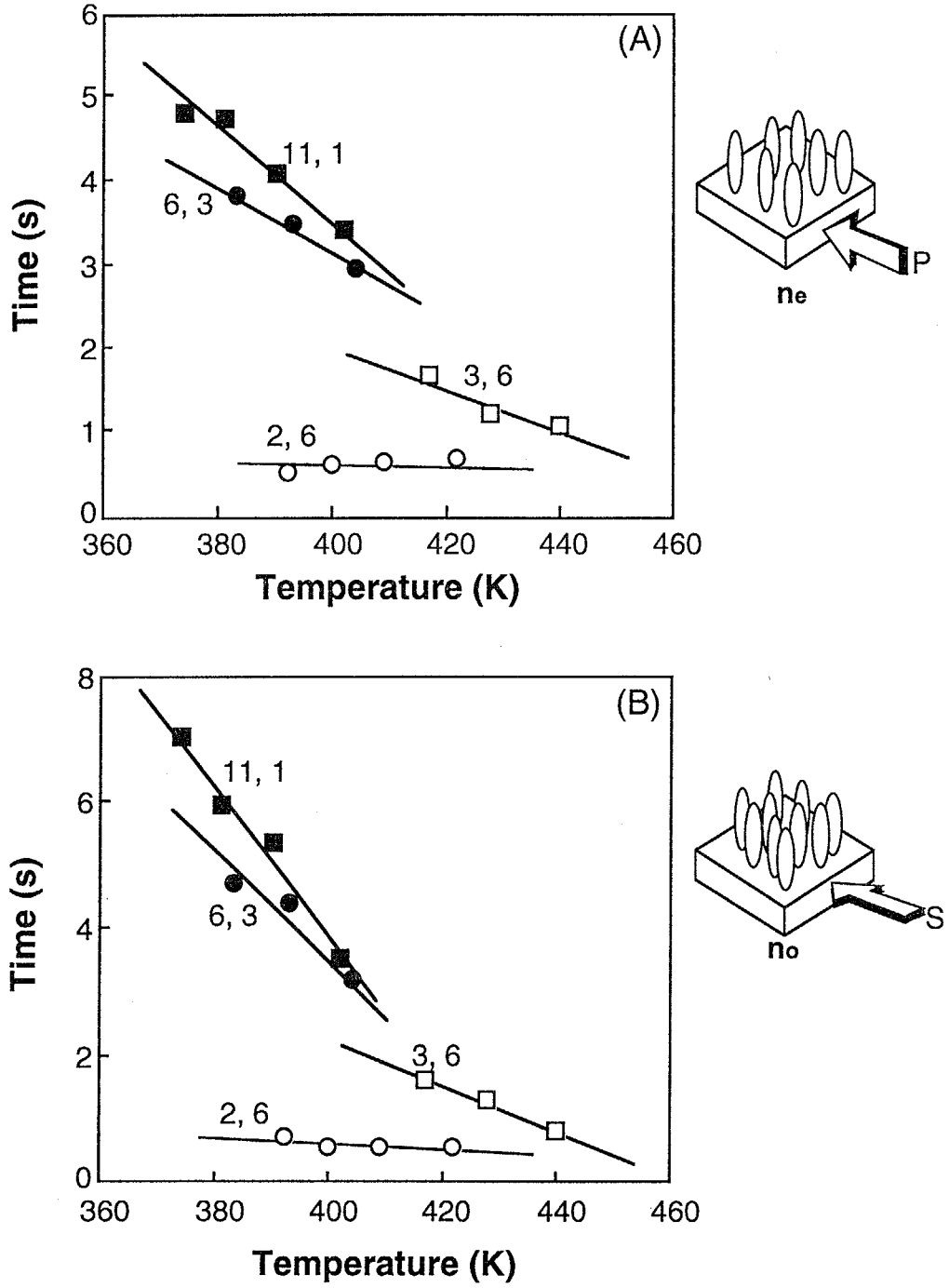

Figure 3-8. Time necessary for thermal recovery of the LC phase as a function of temperature: (○), **PA2AB6**; (□), **PA3AB6**; (●), **PA6AB3**; (■), **PA11AB1**.
(A), *p*-polarized light; (B), *s*-polarized light.

mesogens was restricted by the polymer main chain. In fact, these polymers were very viscous in the LC phase, and this suggests restriction of motion of the mesogens. In the sample with a long spacer (**PA6AB3** and **PA11AB1**), perturbation in the form of the *trans-cis* isomerization of the azobenzenes was propagated through the LC phase and orientational relaxation of the mesogens occurred, then the LC-I phase transition took place almost completely. In **PA2AB6** and **PA3AB6**, the relaxation process would be difficult to occur because the motion of the mesogens was restricted, and the photochemical phase transition was induced only locally.

The photochemical phase transition behavior of copolymers with azobenzenes and phenyl benzoate or cyanobiphenyl mesogens in the side chain has been reported previously.[1-3] It is worth comparing the photochemical phase transition behavior between those copolymers and the present polymer azobenzene LCs. The photochemical phase transition was induced more effectively in the copolymers with three methylene units in the spacer than in those with six or eleven methylene units because the LC phase in the former was unstable. These results are different from the results obtained in the present study where the photochemical phase transition did not occur completely in the polymer with a spacer of three methylene units (**PA3AB6**). It was reported that polymer LCs with a short spacer but a long alkoxyl end-group of the rigid core showed a much stabilized LC phases due to the long alkoxyl tail.[6] The different behavior in the photochemical phase transition, therefore, may be interpreted as the long alkoxyl tail plays a crucial role in the phenomena. In **PA3AB6**, owing to the long alkoxyl end-group, the phase structure could be stabilized, which may result in less effective phase transition on photoirradiation.

CONCLUSION

Photochemical phase transition behavior of the polymer LCs with azobenzene moiety at different position in the side chain was explored by transmission-mode analysis and reflection-mode analysis. The photochemical LC-I phase transition was induced in 100 ~ 200 μs on laser pulse irradiation . In the sample with an azobenzene located apart from the main chain of the polymer by spacers, the LC-I phase transition took place almost completely with a single pulse of the laser. In the sample with the azobenzene moiety in the vicinity of the main chain, however, the photochemical phase transition was induced only locally. These phenomena are interpreted in terms of the mobility of the azobenzene moiety and the stability of the LC phase. In the polymer LCs with a short spacer but a long alkoxyl end-group, the relaxation process would be difficult to occur because the motion of the mesogens was restricted by the polymer main chain and the LC phase was stabilized by the alkoxyl end-group. Thus the photochemical phase transition was induced only locally in these polymers.

References and Notes

(1) Ikeda, T.; Horiuchi, S.; Karanjit, D.B.; Kurihara, S.; Tazuke, S. *Macromolecules* **1990**, *23*, 36.

(2) Ikeda, T.; Horiuchi, S.; Karanjit, D.B.; Kurihara, S.; Tazuke, S. *Macromolecules* **1990**, *23*, 42.

(3) Ikeda, T.; Kurihara, S.; Karanjit, D.B.; Tazuke, S. *Macromolecules* **1990**, *23*, 3938.

(4) Kanazawa, A.; Hirano, S.; Shishido, A.; Hasegawa, M.; Tsutsumi, O.; Shiono, T.; Ikeda, T.; Nagase, Y.; Akiyama, E.; Takamura, Y. *Liq. Cryst.* **1997**, *23*, 293.

(5) Kanazawa, A.; Shishido, A.; Hasegawa, M.; Tsutsumi, O.; Shiono, T.; Ikeda, T.; Nagase, Y.; Akiyama, E.; Takamura, Y. *Mol. Cryst. Liq. Cryst.* **1997**, *300*, 201.

(6) Angeloni, A.S.; Caretti, D.; Carlini, C.; Chiellini, G.; Galli, G.; Altomare, A.; Solaro, R. *Liq. Cryst.* **1989**, *4*, 513.

(7) Shishido, A.; Tsutsumi, O.; Kanazawa, A.; Shiono, T.; Ikeda, T.; Tamai, N. *J. Phys. Chem. B* **1997**, *101*, 2806.

(8) Shishido, A.; Tsutsumi, O.; Kanazawa, A.; Shiono, T.; Ikeda, T.; Tamai, N. *J. Am. Chem. Soc.* **1997**, *119*, 7791.

(9) Finkelmann, H.; Ringsdorf, H.; Wendorff, J. *Makromol. Chem.* **1978**, *179*, 273.

Chapter 4

Acceleration of Thermal Recovery of Liquid-Crystalline Phase with Various Donor-Acceptor Azobenzenes

INTRODUCTION

In the preceding chapters, it was demonstrated that the photochemical N-to-I phase transition took place in 200 μs in low-molecular-weight and polymer NLCs with azobenzene moieties as both mesogens and photosensitive chromophores in each molecule. When photoirradiation was ceased, the initial N phase was restored thermally after some time. Above 100 °C, the N phase recovered in several seconds in both low-molecular-weight and polymer azobenzene LCs. However, this response is about 10^4 times slower than that of the photochemical N-I phase transition. One, therefore, has to accelerate the thermal I-N phase transition to utilize the photoresponsive LC systems for all-optical switching materials.

The thermal I-N phase transition is composed of two processes: the *cis-trans* thermal back-isomerization of the azobenzene moieties and the reorientation of the mesogenic *trans*-azobenzenes. As described in Chapter 2, the rate-determining step of the thermal I-N phase transition is

the *cis-trans* back-isomerization. Thus, one must accelerate the *cis-trans* isomerization of the azobenzene to cause the I-N phase transition more quickly. One approach for acceleration of the thermal isomerization process is the use of donor-acceptor azobenzenes, which contain both an electron donor and an acceptor at both ends of the azobenzene moiety. It is well known that the thermal *cis-trans* isomerization of the donor-acceptor azobenzenes is faster than that of the non-donor-acceptor azobenzene derivatives.[1] When the donor-acceptor azobenzenes are used as a photosensitive chromophore, the thermal recovery of the N phase may occur more quickly. In this chapter, the author investigated the photochemical N-I and the thermal I-N phase transition behavior of low-molecular-weight LCs with the donor-acceptor azobenzenes and discussed the effects of the structure of the donor and the acceptor on the thermal I-N phase transition.

EXPERIMENTAL

1. Materials.

Structures of the donor-acceptor azobenzenes used in this chapter are shown in Figure 4-1. 1-Octyl-4-[4-(4-nitrophenyl-azo)phenyl]piperazine (**Azo4-1**) and 1-octyl-4-[4-(4-cyanophenyl-azo)phenyl]piperazine (**Azo4-2**) were prepared through modification of the method reported previously (Scheme 4-1).[2] 4-Nitro-4'-octyloxyazobenzene (**Azo4-3**) was synthesized as reported previously.[3] 4-Cyano-4'-(8-bromooctyloxy)azobenzene (**Azo4-4**) was kindly given by Professor Lee-Soon Park (Kyungpook National University, Korea). 4-

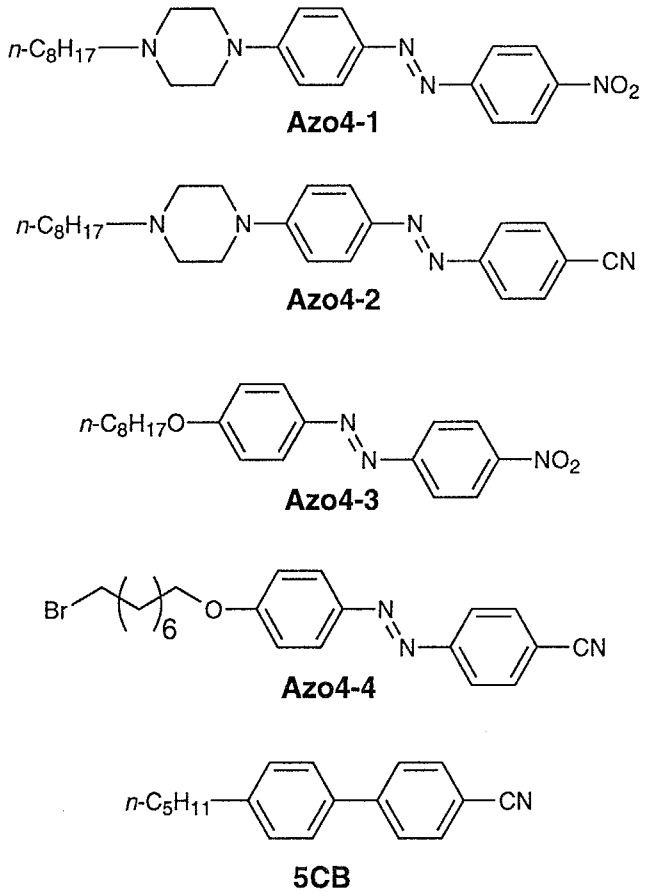

Figure 4-1. Structures of the donor-acceptor azobenzenes and host LC used in this chapter and their abbreviations.

Schem 4-1. Synthetic route for donor-acceptor azobenzene LCs

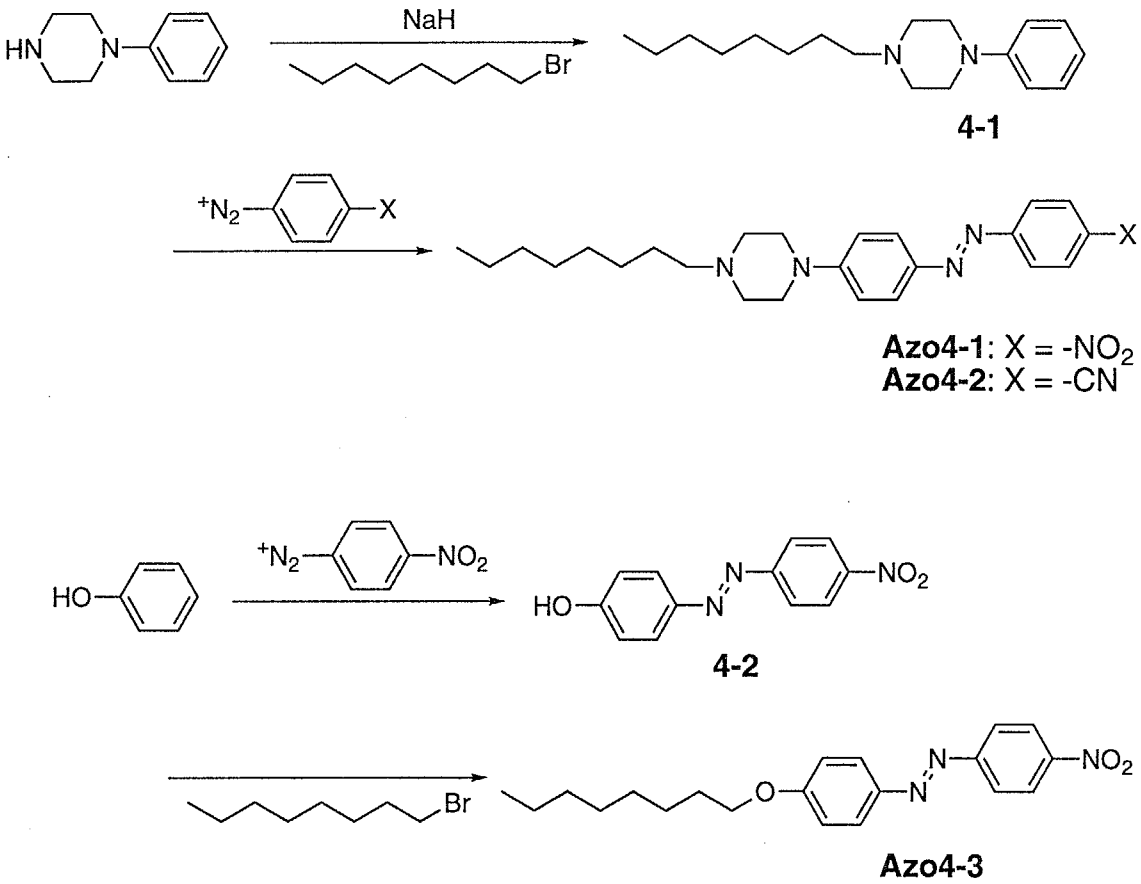

Cyano-4'-pentylbiphenyl (**5CB**) was purchased from Merck Co. and was used without further purification.

General Method of Preparation. THF was distilled over calcium hydride. Unless otherwise noted, all materials and other solvents were commercially available and used as received. The products were characterized by ^{1}H-NMR spectroscopy as described in Chapter 2.

1-Octyl-4-phenylpiperazine (4-1). Under a nitrogen atmosphere, a solution of 1-phenylpiperazine (3.0 g, 18 mmol) in THF (5 mL) was added dropwise to a suspension of sodium hydride (in oil, 60 wt%; 0.77 g, 20 mmol) in THF (10 mL) at room temperature. After the mixture was stirred for 1 h, a solution of 1-bromooctane (3.5 g, 18 mmol) in THF (5 mL) was added dropwise at 0 °C. After 36 h of stirring at room temperature, the solution was poured into saturated aqueous sodium hydrogen carbonate, and the product was extracted with ether. The organic layer was dried with sodium sulfate and evaporated. The crude product was purified by column chromatography on silica gel (ethyl acetate) to give yellow oil. The yellow oil was added into 50 mL of hydrochloric acid (1 M), and then white precipitate formed. The precipitate was collected and washed with *n*-hexane. The white solid was added into saturated aqueous solution of sodium hydrogen carbonate and extracted with ether. The ether was evaporated and the residue was dried under vacuum to yield 3.2 g (67 %) of **4-1**. ^{1}H-NMR ($CDCl_3$): δ 0.88 (t, J = 7 Hz; 3H; CH_3), 1.3 (m; 12H; CH_2), 2.4 (t, J = 7 Hz; 2H; NCH_2), 2.6 (t, J = 5 Hz; 4H; CH_2 in piperazine), 3.2 (t, J = 5 Hz; 4H; CH_2 in piperazine), 6.8 - 6.9 (m; 3H; *CH* in aromatic), 7.2 (d, J = 16 Hz; 2H; *CH* in aromatic).

1-Octyl-4-[4-(4-nitrophenylazo)phenyl]piperazine (Azo4-1). A stirred suspension of 4-nitroaniline (1.7 g, 11 mmol) in 44 mL of aqueous fluoboric acid (4.8 %) was cooled at 0 ~ 5 °C and treated dropwise with 0.76 g of sodium nitrite (11 mmol) dissolved in water (10 mL). After 2 h of stirring, a solution of **4-1** (3.0 g, 11 mmol) in acetic acid (10 mL) was added dropwise at 0 °C, and red precipitate began to form. After 30-min stirring, 1.6 g of sodium acetate (20 mmol) was added. The reaction mixture was stirred for 2 h at room temperature, and then the solid produced was collected. The solid was washed with water and dried under vacuum. The product was recrystallized from methanol to produce 1.3 g (28 %) of red crystal (**Azo4-1**). mp: 126 °C. ^{1}H-NMR ($CDCl_3$): δ 0.89 (t, J = 7 Hz; 3H; CH_3), 1.2 - 1.6 (m; 12H; CH_2), 2.4 (t, J = 8 Hz; 2H; NCH_2), 2.6 (t, J = 5 Hz; 4H; CH_2 in piperazine), 3.4 (t, J = 5 Hz; 4H; CH_2 in piperazine), 6.9 (d, J = 7 Hz; 2 H; *CH* in aromatic), 7.8 - 7.9 (m; 4H; *CH* in aromatic), 8.6 (d, J = 7 Hz; 2H; *CH* in aromatic).

1-Octyl-4-[(4-cyanophenylazo)phenyl]piperazine (Azo4-2). The above procedure was repeated using 1.4 g of *p*-aminobenzonitrile (12 mmol), 3.0 g of **4-1** (11 mmol), and 0.76 g of sodium nitrite (11 mmol). The product was recrystallized from methanol and dried under vacuum. The yield was 1.7 g (red crystal). mp: 106 °C. ^{1}H-NMR ($CDCl_3$): δ 0.89 (t, J = 7 Hz; 3H; CH_3), 1.2 - 1.6 (m; 12H; CH_2), 2.4 (t, J = 8 Hz; 2H; NCH_2), 2.6 (t, J = 5 Hz; 4H; CH_2 in piperazine), 3.4 (t, J = 5 Hz; 4H; CH_2 in piperazine), 7.0 (d, J = 9 Hz; 2H; *CH* in aromatic), 7.8 (d, J = 9 Hz; 2H; *CH* in aromatic), 7.9 - 8.0 (m; 2H; *CH* in aromatic).

4-Hydroxy-4-nitroazobenzene (4-2). A stirred solution of 4-nitroaniline (5.0 g, 36 mmol) in 19 wt% aqueous fluoboric acid (33 mL) was cooled at 0 ~ 5 °C and treated dropwise with 2.5 g of sodium nitrite

(36 mmol) dissolved in water (20 mL). After 2 h of stirring, a solution of phenol (3.4 g, 36 mmol) and sodium hydroxide (4.3 g, 108 mmol) in water (50 mL) was added dropwise at 0 °C, and red precipitate formed. After 90-min stirring at room temperature, the solution was neutralized with acetic acid, and then the solution was filtered. The collected brown solid was washed with water and dried under vacuum. The crude product was purified by recrystallization from chloroform to produce 4.8 g (56 %) of red crystal (**4-2**). ^{1}H-NMR ($CDCl_3$): δ 5.3 (s; 1H; *OH*), 7.0 (d, J = 9 Hz; 2H; *CH* in aromatic), 7.9 (d, J = 9 Hz; 2H; *CH* in aromatic), 8.0 (d, J = 9 Hz; 2H; *CH* in aromatic), 8.4 (d, J = 9 Hz; 2H; *CH* in aromatic)

4-Octyloxy-4-nitroazobenzene (Azo4-3). A solution of **4-2** (2.0 g, 8.2 mmol), 1-bromooctane (2.0 g, 10 mmol), and sodium hydroxide (0.40 g, 10 mmol) in DMF (50 mL) was stirred at 120 °C for 72 h. After the reaction mixture was cooled to room temperature, 500 mL of water was added to the mixture. The precipitate was collected and recrystallized from methanol to yield 1.0 g (34 %) of brown crystal (**Azo4-3**). mp: 84 °C. ^{1}H-NMR ($CDCl_3$): δ 0.9 (t, J = 7 Hz; 3H; CH_3), 1.3 - 1.5 (m; 10H; CH_2), 1.8 (m; 2H; CH_2), 4.1 (t, J = 7 Hz; 2H; OCH_2), 7.0 (d, J = 9 Hz; 2 H; *CH* in aromatic), 7.9 (d, J = 9 Hz; 2H; *CH* in aromatic), 8.0 (d, J = 9 Hz; 2H; *CH* in aromatic), 8.4 (d, J = 9 Hz; 2H; *CH* in aromatic).

2. Characterization of LCs.

LC behavior was examined on a polarizing microscope and thermotropic properties of the LCs were determined with DSC as described in Chapter 2. The thermodynamic properties of the LCs are given in Table 4-1.

3. Photochemical Phase Transition.

The photochemical phase transition behavior of the LCs was investigated by means of the apparatus described in Chapter 2. Sample films were prepared in the same manner as described in the preceding chapter. The LC films were irradiated at 405 nm and 436 nm (40 mW/cm^2) from a 500 W high-pressure mercury lamp through glass filters (Toshiba, V-40 + L-39 + IRA-25), and the intensity of the probe light transmitted through a pair of crossed polarizers, with the sample film between them, was measured with a photodiode.

In time-resolved measurements, the sample was irradiated with a single pulse of a Nd:YAG laser (the second harmonic (532 nm) or the third harmonic (355 nm); 40 mJ/cm^2; 10 ns, fwhm), and transmittance of the probe light through crossed polarizers was measured with a photomultiplier as a function of time.

4. Thermal *cis-trans* Isomerization Behavior of Azobenzenes.

To determine the lifetime of the *cis* isomers, the change in absorbance at absorption maximum of the *trans*-azobenzenes was observed in solutions. DMF and dimethyl sulfoxide (DMSO) (spectroscopic grade) were used as the solvent. For slower decays, the dilute solutions (~ 10^{-5} M) of the azobenzenes were placed in a 1-cm cell and irradiated at 405 nm and 436 nm (40 mW/cm^2) for 5 min, then the cell was placed in an absorption spectrometer. The change in absorbance at absorption maximum was measured at room temperature (23 °C) as a function of time.

Fast decay times (< 1 s) were determined by transient absorption spectroscopy with a spectroscopic multichannel analyzer (SMA; Princeton, IDPDA-512G/B) as a detector (Figure 4-2). The samples were excited

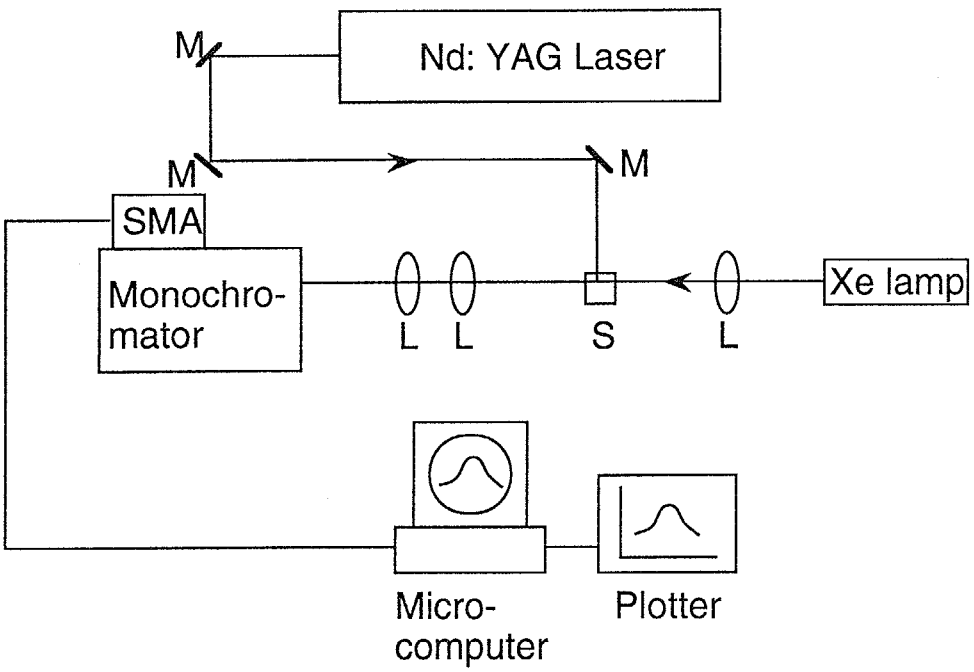

Figure 4-2. Schematic diagram for the time-resolved measurement of isomerization behavior of donor-acceptor azobenzenes: L, lens; M, mirror; S, sample.

with a laser pulse at 532 nm, and the analyzing light from a Xe flash-lamp was irradiated to the sample cell perpendicular to the direction of the laser pulse. The analyzing light passed through the sample solutions was collimated on a Jobin-Ybon HR-320 monochromator. Intensity of the analyzing light through the sample solution was measured with the SMA (gate width: 800 ns) synchronized with the analyzing light by a delay generator (Princeton, DG-535).

RESULTS AND DISCUSSION

1. Characterization of Donor-Acceptor Azobenzene LCs.

Figure 4-3 shows the absorption spectra of the azobenzene derivatives in DMSO solution. *trans*-Azobenzenes exhibit their absorption maximum at around 350 ~ 500 nm due to a π-π^* transition. The absorption maximum shifted toward longer wavelength region as the strength of the donor and the acceptor increased. This is owing to electronic effects of the donor and acceptor. In general, substituents with increasing electron-donating and electron-accepting properties cause a red shift in the absorption spectra, which is ascribed to the depression of energy of the excited state due to the intramolecular charge transfer.[4] As shown in Figure 4-3, irradiation with the laser pulse at 532 nm or 355 nm induced *trans-cis* photoisomerization of the azobenzene derivatives. When the irradiated solutions were kept in the dark, the *cis-trans* back-isomerization took place thermally.

The *trans* form of all the azobenzene derivatives used in this chapter showed the LC phase. Phase structures and phase transition temperatures are summarized in Table 4-1. **Azo4-3** and **Azo4-4** were aligned in the

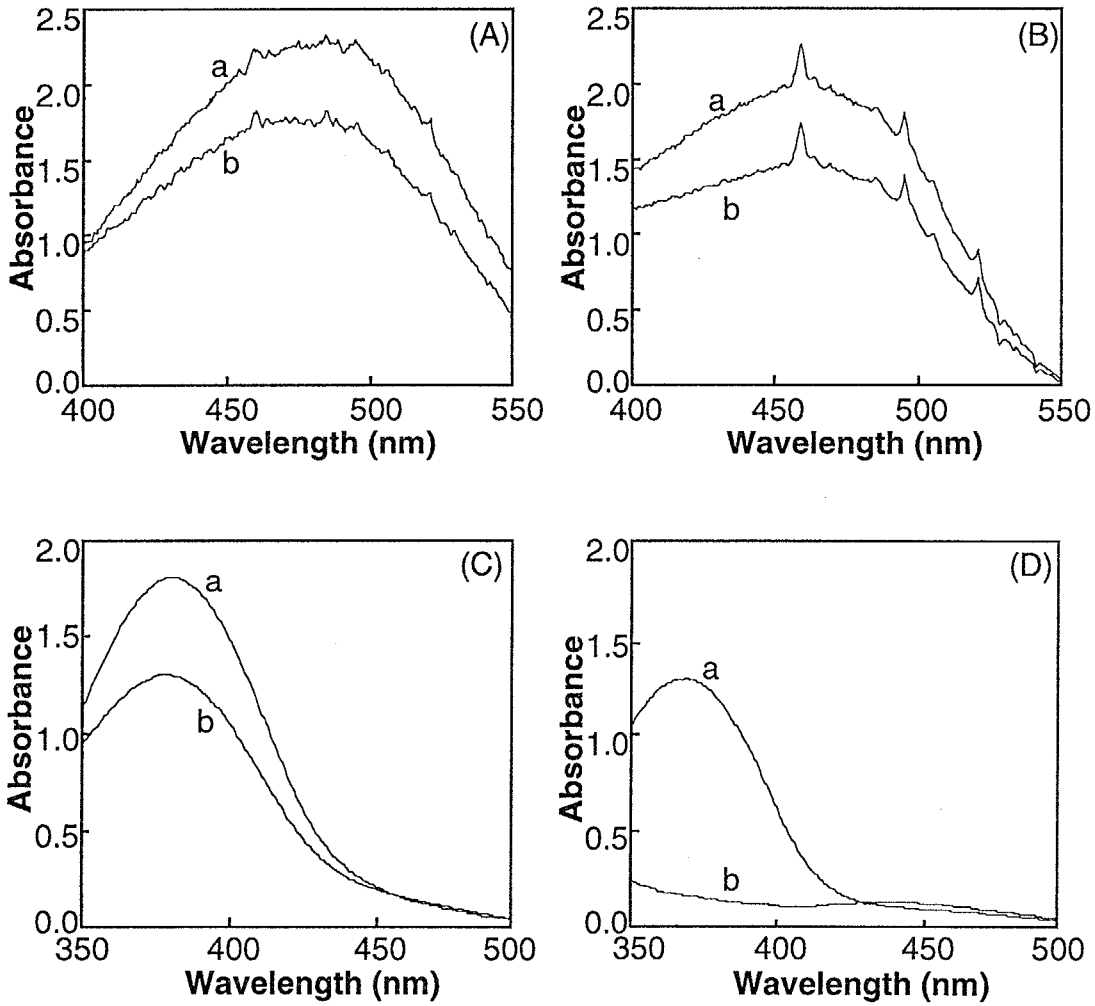

Figure 4-3. Absorption spectra of the donor-acceptor azobenzenes in DMSO solution at room temperature before irradiation (a) and after irradiation (b): (A), **Azo4-1** (9.6 X 10^{-5} M); (B), **Azo4-2** (9.2 X 10^{-5} M); (C), **Azo4-3** (8.2 X 10^{-5} M) ; (D), **Azo4-4** (4.8 X 10^{-5} M). (A) and (B) were measured with SMA before and immediately after irradiation with the laser pulse at 532 nm (10 ns fwhm; 25 mJ/cm^2).

homogeneous manner in the LC phase. On the other hand, **Azo4-1** and **Azo4-2** were aligned in the homeotropic manner on the glass substrate in the LC phase and they exhibited no birefringence by observation with the polarizing microscope when viewed in the direction normal to the glass substrate. Thus, it was not possible to evaluate the phase transition behavior of **Azo4-1** and **Azo4-2** by observation of change in the transmittance of the probe light. Furthermore, since the phase structures and the phase transition temperatures varied with structures of the donor-acceptor, it was difficult to compare the phase transition behavior of the azobenzene LCs under the same condition. The photochemical phase transition behavior of the LCs, therefore, was examined in the guest-host system to reveal the effect of the donor and the acceptor on the photochemical phase transition behavior. **5CB** was used as a host LC. Structure of **5CB** was also shown in Figure 4-1.

Table 4-1. Thermodynamic Properties of Azobenzene LCs and Azobenzene/**5CB** Mixtures[a]

compound	phase transition temperature of azobenzene LCs,[b] °C	phase transition temperature of azobenzene/**5CB** mixtures,[c,d] °C
Azo4-1	K 126 Sm 213 I	N 38 I
Azo4-2	K 106 Sm 213 N 224 I	N 40 I
Azo4-3	K 84 Sm 95 N 96 I	N 39 I
Azo4-4	K 94 Sm 96 I	N 40 I

[a] Abbreviations: K, crystal; Sm, smectic; N, nematic; I, isotropic.

[b] Determined by DSC.

[c] Determined by polarizing microscopy.

[d] The concentration of azobenzene was 1 mol% in the mixtures.

Figure 4-4 shows phase diagrams of the mixtures of the azobenzenes and **5CB**. When **Azo4-1**, **Azo4-3** and **Azo4-4** were added in **5CB** more than 10 mol%, the azobenzenes separated from **5CB** and one could not mix homogeneously the azobenzenes at the concentration more than 10 mol% with **5CB**. To avoid the phase separation, the author employed 1 mol% as a concentration of the azobenzenes in the mixtures. All the mixtures of the azobenzenes (1 mol%) and **5CB** showed N phase and aligned in the homogeneous manner on the glass substrate coated with PVA. The N-I phase transition temperatures of the mixtures were also listed in Table 4-1.

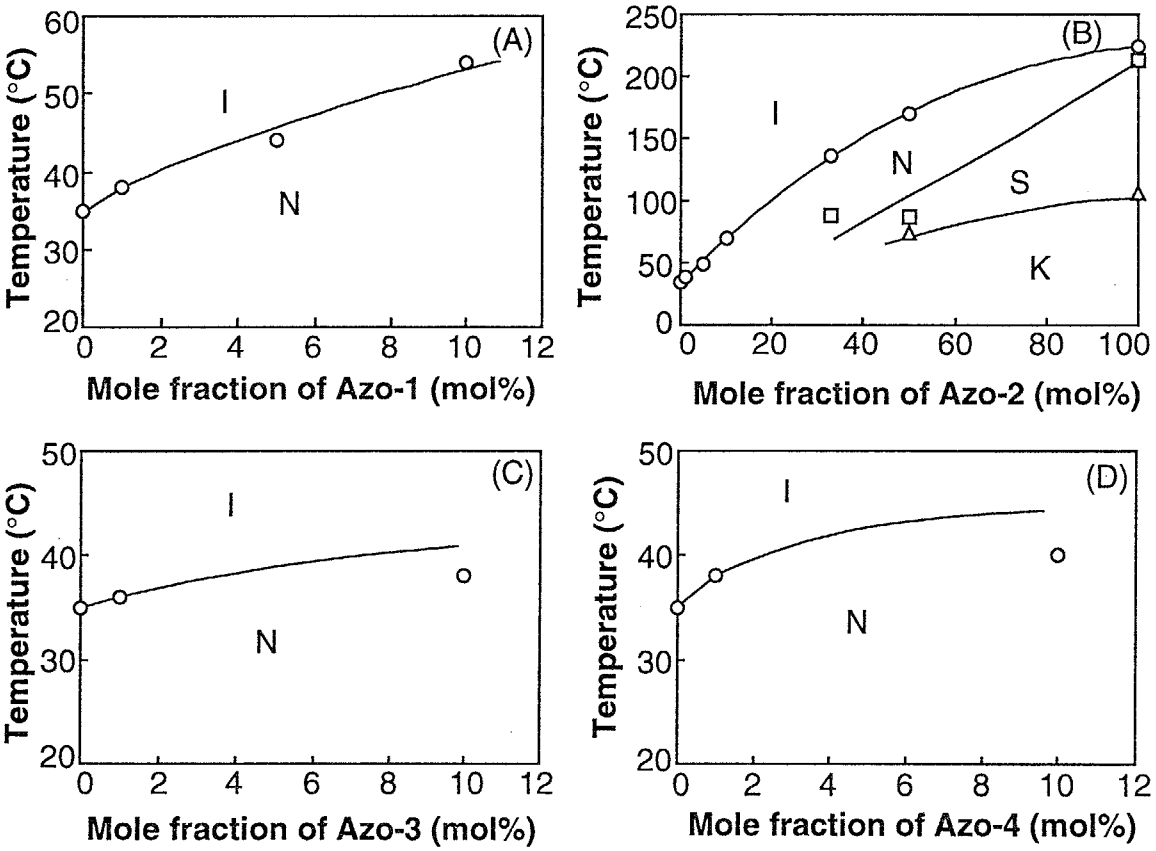

Figure 4-4. Phase diagrams of azobenzene/**5CB** mixtures: (A), **Azo4-1**; (B), **Azo4-2**; (C), **Azo4-3**; (D), **Azo4-4**.

2. Photochemical Phase Transition Behavior of the Mixtures of the Azobenzenes and 5CB.

When the thin films of the mixtures were irradiated at 405 nm and 436 nm in the N phase (37 °C), transmittance of the probe light at 633 nm decayed immediately as shown in Figure 4-5. This was caused by the N-I phase transition due to the photoisomerization of the azobenzenes. As shown in Figure 4-6 (A), the photochemical N-I phase transition was induced in 200 ~ 300 μs in all samples, and this response is similar to that observed in the alkoxyl-type azobenzene LCs (Chapter 2).

In the mixture of **Azo4-1** and **5CB** the transmittance of the probe light recovered instantly when photoirradiation was ceased (Figure 4-5 (A)). The *trans* form of **Azo4-1** restored thermally, followed by reorientation of the mesogens, then the initial N phase was recovered rapidly when the LC sample was kept in the dark. Time-resolved measurement of the thermal I-N phase transition for the mixture of **Azo4-1/5CB** showed that the N phase recovered in 500 ms at 37 °C (Figure 4-6 (B)). As described in Chapter 2, the I-N phase transition of the alkoxyl-type azobenzene LCs occurred in several hours at 35 °C, so that this response is faster by 5 orders of magnitude than that in the alkoxyl-type azobenzene LCs. It is known that the *cis-trans* back-isomerization of the donor-acceptor azobenzenes takes place more effectively than that of the non-donor-acceptor azobenzene, because the dipolar transition state is stabilized by charge-transfer interaction of the donor-acceptor.[5-13] In addition, Asano et al. and Whitten et al. reported that in polar solvents the dipolar transition state was further stabilized and the rate constant for the *cis-trans* isomerization was much larger.[5,11,13] **5CB** is a relatively polar solvent: dielectric constants (ε) of **5CB** are 17 and 6 for parallel and perpendicular direction to the molecular long axis, respectively.[14] Therefore, *cis-trans* isomerization of **Azo4-1** proceeded very fast in **5CB**.

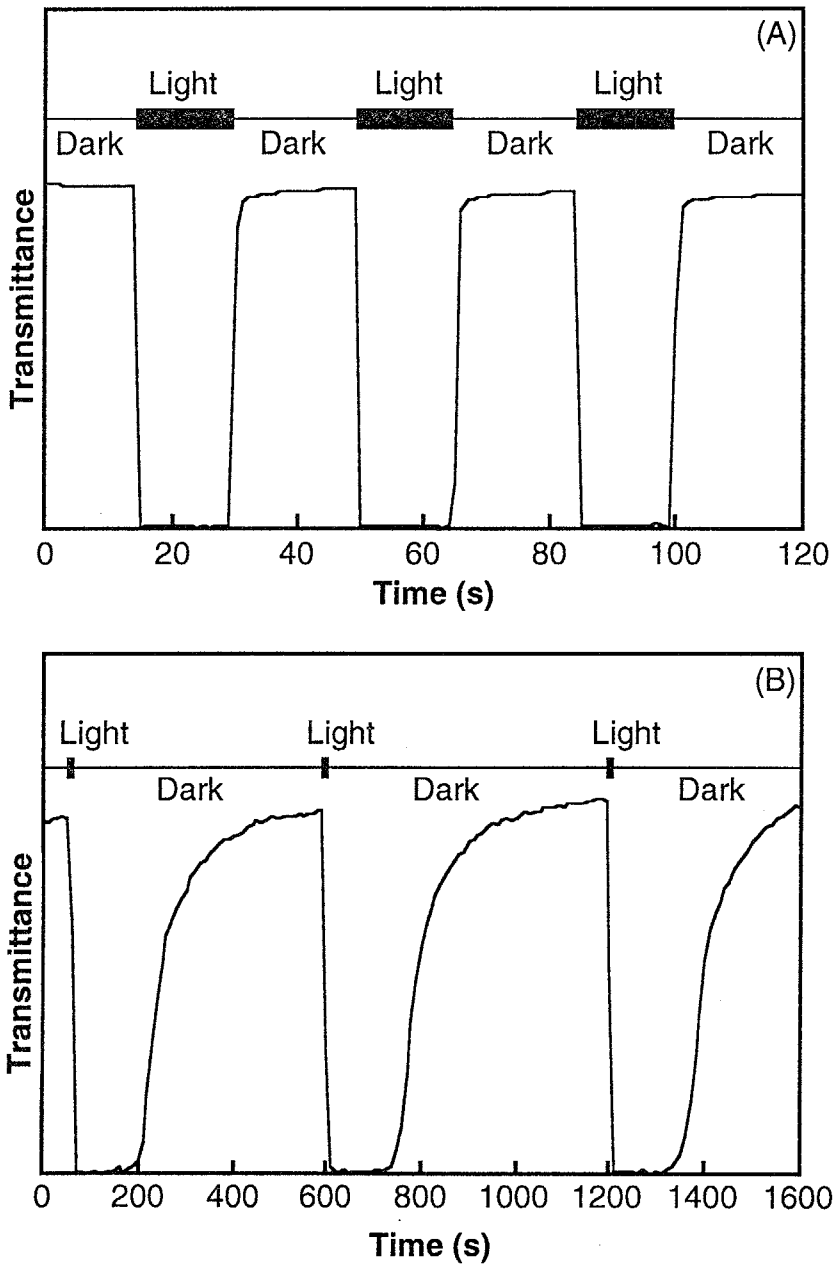

Figure 4-5. Photochemical N-I phase transition and thermal I-N phase transition of azobenzene/**5CB** mixtures: (A), **Azo4-1**; (B), **Azo4-3**.
Photoirradiation at 405 nm and 436 nm was performed at 37 °C.

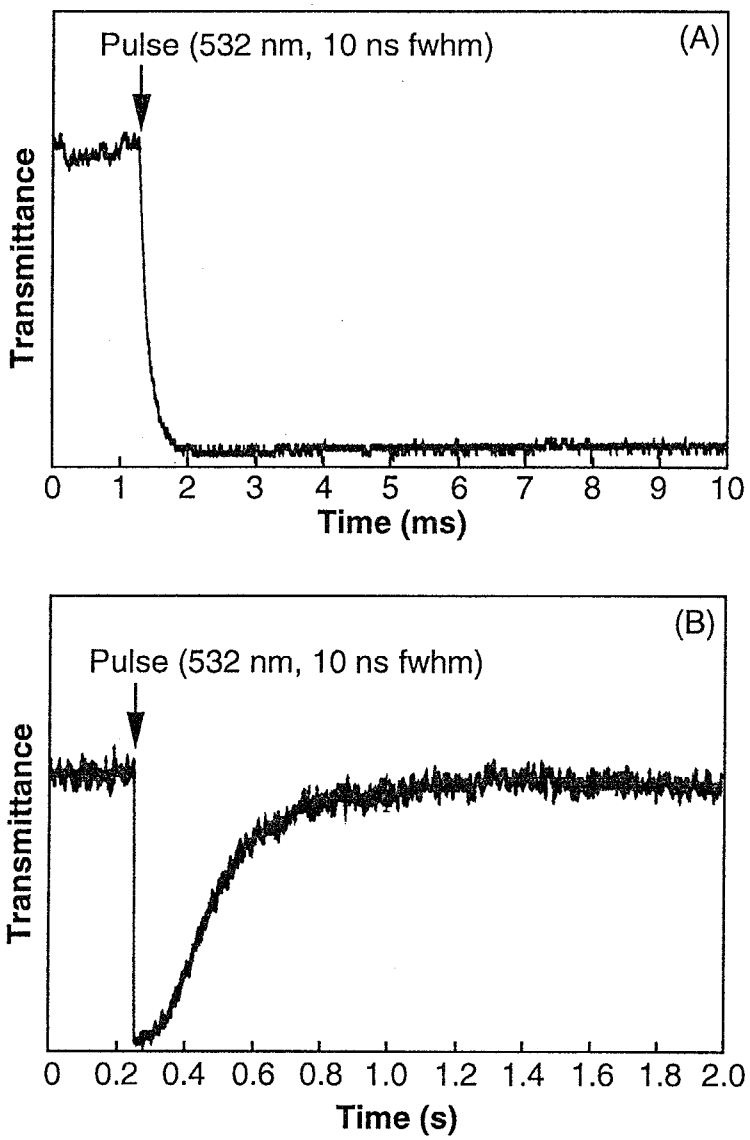

Figure 4-6. Time-resolved measurements of the photochemical N-I and the thermal I-N phase transition of **Azo4-1/5CB**. Irradiation with laser pulse at 532 nm (10 ns fwhm; 30 mJ/cm^2) was performed at 37 °C: (A), photochemical N-I phase transition; (B), thermal I-N phase transition.

As described in Chapter 2, the rate-determining step of the thermal I-N phase transition is the *cis-trans* isomerization process. Since the rate-determining step was accelerated, the thermal recovery of the N phase occurred very rapidly in the mixture of **Azo4-1/5CB**. As shown in Figure 4-5 (B), however, the I-N phase transition in the mixture of **Azo4-3/5CB** needed relatively long time; it took 5 min. These results indicate that the thermal recovery of the N phase in the mixtures is affected strongly by the structure of the donor and the acceptor of the photosensitive azobenzene guest molecules.

Figure 4-7 shows the effect of strength of the donor-acceptor on the thermal I-N phase transition. To discuss the effects of the structure of the donor-acceptor quantitatively, the strength of electron-donating and electron-accepting properties of the substituents was estimated with the absolute value of Hammett's substituent constant ($|\sigma|$).[15] As shown in Figure 4-7, time necessary for the recovery of the N phase varied significantly with structure of the donor-acceptor: the response time of the slowest phase transition (**Azo4-4**) was about 10^5 times longer than that of the fastest phase transition (**Azo4-1**). The rate of the I-N phase transition increased with increasing the $|\sigma|$ value of the donors in both cases where the azobenzenes contained the nitro group or the cyano group as the acceptor. Similarly, it occurred quickly with increasing the $|\sigma|$ value of the acceptors. In other words, time necessary for the thermal I-N phase transition decreased with increasing the strength of the electron-donating and electron-accepting properties of the substituents at 4,4'-positions of the azobenzenes.

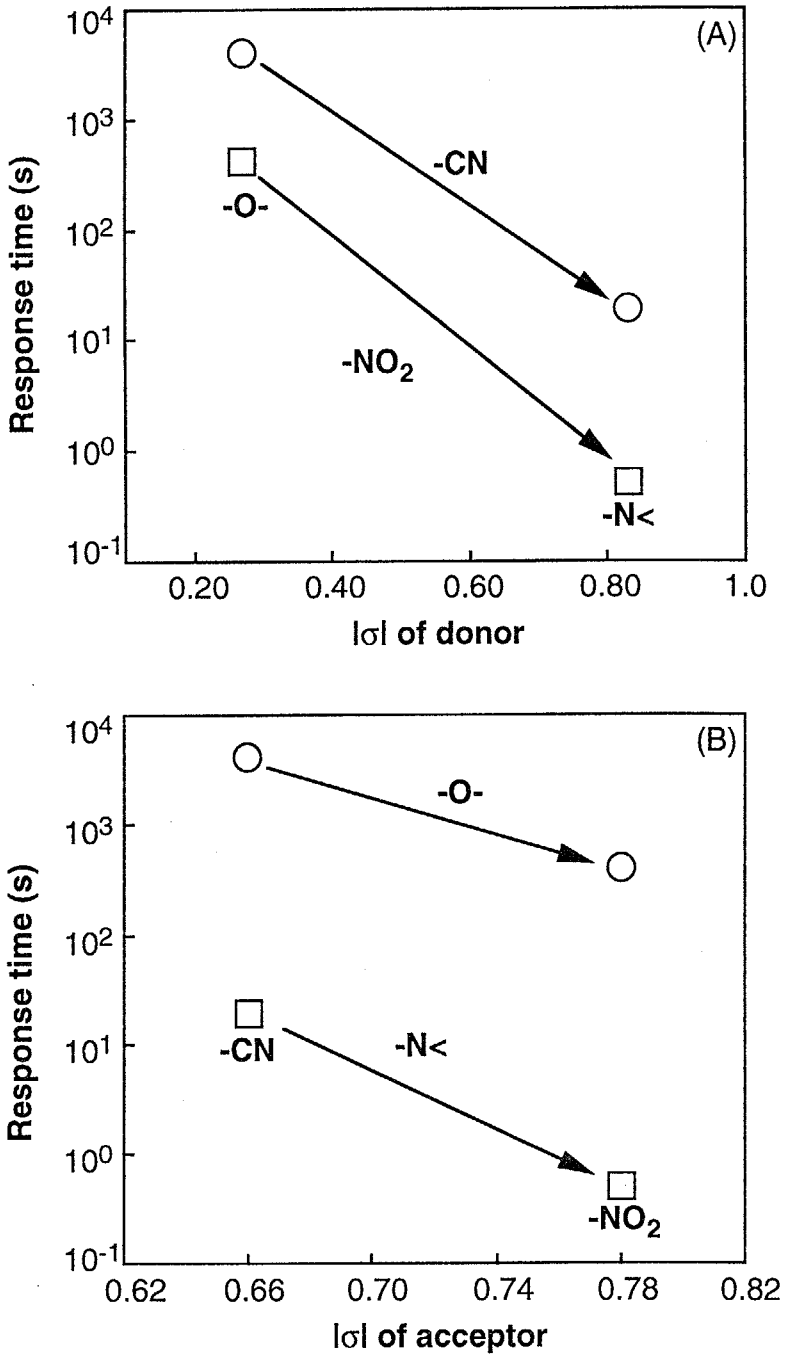

Figure 4-7. Effects of the strength of the donor and the acceptor on the thermal I-N phase transition of azobenzene/**5CB** mixtures at 37 °C: (A), effect of donor; (B), effect of acceptor.

3. Thermal *cis-trans* Isomerization Behavior of the Donor-Acceptor Azobenzenes.

To explore the difference in response time for the recovery of the N phase, the author investigated the thermal *cis-trans* back-isomerization behavior of the azobenzenes in solutions. The thermal isomerization was examined by observation of change in the absorbance at the absorption maximum of the *trans* isomer. Figure 4-8 shows a typical example of the time-resolved absorption spectra of **Azo4-1** at room temperature. The first-order rate constant was determined by fitting the experimental data to eq 2-4. Figure 4-9 shows first-order plots according to eq 2-4 for the *cis-trans* isomerization of the azobenzenes in the solution at room temperature. As shown in Figure 4-9, eq 2-4 gives a good fit to the thermal *cis-trans* isomerization of the donor-acceptor azobenzenes. From the slope of the first-order plots, values of k_{C-t} were obtained and lifetimes of the *cis* isomer were determined as reciprocal of the k_{C-t} value.

The lifetimes of the *cis* isomers of the donor-acceptor azobenzenes were listed in Table 4-2. The lifetimes depended on solvent: the lifetimes in DMSO solution tended to be shorter than those in DMF solution except for **Azo4-4**. Because DMSO (ε = 48.9) is more polar than DMF (ε = 36.7),[5] the *cis* isomer decayed more quickly in the DMSO solution. At present, the reason for the reverse effect of solvent on the isomerization in **Azo4-4** is not clear.

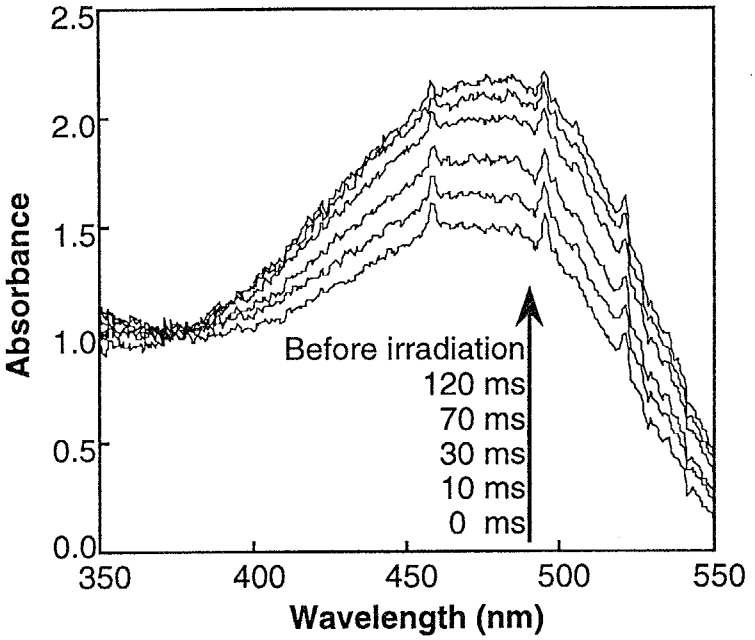

Figure 4-8. Time-resolved absorption spectra of **Azo4-1** in DMF at room temperature (25 °C). Delay times after pulse irradiation were indicated in the figure.

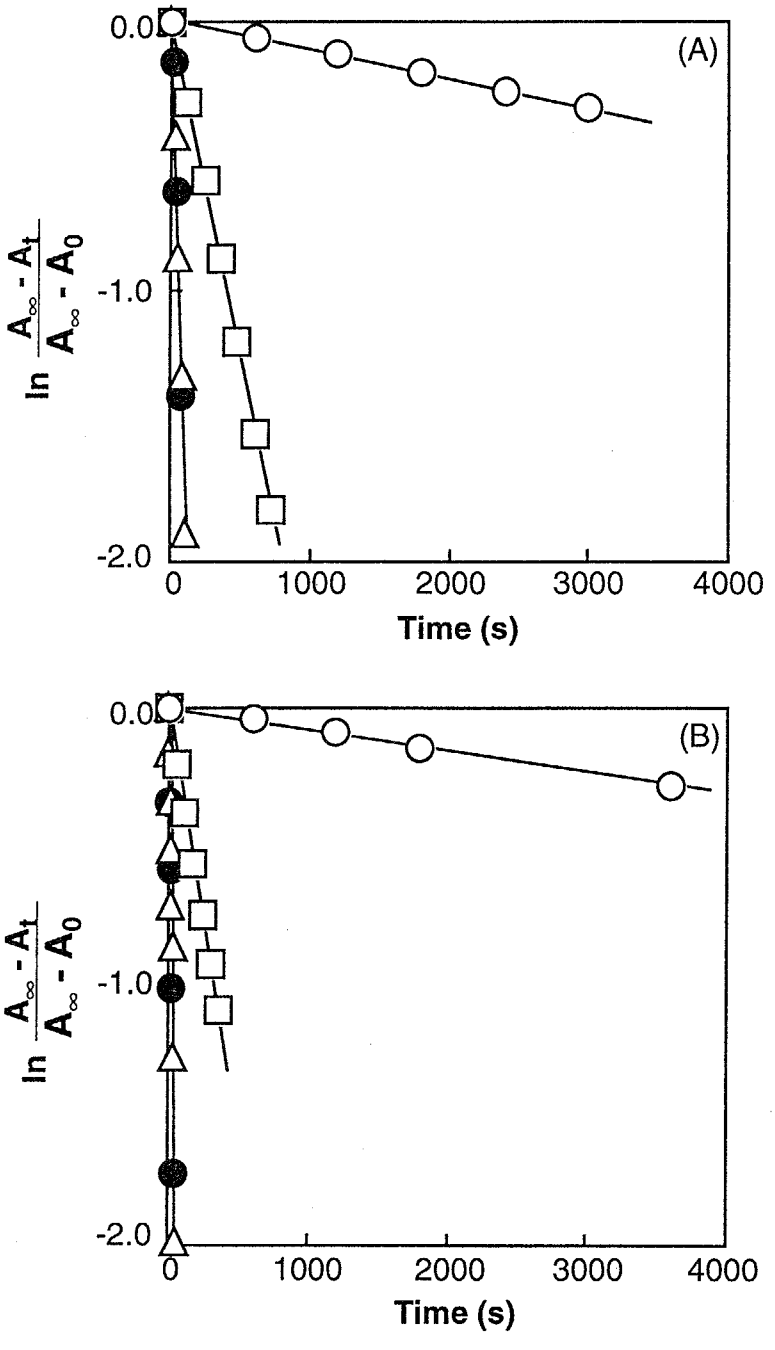

Figure 4-9. First-order plots for the *cis-trans* thermal isomerization of the donor-acceptor azobenzenes at room temperature (25 °C).
(A), in DMF; (B), in DMSO: ●, **Azo4-1**; △, **Azo4-2**; □, **Azo4-3**; ○, **Azo4-4**.

Table 4-2. Lifetime of *cis* Isomer of the Donor-Acceptor Type Azobenzenes in Solution at Room Temperature (25 °C).

			lifetime, s	
compound	donor (|σ|)	acceptor (|σ|)	in DMF	in DMSO
Azo4-1	-N< (0.83)	$-NO_2$ (0.78)	5.1×10^{-2} [a]	1.8×10^{-2} [a]
Azo4-2	-N< (0.83)	-CN (0.66)	6.4×10^{1}	3.0×10^{1}
Azo4-3	-O- (0.27)	$-NO_2$ (0.78)	4.0×10^{2}	3.2×10^{2}
Azo4-4	-O- (0.27)	-CN (0.66)	8.9×10^{3}	1.2×10^{4}

[a] Determined with SMA.

Both in DMF and DMSO solutions, increase in the strength (|σ| value) of the donor and the acceptor tended to reduce the lifetime of the *cis* isomer. For example, the lifetime of **Azo4-4** (with the weakest donor-acceptor pair), 8.9×10^3 s (2.5 h) in DMF solution at room temperature, is approximately 10^5 times as long as that of **Azo4-1** (with the strongest donor-acceptor pair), 51 ms. This tendency agreed closely with the tendency of the response time of the thermal I-N phase transition. Therefore, it can be concluded that the difference in time necessary for the thermal recovery of the N phase is attributable to difference in the rate of the thermal *cis-trans* isomerization process of the azobenzene derivatives.

It is well known that the thermal isomerization of azobenzene derivatives consists of two processes: an inversion mechanism involving flip-flop inversion of one of the nitrogen atoms or a rotation mechanism involving rotation about N=N bond (Scheme 4-2).[11,12] It is now accepted that the thermal isomerization of non-donor-acceptor azobenzenes occurs mainly through the inversion mechanism because the activation energy for the inversion mechanism is lower than that for the rotation mechanism.[5-13]

Scheme 4-2. Mechanism of the thermal *cis-trans* isomerization of donor-acceptor azobenzenes.

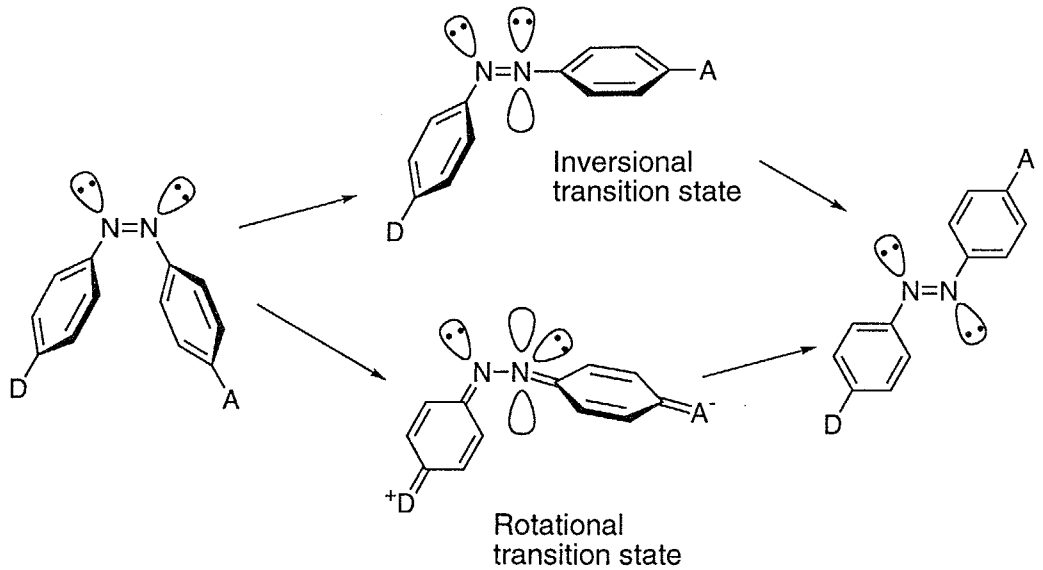

In this mechanism, one of the nitrogen atoms undergoes rehybridization to sp-hybrid state during activation.[11,12] On the other hand, the rotation mechanism proceeds through a dipolar transition state where the N=N π-bond is heterolytically ruptured and rotation around remaining σ-bond takes place.[11,12] In the donor-acceptor azobenzenes, the activation energy for the two mechanisms is close to each other, because intramolecular charge transfer from the donor to the acceptor stabilizes the dipolar transition state of the rotational route. Consequently, the thermal *cis-trans* isomerization of the donor-acceptor azobenzenes involves both the inversion and the rotation processes, and it proceeds quickly.[5-13] Since the charge transfer occurs more effectively in the azobenzene with the stronger donor-acceptor pair, the lifetime of the *cis* isomer becomes shorter.[5,11]

CONCLUSION

The photochemical N-I phase transition and the thermal I-N phase transition of LC were induced rapidly with the donor-acceptor azobenzenes. In these azobenzenes, the thermal *cis-trans* back-isomerization occurred quickly, thus the thermal I-N phase transition was induced quickly in the mixtures of the donor-acceptor azobenzene and **5CB**. Furthermore, it was found that the time required for the I-N phase transition decreased with increasing the strength of the donor and the acceptor. The N phase recovered in 500 ms in a mixture of **Azo4-1** (with nitro group as the acceptor and tertiary amine as the donor) and **5CB** at 37 °C. This response is faster by 5 orders of magnitude than that of alkoxyl-type azobenzene LCs at 35 °C.

References and Notes

(1) Xie, S.; Natansohn, A.; Rochon, P. *Chem. Mater.* **1993**, *5*, 403.

(2) Schilling, M.L.; Katz, H.E. *Chem. Mater.* **1989**, *1*, 668.

(3) Ringsdorf, H.; Schmidt, H.-W. *Makromol. Chem.* **1984**, *185*, 1327.

(4) Ross, D.; Reissner, E. *J. Org. Chem.* **1966**, *31*, 2571.

(5) Wildes, P.D.; Pacifici, J.G.; Irick, G.; Whitten, D.G. *J. Am. Chem. Soc.* **1971**, *93*, 2004.

(6) Asano, T. *J. Am. Chem. Soc.* **1980**, *102*, 1205.

(7) Asano, T.; Okada, T.; Shinkai, S.; Shigematsu, K.; Kusano, Y.; Manabe, O.; *J. Am. Chem. Soc.* **1981**, *103*, 5161.

(8) Asano, T.; Yano, T; Okada, T. *J. Am. Chem. Soc.* **1982**, *104*, 4900.

(9) Schanze, K.S.; Mattox, T.F.; Whitten, D.G. *J. Am. Chem. Soc.* **1982**, *104*, 1733.

(10) Schanze, K.S.; Mattox, T.F.; Whitten, D.G. *J. Org. Chem.* **1983**, *48*, 2808.

(11) Asano, T.; Okada, T. *J. Org. Chem.* **1984**, *49*, 4387.

(12) Asano, T.; Okada, T. *J. Org. Chem.* **1986**, *51*, 4454.

(13) Shin, D.-M.; Whitten, D.G. *J. Am. Chem. Soc.* **1988**, *110*, 5206.

(14) Kelker, H.; Hatz, R. In *Handbook of Liquid Crystals*, Verlag Chemie, Weinheim; **1980**, p. 179.

(15) Pine, S.H. In *Organic Chemistry*, McGraw Hill, New York; **1987**, p. 634.

Chapter 5

Effect of Mole Fraction and Structure of Azobenzenes with Strong Donor-Acceptor Pairs on Photochemical and Thermal Phase Transition Behavior of Polymer Liquid Crystals

INTRODUCTION

In Chapter 4, it was found that the photochemical N-I phase transition and the thermal I-N phase transition of low-molecular-weight LCs were induced rapidly with the donor-acceptor azobenzenes because their thermal *cis-trans* isomerization took place very effectively. Furthermore, it became apparent that the time required for the I-N phase transition decreased with increasing the strength of the donor and the acceptor. The N phase recovered in 500 ms in a mixture of the donor-acceptor azobenzene (with nitro group as the acceptor and tertiary amine as the donor) and the host LC at 37 °C. When the donor-acceptor azobenzenes were added in the host LC with high concentration (more than 10 mol%), however, the azobenzenes separated from the host LC. To avoid the phase separation, a concentration of the azobenzenes has to be low (~ 1mol%) in the mixtures. If one introduces the azobenzene moiety

with a stronger donor-acceptor pair in polymer LCs by copolymerization, one can avoid the phase separation. In this chapter, the author investigated the photochemical N-I phase transition and the thermal I-N phase transition behavior of polymer LCs containing azobenzene moieties with strong donor-acceptor pairs and discussed the effect of mole fraction and structure of the azobenzenes on the phase transition behavior.

EXPERIMENTAL

1. Materials.

Structures of the polymer LCs used in this chapter are shown in Figure 5-1. All polymers contain azobenzene moieties with a tertiary amine as an electron donor and a nitro group as an acceptor. **P5-1** and **P5-2** were synthesized as reported by Robello (Scheme 5-1).[1] **P5-3** which contained a piperazine moiety in the donor unit was prepared through modification of the method reported previously (Scheme 5-2).[2] Cyanobiphenyl monomers (**5-7**) were synthesized and purified as reported previously.[3]

General Method of Preparation. THF, DMF, and dichloromethane were distilled over calcium hydride. Other solvents and materials were commercially available and used as received. The products were characterized by ^{1}H-NMR spectroscopy as described in Chapter 2.

***N*-(6-Hydroxyhexyl)-*N*-methylaniline (5-1).** Under a nitrogen atmosphere, a solution of *N*-methylaniline (15 g, 140 mmol) in THF (20 mL) was added dropwise with vigorous stirring to a suspension of sodium

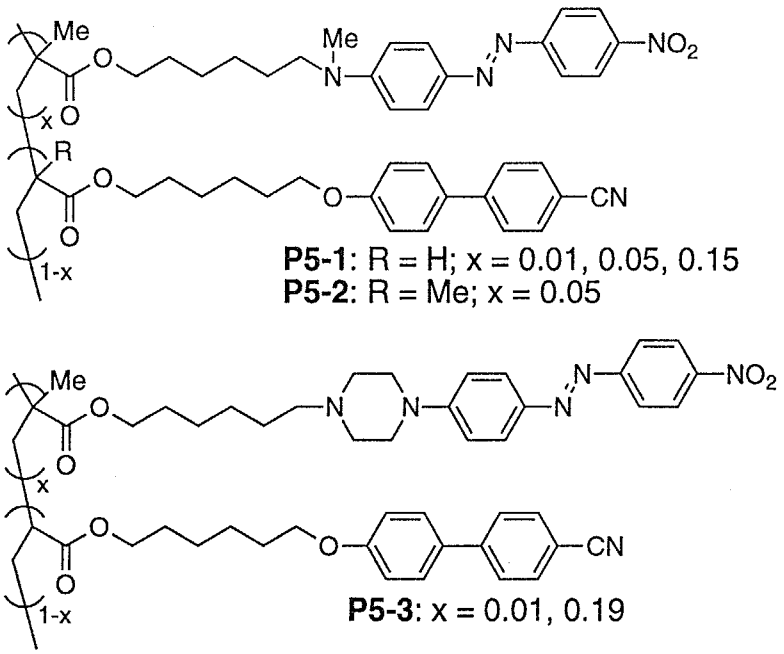

Figure 5-1. Structures of polymer LCs used in this chapter and their abbreviations.

Schem 5-1. Synthetic route for **P5-1**, and **P5-2**

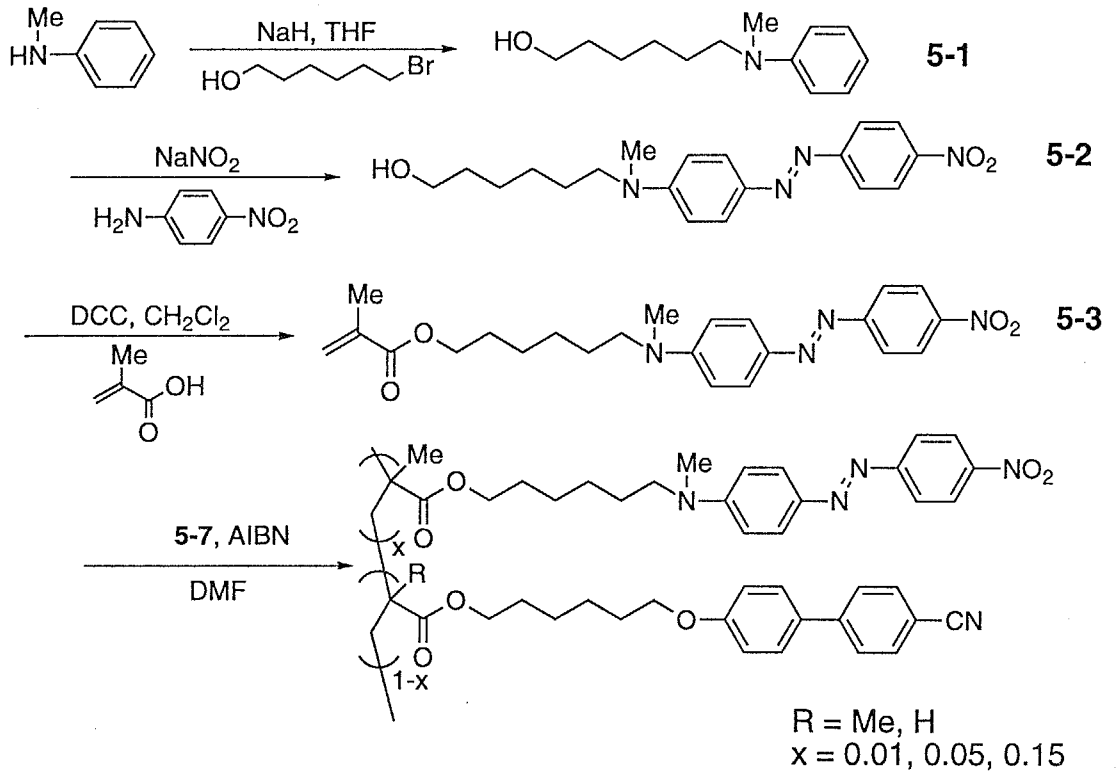

Schem 5-2. Synthetic route for **P5-3**

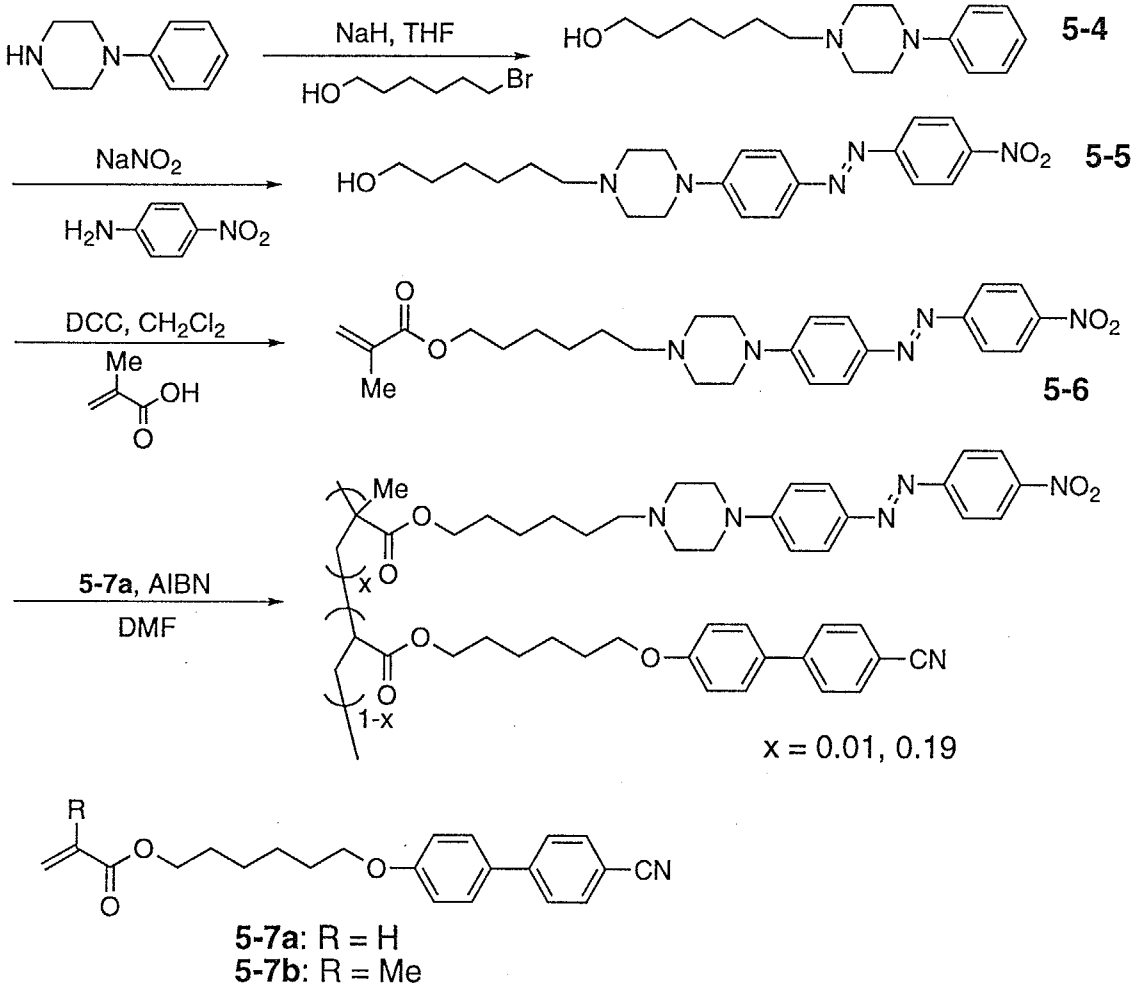

hydride (in oil, 60 %; 5.6 g, 140 mmol) in THF (50 mL) at 0 °C. After the mixture was stirred at room temperature for 3 h, 6-bromo-1-hexanol (25 g, 140 mmol) was added dropwise at 0 °C. After 48 h of stirring at room temperature, the solution was poured into saturated solution of sodium hydrogen carbonate in water, and extracted with ether. The organic layer was dried with sodium sulfate and evaporated to dryness. The crude product was purified by distillation under reduced pressure to obtain **5-1** (11 g) in 36 % yield. ^{1}H-NMR ($CDCl_3$): δ 1.3-1.8 (m; 8H; CH_2), 2.9 (s; 3H; NCH_3), 3.4 (t, J = 8 Hz; 2H; CH_2OH), 3.6 (t, J = 4 Hz; 2H; NCH_2), 6.6-6.7 (m; 2H; *CH* in aromatic), 7.1-7.2 (m; 3H; *CH* in aromatic).

4-Nitro-4'-[*N*-(6-hydroxyhexyl)-*N*-methylamino]azobenzene (5-2). A solution of sodium nitrite (3.3 g, 40 mmol) in 20 mL of water was added dropwise at 0 °C to a mixture of *p*-nitroaniline (6.6 g, 40 mmol) and fluoboric acid (48 wt%; 8.8 g, 48 mmol) in 50 mL of water. After the resulting solution was stirred at 0 °C for 1 h to produce diazonium salt, a mixture of 10 g (48 mmol) of **5-1** and 13 g (96 mmol) of potassium carbonate in water was added dropwise at 0°C. The reaction mixture was stirred at room temperature for 3 h, then a red precipitate appeared. The precipitate was collected and washed with water. The solid was dried and purified by reprecipitation of the chloroform solution into *n*-hexane to obtain **5-2** (2.6 g, 7.2 mmol) in 15 % yield. mp: 120-122 °C. ^{1}H-NMR ($CDCl_3$): δ 1.4-1.6 (m; 8H; CH_2), 3.1 (s; 3H; NCH_3), 3.4 (t, J = 8 Hz; 2H; CH_2OH), 3.6 (t, J = 6 Hz; 2H; NCH_2), 6.7 (d, J = 9 Hz; 2H; *CH* in aromatic), 7.8-7.9 (m; 4H; *CH* in aromatic), 8.3 (d, J = 9 Hz; 2H; *CH* in aromatic). Anal. Calcd for $C_{19}H_{23}N_4O_3$: C, 64.2; H, 6.68; N, 15.8; Found: C,65.1; H, 6.85; N, 16.2.

6-*N*-Methyl-*N*-[4-(4-nitrophenylazo)phenyl]aminohexyl methacrylate (5-3). A solution of dicyclohexylcarbodiimide (DCC; 3.5 g, 17 mmol) in dichloromethane (20 mL) was added dropwise at 0 °C to a mixture of **5-2** (2.0 g, 5.6 mmol), methacrylic acid (1.4 g, 16 mmol) and 4-dimethylaminopyridine (DMAP; 0.68 g, 5.6 mmol) in dichloromethane (20 mL) under an atmosphere of nitrogen. After the reaction mixture was stirred at room temperature for 3 h, the precipitate was filtered off. The filtrate was washed with hydrochloric acid (2 M) and a saturated solution of sodium hydrogen carbonate in water, and evaporated to dryness. The crude product was purified by column chromatography on silica gel (dichloromethane) and recrystallized from ethanol to yield a red crystal of **5-3** (0.52 g, 1.2 mmol) in 21 % yield. mp: 93-95 °C. ^{1}H-NMR ($CDCl_3$): δ 1.4-1.7 (m; 8H; CH_2), 1.9 (s; 3H; CH_2=CH(CH_3)), 3.1 (s; 3H; NCH_3), 3.4 (t, J = 8 Hz; 2H; OCH_2), 4.1 (t, J = 6 Hz; 2H; NCH_2), 5.5 (dd, J = 9, 2 Hz; 1H; *trans*-CH_2=CH(CH_3)), 6.1 (dd, J = 15, 2 Hz; 1H; *cis*-CH_2=CH(CH_3)), 6.7 (d, J = 10 Hz; 2H; *CH* in aromatic), 7.8-7.9 (m; 4H; *CH* in aromatic), 8.3 (d, J = 9 Hz; 2H; *CH* in aromatic). Anal. Calcd for $C_{23}H_{28}N_4O_4$: C, 65.1; H, 6.64; N, 13.2; Found: C,64.9; H, 6.62; N, 13.1.

4-(6-Hydroxyhexyl)-1-phenylpiperazine (5-4). Under a nitrogen atmosphere, a solution of 1-phenylpiperazine (10 g, 62 mmol) in THF (20 mL) was added dropwise with vigorous stirring to a suspension of sodium hydride (in oil, 60 %; 2.4 g, 62 mmol) in THF (50 mL) at 0 °C. After the mixture was stirred at room temperature for 1 h, 6-bromo-1-hexanol (11 g, 62 mmol) was added dropwise at 0 °C. After 18 h of stirring at room temperature, the solution was poured into saturated aqueous sodium hydrogen carbonate, and the product was extracted with ether. The organic layer was dried with sodium sulfate and evaporated to dryness. The crude product was purified by column chromatography on silica gel

(acetone) to give **5-4** (4.1 g) in 26 % yield. ^{1}H-NMR ($CDCl_3$): δ 1.3-1.4 (m; 8H; CH_2), 2.4 (t, J = 7 Hz; 2H; NCH_2), 2.6 (t, J = 5 Hz; 4H; CH_2 in piperazine), 3.2 (t, J = 5 Hz; 4H; CH_2 in piperazine), 3.4 (t, J = 6 Hz; 1H; *OH*), 3.6 (dt, J = 6, 6 Hz; 2H; CH_2OH), 6.8-6.9 (m; 3H; *CH* in aromatic), 7.1-7.3 (m; 2H; *CH* in aromatic).

4-(6-Hydroxyhexyl)-1-[4-(4-nitrophenylazo)phenyl]piperazine (5-5). A solution of sodium nitrite (0.55 g, 7.9 mmol) in 10 mL of water was added dropwise at 0 °C to a mixture of *p*-nitroaniline (1.1 g, 7.9 mmol) and fluoboric acid (48 wt%; 3.0 g, 16 mmol) in 50 mL of water. After the resulting solution was stirred at 0 °C for 1 h to produce diazonium salt, a solution of 2.0 g (7.6 mmol) of **5-4** and 6.0 mL of acetic acid in water (50 mL) was added dropwise at 0°C. After the mixture was stirred at room temperature for 4 h, the solution was neutralized with sodium acetate and stirred for 2 h. The produced precipitate was collected and washed with water. The crude product was dried and purified by column chromatography on silica gel (dichloromethane) and recrystallized from ethanol to give the title compound (0.41 g, 1.0 mmol) in 13 % yield. ^{1}H-NMR ($CDCl_3$): δ 1.3-1.4 (m; 8H; CH_2), 2.4 (t, J = 8 Hz; 2H; NCH_2), 2.6 (t, J = 5 Hz; 4H; CH_2 in piperazine), 3.4 (t, J = 5 Hz; 4H; CH_2 in piperazine), 3.7 (t, J = 6 Hz; 2H; CH_2OH), 6.8 (d, J = 9 Hz; 2H; *CH* in aromatic), 7.9 (d, J = 9 Hz; 2H; *CH* in aromatic), 7.9 (d, J = 9 Hz; 2H; *CH* in aromatic), 8.3 (d, J = 9 Hz; 2H; *CH* in aromatic).

6-[1-(4-(4-Nitrophenylazo)phenyl)piperazino]hexyl methacrylate (5-6). A solution of DCC (640 mg, 2.4 mmol) in dichloromethane (10 mL) was added dropwise at 0 °C to a mixture of **5-5** (490 mg, 1.2 mmol), methacrylic acid (210 mg, 2.4 mmol) and DMAP (150 mg, 1.2 mmol) in dichloromethane (20 mL). After the reaction mixture was stirred at room

temperature for 3 h, the precipitate was filtered off. The filtrate was washed with hydrochloric acid (2 M) and saturated aqueous hydrogen carbonate, and evaporated to dryness. The crude product was purified by column chromatography on silica gel (methanol/chloroform = 1/4) and recrystallized from methanol to obtain **5-6** (290 mg, 610 μmol) in 50 % yield. mp: 129-131 °C. ^{1}H-NMR ($CDCl_3$): δ 1.4-1.6 (m; 8H; CH_2), 1.9 (s; 3H; CH_2=CH(CH_3)), 2.4 (t, J = 7 Hz; 2H; NCH_2), 2.6 (t, J = 4 Hz; 4H; CH_2 in piperazine), 3.4 (t, J = 4 Hz; 4H; CH_2 in piperazine), 4.2 (t, J = 7 Hz; 2H; CH_2OH), 5.6 (s, 1H; *trans*-CH_2=CH(CH_3)), 6.1 (s, 1H; *cis*-CH_2=CH(CH_3)), 6.9 (d, J = 9 Hz; 2H; *CH* in aromatic), 7.9 (d, J = 10 Hz; 2H; *CH* in aromatic), 7.9 (d, J = 9 Hz; 2H; *CH* in aromatic), 8.3 (d, J = 10 Hz; 2H; *CH* in aromatic).

Polymerization. **P5-1**, **P5-2**, and **P5-3** were prepared from the corresponding azobenzene monomers and cyanobiphenyl monomers. Polymerization was conducted in DMF with AIBN as an initiator similarly to **PA6AB2** described in Chapter 2 (see Table 5-1). Each polymer was purified by reprecipitation of a THF solution into a large excess of methanol.

Table 5-1. Conditions for Polymerization[a]

polymer	amount of azobenzene monomer, mg	amount of cyanobiphenyl monomer, g	amount of initiator, mg	amount of solvent, mL	conversion, %
P5-1a	12	1.0	7.2	5	54
P5-1b	40	1.0	7.2	5	46
P5-1c	120	1.0	7.2	5	37
P5-2	58	1.0	7.2	5	60
P5-3a	14	1.0	7.2	5	35
P5-3b	140	1.0	7.2	5	25

[a] Polymerization was carried out at 60 °C for 48 h.

2. Characterization of Polymer LCs.

Molecular weight of the polymers was determined by GPC and thermotropic properties of the LCs were determined with DSC as described in Chapter 2. The thermodynamic properties and molecular weight of the polymer LCs are given in Table 5-2. Mole fraction of the azobenzenes introduced into the copolymers was determined by absorption spectroscopy based on molar extinction coefficient separately obtained from the model azobenzene compounds.

3. Photochemical Phase Transition.

The photochemical phase transition behavior of the LCs was investigated by means of the apparatus described in Chapter 2. Sample films were prepared in the same manner as described in the preceding

chapter. The LC films were placed in a thermostated block and irradiated with steady light at 488 nm from an Ar^+ laser (National Laser Co., H210), and the intensity of the probe light (NEC, GLG5370 He-Ne laser; 633 nm; 1 mW) transmitted through a pair of crossed polarizers, with the sample film between them, was measured with a photodiode.

In time-resolved measurements, the sample was irradiated with a single pulse of a Nd:YAG laser at 532 nm (the second harmonic; 10 ns, fwhm), and transmittance of a probe light through crossed polarizers was measured with a photomultiplier as described in Chapter 2.

4. Isomerization Behavior of Azobenzenes.

Isomerization behavior of the azobenzenes in the LC phase was evaluated by transient absorption spectroscopy as described in Chapter 4. The film of the polymer LCs was excited with a laser pulse at 532 nm under exposure to an analyzing light from a Xe flash-lamp. The analyzing light passed through the LC film was collimated on a monochromator, and its intensity was measured with the SMA (gate width: 800 ns) synchronized with the analyzing light.

RESULTS AND DISCUSSION

1. LC Behavior of Polymers.

It was observed with a polarizing microscope that all polymers used in this chapter showed an LC phase. Phase structures and phase transition temperatures are summarized in Table 5-2. As listed in Table 5-2, **P5-1** and **P5-3** exhibited the N phase, while **P5-2** exhibited the Sm phase.

Annealing of the LC films at temperature just below their Tc gave a well-aligned monodomain of the LC phase.

Table 5-2. Phase Transition Temperature of LCs and Molecular Weight of Polymers Used in This Chapter[a]

polymer	mole fraction of azobenzene	*Mn*	*Mw / Mn*	phase transition temperature, °C
P5-1a	0.01	5,800	1.8	G 34 N 121 I
P5-1b	0.05	15,000	1.3	G 27 N 110 I
P5-1c	0.15	9,300	1.7	G 35 N 104 I
P5-2	0.05	31,000	1.4	G 33 Sm 105 I
P5-3a	0.01	13,000	1.4	G 30 N 116 I
P5-3b	0.19	16,000	1.5	G 38 N 156 I

[a] Abbreviations: G, glass; N, nematic; Sm, smectic; I, isotropic; *Mn*, number-average molecular weight; *Mw*, weight-average molecular weight.

In **P5-1**, temperature range of the N phase becomes narrow with increasing mole fraction of the azobenzene. This suggests that the azobenzene incorporated in **P5-1** destabilizes the phase structure of the N phase. On the other hand, temperature range of the N phase in **P5-3** increased with an increase of the azobenzene content in the copolymer. Thus, it may be considered that the azobenzene in **P5-3** stabilizes the N phase. The *N*-methyl substituent of the azobenzene in **P5-1** occupies some pocket in the side of the molecule and broadens the azobenzene moiety. In general, broadening a molecule by introducing a substituent in a position

along the side of the core structure tends to decrease the thermal stability of the N phase.[4,5] As a result, the N phase in **P5-1** was destabilized with increasing the azobenzene content. In contrast, the azobenzene in **P5-3** which has a 3-ring structure in the core unit stabilized the N phase, because increasing the number of the ring units enhances the N-I phase transition temperature.[5] Therefore, **P5-3** with a larger amount of the azobenzene shows a higher N-I phase transition temperature.

2. Isomerization Behavior of Azobenzenes.

Figure 5-2 shows the time-resolved absorption spectra of the polymer films in the LC phase (at 100 °C). Absorption maximum appeared at around 500 nm in the absorption spectra due to a π-π^* transition of the *trans*-azobenzenes.[6] The absorbance at the π-π^* band was reduced by irradiation with a laser pulse at 532 nm in the LC phase owing to the *trans-cis* photoisomerization of the azobenzene moieties. After pulse irradiation, the absorbance recovered almost completely in 2 ms at 100 °C because of the *cis-trans* thermal back-isomerization. The *trans-cis* photoisomerization and the *cis-trans* thermal isomerization of the azobenzene moieties were observed in both N phase (Figure 5-2 (A) and (C)) and Sm phase (Figure 5-2 (B)).

3. Photochemical Phase Transition Behavior of Polymer NLCs. Effect of Mole Fraction of Azobenzene Moiety.

As shown in Figure 5-3 for **P5-1b**, the transmittance of the probe light decayed immediately upon irradiation at 488 nm in the N phase. As described in Chapter 2, this was caused by the photochemical N-I phase transition of the polymer LC due to the *trans-cis* photoisomerization of the

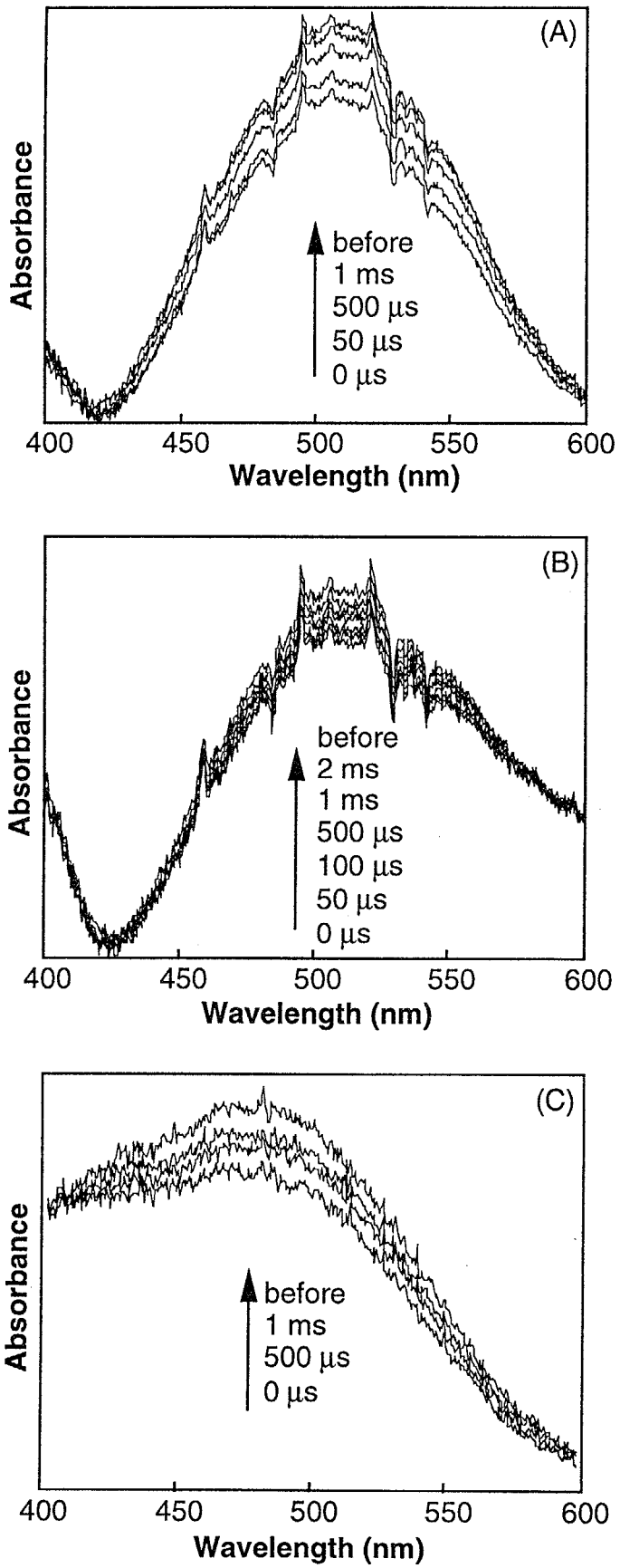

Figure 5-2. Time-resolved absorption spectra of polymer LC films in the LC phase at 100 °C. Delay times after pulse irradiation were indicated in the figure.
(A), **P5-1b** in N phase; (B), **P5-2** in Sm phase; (C), **P5-3b** in N phase.

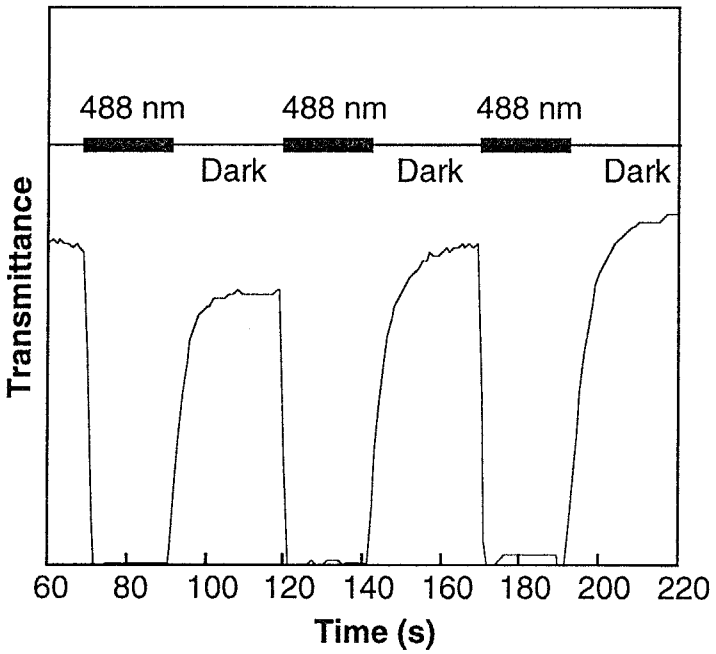

Figure 5-3. Photochemical N-I and thermal I-N phase transition of **P5-1b**.
Photoirradiation at 488 nm (27 mW/cm^2) was performed at 100 °C.

azobenzene moiety. When the irradiated film was kept in the dark, the transmittance recovered completely. Because the *trans*-azobenzene was restored thermally, the initial N phase appeared when photoirradiation was ceased. The photochemical N-I and the thermal I-N phase transition could be induced repeatedly by irradiation at 488 nm.

Figure 5-4 shows the time-resolved measurements of the photochemical N-I phase transition in the polymer LCs of **P5-1** series. The N-I phase transition was induced completely in 300 μs in the polymer with the azobenzene moieties of 15 mol% (**P5-1c**). This response in **P5-1c** is the same as that in the non-donor-acceptor azobenzene LCs described in Chapter 2. In **P5-1b** with the azobenzene of 5 mol%, however, the transmittance of the probe light decreased only to about half of the level in the I phase by laser pulse irradiation. This means that the photochemical phase transition was induced only locally in **P5-1b**. Furthermore, no change in the transmittance of the probe light was observed in **P5-1a** which contained the azobenzene of only 1 mol%, thus the photochemical phase transition could not occur in **P5-1a**. The photochemical N-I phase transition of the **P5-1** series depended strongly on mole fraction of the azobenzene moiety.

A similar photochemical N-I phase transition behavior was also observed in **P5-3b** at 146 °C (Figure 5-5). The photochemical N-I and the thermal I-N phase transition were also caused repeatedly by laser pulse irradiation (Figure 5-6). Furthermore, the same dependence on the mole fraction of the azobenzene moiety was observed in the **P5-3** series: the photochemical phase transition was not observed in **P5-3a**. Thus, it can be concluded that there is a threshold concentration of the azobenzenes in the photochemical phase transition of the polymer LCs. In the polymer LCs with the azobenzene moieties of more than 10 mol%, perturbation in the form of the *trans-cis* photoisomerization of the azobenzenes was

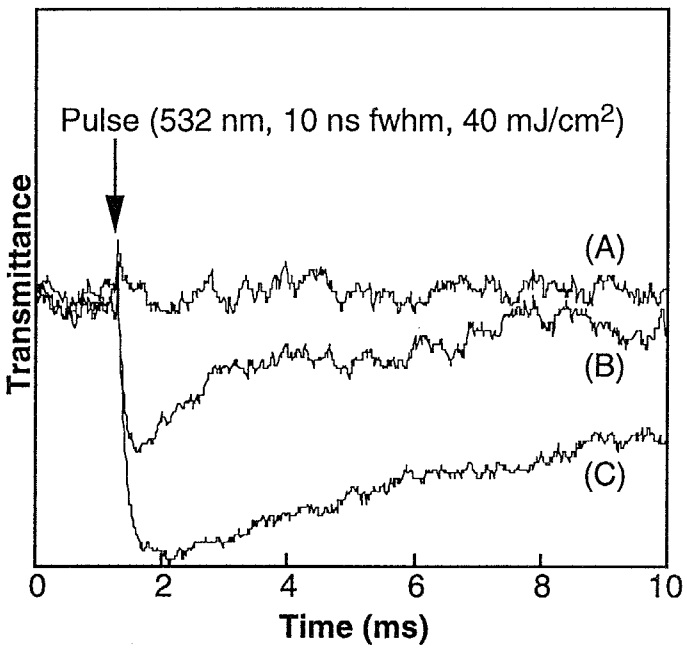

Figure 5-4. Time-resolved measurements of photochemical N-I phase transition of **P5-1**. Laser pulse irradiation at 532 nm (40 mJ/cm^2; 10 ns fwhm) was carried out at 100 °C.
(A), **P5-1a**; (B), **P5-1b**; (C), **P5-1c**.

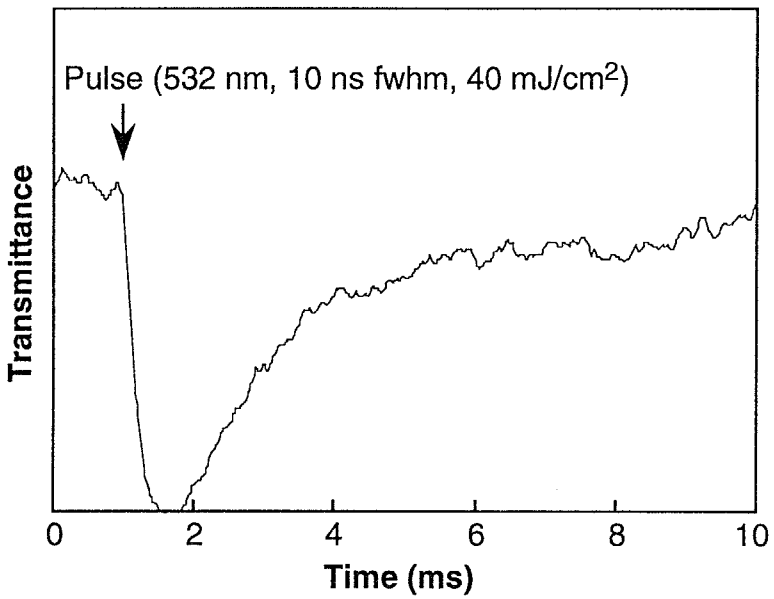

Figure 5-5. Time-resolved measurement of photochemical phase transition of **P5-3b**. Irradiation with a laser pulse at 532 nm (40 mJ/cm^2) was performed at 146 °C (T_{red} = 0.974).

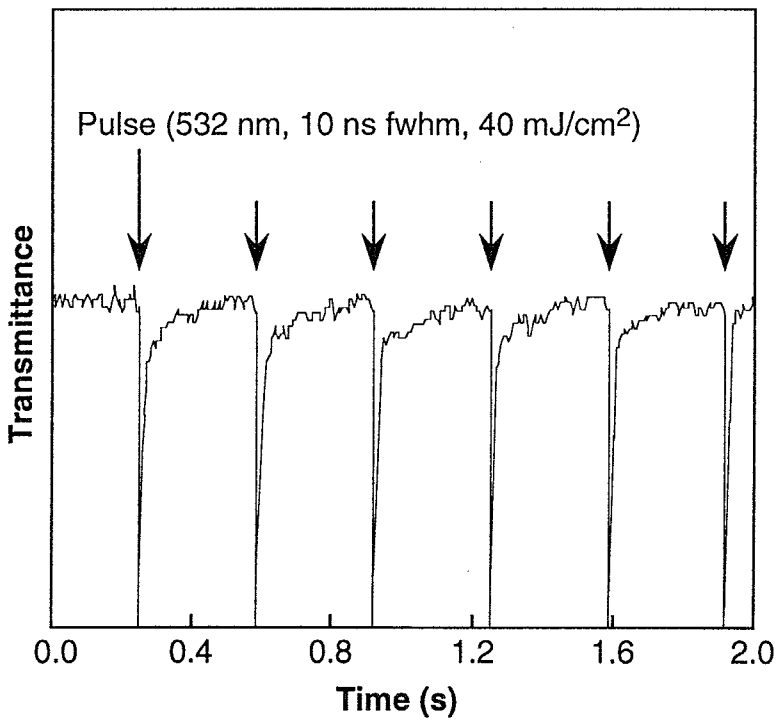

Figure 5-6. Photochemical N-I and thermal I-N phase transition of **P5-3b** induced by repeated irradiation with laser pulses at 532 nm (40 mJ/cm^2) at 134 °C. Repetition rate of the pulse irradiation was 3 Hz.

propagated through the LC phase and orientational relaxation of the mesogens occurred, then the N-I phase transition took place completely. In the polymer LCs with the azobenzene moiety of less than 5 mol%, however, the perturbation of the photoisomerization was not enough to bring about the relaxation of the mesogens completely. The photochemical N-I phase transition, therefore, can not be induced in the polymer LCs with the azobenzene moiety of less than the threshold concentration.

4. Thermal I-N Phase Transition Behavior of the Polymer LCs. Effect of Structure of Azobenzene Moiety.

Figure 5-7 shows the time-resolved measurement of the thermal I-N phase transition in **P5-1c**. It became apparent that the N phase recovered thermally in 50 ms at 95 °C in **P5-1c**. The thermal I-N phase transition in **P5-3b**, however, occurred in 8 ms at 146 °C as shown in Figure 5-5. The thermal recovery of the N phase in the non-donor-acceptor azobenzene LCs took place in 7 ~ 8 s at 145 °C (Chapter 2), because the thermal *cis-trans* isomerization process needed a time scale of several seconds to take place. As described in Chapter 4, however, the thermal *cis-trans* isomerization of the donor-acceptor azobenzenes proceeded very effectively: it occurred almost completely in 2 ms at 100 °C (Figure 5-2). Thus, the response of the I-N phase transition in the present polymer LCs was faster by 2 ~ 3 orders of magnitude than that in the non-donor-acceptor azobenzene LCs. In Chapter 4, the author described that the response time of the thermal recovery of the N phase in low-molecular-weight LCs with donor-acceptor azobenzenes was 500 ms at 37 °C. The response in the present polymer LCs, therefore, was faster by 1 ~ 2 orders of magnitude than that in low-molecular-weight LCs. This difference

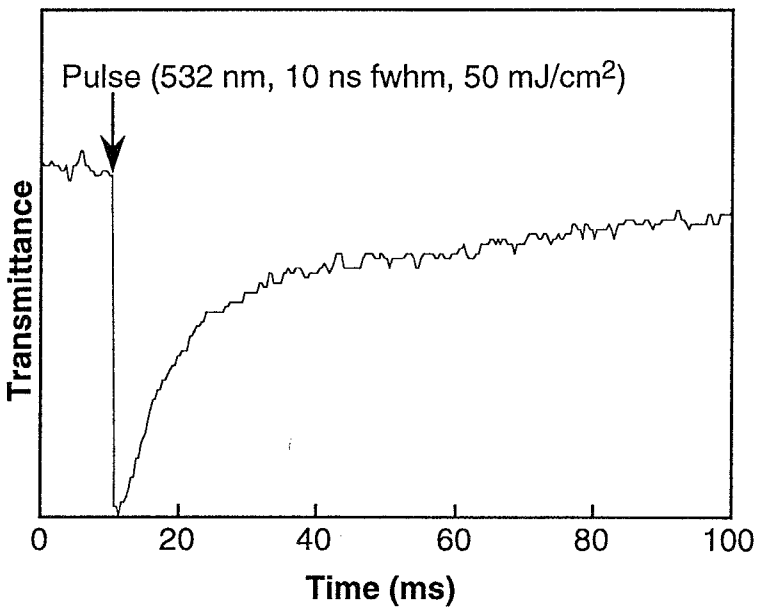

Figure 5-7. Time-resolved measurement of thermal I-N phase transition of **P5-1c** at 95 °C (T_{red} = 0.974).

between low-molecular-weight and polymer LCs may be due to difference in temperature. At 37 °C, the thermal *cis-trans* back-isomerization occurs slowly, so that the thermal recovery of the N phase needed a longer time in low-molecular-weight LCs.

Figure 5-8 shows the temperature dependence of the response time of the thermal I-N phase transition in **P5-1c** and **P5-3b**. In both **P5-1c** and **P5-3b**, the photochemical phase transition was not induced completely below temperature which is about 30 °C below their Tc. The N phase appeared more slowly at lower temperature in both samples. Since the rate of the thermal *cis-trans* isomerization of the azobenzenes and the mobility of the mesogens decreased with decreasing temperature, isomerization and reorientation process took place ineffectively. Consequently, the I-N phase transition was slower at lower temperature. In addition, the thermal recovery of the N phase became slower at temperature just below the N-I phase transition temperature. At this temperature, although the *cis-trans* isomerization occurred quickly, the reorientation process was depressed because the mobility of the mesogen is close to that in the I phase.

It is difficult to compare the thermal I-N phase transition behavior in **P5-1c** and **P5-3b** at the same temperature, because the temperature range in which the photochemical phase transition took place was different. The author, therefore, discussed it at the same reduced temperatures (T_{red}). T_{red} was defined as the ratio of the measurement temperature to their Tc. The T_{red} for **P5-1c** at 95 °C (T_{red} = 0.974) was the same as that for **P5-3b** at 146 °C. At this temperature, the N phase recovered in 50 ms in **P5-1c** (Figure 5-7), while it recovered in 8 ms in **P5-3b** (Figure 5-5). As described above, the *cis* isomer of the azobenzenes in both polymers showed nearly the same lifetimes: it disappeared almost completely in 2 ms. Hence, the difference in the response time of the thermal I-N phase transition between these polymers may be interpreted as the reorientation

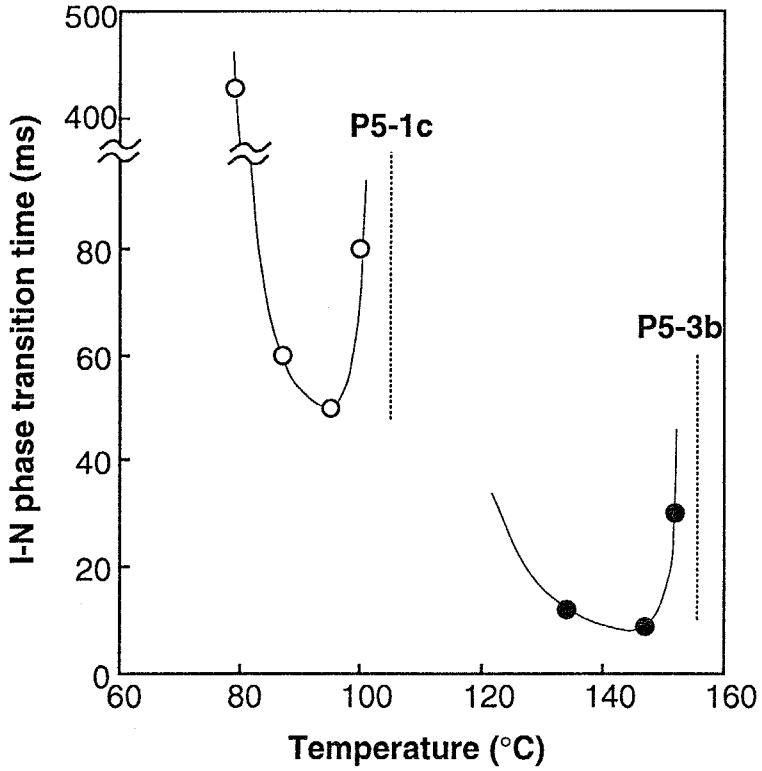

Figure 5-8. Temperature dependence of the response time of the thermal I-N phase transition: ○, **P5-1c**; ●, **P5-3b**.
Dotted line indicates the N-I phase transition temperature of the polymer LCs.

process of the mesogens plays a crucial role in the phenomena. Although the isomerization process took place in 2 ms, the N phase recovered in 50 ms in **P5-1c**. This suggests that the reorientation of the mesogens in **P5-1c** needs a timescale of about 50 ms to take place. This slow reorientation of **P5-1c** may be due to the instability of the LC phase. Since the azobenzene introduced in the **P5-1** series destabilizes the N phase, the reorientation process was depressed and occurred slowly. The azobenzene introduced in the **P5-3** series, however, stabilizes the LC phase and the reorientation process of **P5-3b** may proceed more effectively than that of **P5-1c**. As a result, **P5-3b** showed faster response in the thermal I-N phase transition.

As described in Chapter 4, the response time of the thermal recovery in the low-molecular-weight LCs was 500 ms at 37 °C, thus the response time of the polymer LCs was 10 ~ 100 times faster than that of the low-molecular-weight LCs. This difference between the two types of the LCs is attributable to the difference in temperature. The polymer LCs show a much wider temperature range in general for the N phase, so that they are advantageous in view of a quick response and a wide temperature range available for the optical switching.

5. Effect of Phase Structure on Photochemical Phase Transition.

In the N phase, when the azobenzene moiety stabilized the LC phase, the thermal recovery of the N phase became faster. From these results, one can expect that the thermal recovery of the LC phase may be brought about more quickly when the photochemical phase transition is induced in a more stable LC phase, such as an Sm phase. Thus, the author investigated the photochemical phase transition behavior of the polymer LC in the Sm phase. In **P5-2** which showed the Sm phase, however, no change in the transmittance of the probe light was observed by irradiation

with the steady light at 488 nm nor the laser pulse at 532 nm (Figure 5-9). This means that the photochemical phase transition of the polymer LCs could not be induced in the Sm phase under the present experimental condition. In the Sm phase, the mesogens are packed closely and form more stable LC phase than in the N phase. In the Sm phase, therefore, it may need a larger amount of the azobenzene to destroy the phase structure than in the N phase. Namely, the threshold concentration of the azobenzene was higher in the Sm phase, and the photochemical phase transition could not occur in **P5-2**.

CONCLUSION

The photochemical phase transition of the polymer LCs with donor-acceptor azobenzenes was induced in 300 μs by irradiation with a laser pulse to bring about the *trans-cis* photoisomerization of the azobenzene. When the irradiated sample was kept in the dark, the initial N phase was restored immediately due to the thermal *cis-trans* back-isomerization. The photochemical phase transition of the polymer LCs depended strongly on mole fraction of the azobenzene; it required a larger amount of the azobenzene than a threshold concentration. Furthermore, the photochemical phase transition was influenced by the phase structure of the LC phase.

The thermal recovery of the N phase was affected by the structure of the azobenzene moiety. When the azobenzene with a strong donor-acceptor pair stabilized the N phase, the *cis-trans* thermal isomerization and the reorientation of the mesogen proceeded effectively, thus the thermal I-N phase transition occurred very quickly: it took 8 ms at 146 °C.

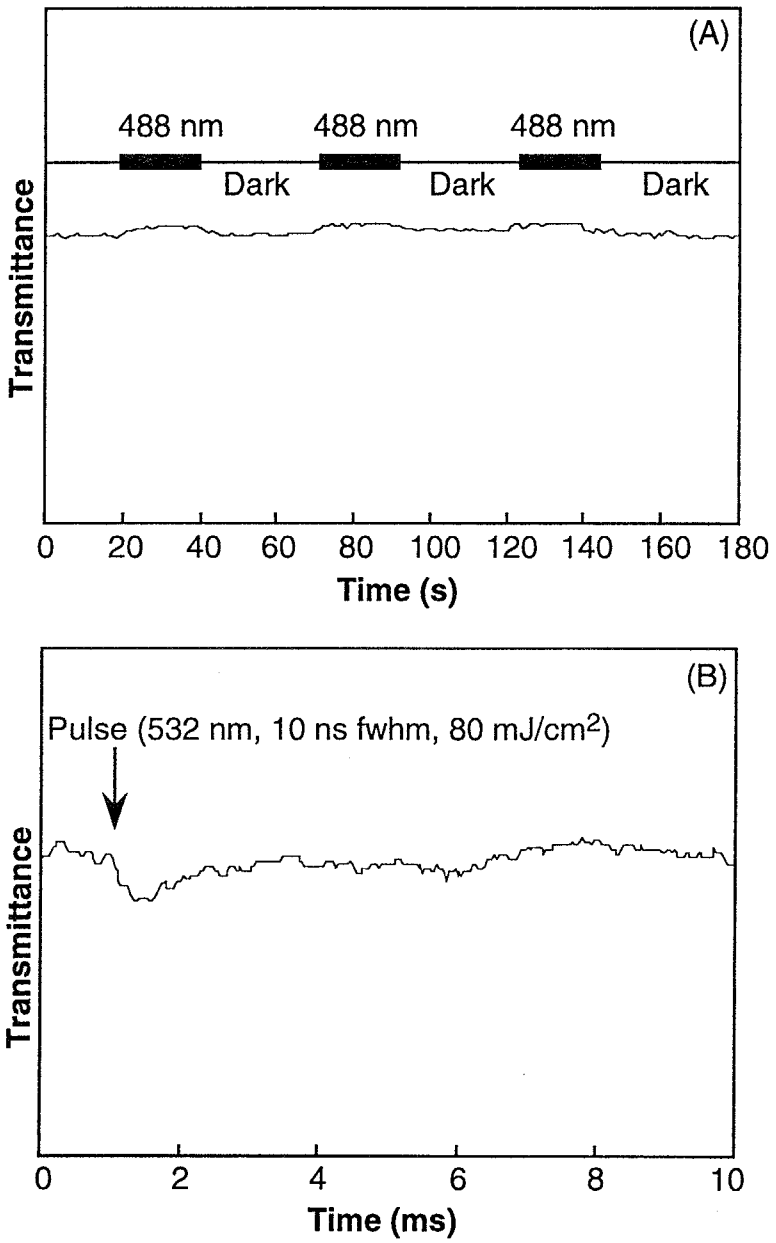

Figure 5-9. Photoresponse of **P5-2** in the Sm phase: (A), irradiation with steady light at 488 nm (27 mW/ cm^2) at 100 °C; (B), irradiation with a single pulse of laser at 523 nm (80 mJ/cm^2) at 95 °C.

References and Notes

(1) Robello, D.R. *J. Polym. Sci. Part A: Polym. Chem.* **1990**, *28*, 1.

(2) Schilling, M.L.; Katz, H.E. *Chem. Mater.* **1989**, *1*, 668.

(3) Shibaev, V.P.; Kostromin, S.G.; Platé, N.A. *Eur. Polym. J.* **1982**, *18*, 651.

(4) Gray, G.W. *Mol. Cryst.* **1966**, *1*, 333.

(5) Gray, G.W. In *The Molecular Physics of Liquid Crystals*; Luckhurst, G.R., Gray, G.W., Eds.; Academic Press: London, U.K., 1979; pp 1-29.

(6) Xie, S.; Natansohn, A.; Rochon, P. *Chem. Mater.* **1993**, *5*, 403.

Chapter 6

Photochemical Phase Transition Behavior of Polymer Azobenzene Liquid Crystals with Donor-Acceptor Pairs

INTRODUCTION

In Chapters 4 and 5, the author preliminarily investigated the photochemical phase transition behavior of LCs with donor-acceptor azobenzenes in the guest/host system, and it became clear that the thermal I-N phase transition was accelerated with donor-acceptor azobenzenes. In the guest/host systems, however, the photochemical phase transition could not be induced in a wide temperature range; it took place just below Tc of the LCs. This nature of the guest/host system would be disadvantageous to photonic materials. As mentioned in Chapters 2 and 3, the photochemical phase transition of the photochromic LCs occurred in a wide temperature range; it took place even below Tg. In azobenzene LCs with a donor-acceptor pair, therefore, quick photoresponse may be obtained in a wide temperature range. In this chapter, the author explored the photochemical N-I phase transition and the thermal I-N phase transition behavior of polymer azobenzene LCs with donor-acceptor substituents at 4,4'-positions. In addition, the author discussed the effect

of structure of main chain of the polymer on the phase transition behavior of the azobenzene LCs.

EXPERIMENTAL

1. Materials.

Figure 6-1 shows the structures of the polymer azobenzene LCs as well as their abbreviations used in this chapter. **PA6AB2** and **PM6AB2** have a 4-ethoxyazobenzene moiety, and **PA6ABCN** and **PM6ABCN** have a donor-acceptor azobenzene moiety as a mesogen and a photoresponsive moiety in the side chain. In Chapters 4 and 5, the author described that the thermal I-N phase transition took place very effectively when the azobenzenes had a strong donor-acceptor pair, such as amine and nitro group. However, it was reported that the azobenzene LCs with such a strong donor-acceptor pair exhibited the Sm phase.[1] Furthermore, as described in Chapter 4, the azobenzene LCs with a strong donor-acceptor pair were aligned in the homeotropic manner in the LC phase and it was not possible to evaluate their phase transition behavior by observation of change in the transmittance of the probe light. Therefore, an alkoxyl group and a cyano group were employed as the donor and the acceptor. In the abbreviations, PA and PM indicate the structure of the main chain of the polymer: the former means polyacrylate and the latter means polymethacrylate. These polymers were prepared and purified as reported previously.[1]

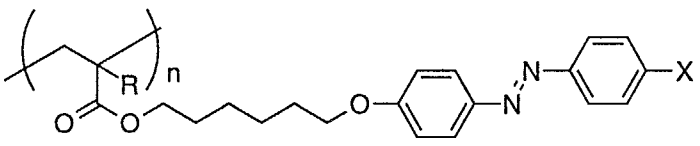

PA6AB2: R = H, X = OC_2H_5
PM6AB2: R = Me, X = OC_2H_5
PA6ABCN: R = H, X = CN
PM6ABCN: R = Me, X = CN

Figure 6-1. Structures of the polymer azobenzene LCs used in this chapter and their abbreviations.

General Method of Preparation. THF and DMF were distilled over calcium hydride. Unless otherwise noted, all materials and other solvents were commercially available and used as received. The products were characterized by ^{1}H-NMR spectroscopy as described in Chapter 2.

4-Cyano-4'-hydroxyazobenzene (6-1). 4-Aminobenzonitrile (10 g, 84 mmol) was dissolved in 30 mL of sulfuric acid (3 M) and the resulting solution was cooled to 0 °C. With stirring, sodium nitrite (5.8 g, 84 mmol) in water (40 mL) was added dropwise to the solution to produce diazonium salt. A mixture of phenol (7.4 g, 84 mmol) and sodium hydroxide (6.8 g, 168 mmol) in water (200 mL) was added slowly to the solution. The reaction mixture was stirred at room temperature for 1 h. After the reaction mixture was neutralized with acetic acid, precipitated solid was collected and washed with water. The solid was dried under vacuum and recrystallized from benzene to obtain 7.3 g (34 mmol) of **6-1** in 40 % yield. mp: > 200 °C (dec.). ^{1}H-NMR ($CDCl_3$): δ 5.4 (s; 1H; *OH*), 6.9 (d, J = 9 Hz; 2H; *CH* in aromatic), 7.8 (d, J = 9 Hz; 2H; *CH* in aromatic), 7.9 (m; 4H; *CH* in aromatic). IR (KBr, cm^{-1}): 3320, 2250, 1600, 1590. Anal. Calcd for $C_{13}H_{19}N_3O$: C, 69.95; H, 4.06; N, 18.82. Found: C, 69.86; H, 3.80; N, 18.94.

4-Cyano-4'-(6-hydroxyhexyloxy)azobenzene (6-2). 6-Chloro-1-hexanol, potassium carbonate (1.2 g, 9.4 mmol) and **6-1** (2.0 g, 9.4 mmol) were dissolved in 50 mL of DMF, and the resulting solution was stirred at 120 °C for 72 h. After the reaction mixture was cooled to room temperature, it was poured into water, and the precipitated orange solid was collected and washed with water. The crude product was dried and purified by recrystallization from acetone to produce 1.8 g (5.7 mmol) of **6-2** in 61 % yield. mp: 155-157 °C. ^{1}H-NMR ($CDCl_3$): δ 1.4-1.8 (m; 8H;

CH$_2$), 3.5 (s; 1H; *OH*), 3.7 (m; 2H; *CH*$_2$OH), 4.0 (t, *J* = 7 Hz; 2H; O*CH*$_2$), 6.9 (d, *J* = 9 Hz; 2H; *CH* in aromatic), 7.8 (d, *J* = 9 Hz; 2H; *CH* in aromatic), 7.9 (m; 4H; *CH* in aromatic). IR (KBr, cm^{-1}): 3500, 2940, 2860, 1600, 1580, 1500, 1260, 1060, 1020, 850, 800. Anal. Calcd for $C_{19}H_{21}N_3O_2$: C, 70.57; H, 6.54; N, 12.99. Found: C, 70.43; H, 6.47; N, 13.01.

6-[4-(4-Cyanophenylazo)phenoxy]hexyl acrylate (6-3). Triethylamine (0.7 g, 8.0 mmol), **6-2** (2.0 g, 6.3 mmol) and a trace amount of hydroquinone were dissolved in 50 mL of THF and the resulting solution was cooled at 0 °C. With stirring, 0.63 g (7.0 mmol) of acryloyl chloride in THF (5 mL) was added dropwise to the solution and the reaction mixture was stirred at room temperature for 24 h. The reaction mixture was poured into water and the product was extracted with ether, and the organic layer was dried with sodium sulfate. After the solvent was evaporated, yellow solid obtained was purified by column chromatography on silica gel (*n*-hexane/ethyl acetate = 6/1) and recrystallized from a mixture of ethanol and acetone (6/1) to give 0.57 g (1.5 mmol) of **6-3** in 24 % yield. mp: 89-92 °C. ^{1}H-NMR ($CDCl_3$): δ 1.4-1.8 (m; 8H; *CH*$_2$), 4.1 (t, *J* = 6 Hz; 2H; O*CH*$_2$), 4.2 (t, *J* = 7 Hz; 2H; COO*CH*$_2$), 5.8 (dd, *J* = 10, 2 Hz; 1H; *cis*-*CH*$_2$=CH), 6.1 (dd, *J* = 17, 10 Hz; 1H; CH$_2$=*CH*), 6.4 (dd, *J* = 17, 2 Hz; 1H; *trans*-*CH*$_2$=CH), 7.0 (d, *J* = 9 Hz; 2H; *CH* in aromatic), 7.8 (d, *J* = 9 Hz; 2H; *CH* in aromatic), 7.9 (m; 4H; *CH* in aromatic). IR (KBr, cm^{-1}): 2950, 2230, 1730, 1640, 1600, 1580, 1500, 1480, 1260. Anal. Calcd for $C_{22}H_{23}N_3O_3$: C, 70.01; H, 6.15; N, 11.13. Found: C, 71.28; H, 6.09; N, 11.33.

6-[4-(4-Cyanophenylazo)phenoxy]hexyl methacrylate (6-4). This compound was prepared from **6-2** (2.0 g, 6.2 mmol), triethylamine (1.8 g,

18 mmol), and methacryloyl chloride (1.9 g, 18 mmol) similarly to **6-3** (1.4 g, 10 mmol) in 56 % yield. ^{1}H-NMR ($CDCl_3$): δ 1.4-1.8 (m; 8H; *CH_2*), 1.9 (s, 3H, CH_2=C-*CH_3*), 4.0 (t, *J* = 6 Hz; 2H; O*CH_2*), 4.2 (t, *J* = 7 Hz; 2H; COO*CH_2*), 5.5 (s, 1H; *cis-CH_2*=C-CH_3), 6.1 (s, 1H; *trans-CH_2*=C-CH_3), 7.0 (d, *J* = 9 Hz; 2H; *CH* in aromatic), 7.8 (d, *J* = 9 Hz; 2H; *CH* in aromatic), 7.9 (m; 4H; *CH* in aromatic).

6-[4-(4-Ethoxyphenylazo)phenoxy]hexyl methacrylate (6-5). The title compound was obtained from **2-2** (1.2 g, 3.1 mmol), triethylamine (0.97 g, 9.6 mmol), and methacryloyl chloride (1.0 g, 9.6 mmol) similarly to **2-3** (0.62 g, 1.5 mmol) in 49 % yield. ^{1}H-NMR ($CDCl_3$): δ 1.4-1.8 (m; 11H; *CH_2*, *CH_3*), 1.9 (s, 3H, CH_2=C-*CH_3*), 3.7 (q, *J* = 6 Hz, 2H, O*CH_2*CH_3), 4.0 (t, *J* = 6 Hz; 2H; O*CH_2*), 4.2 (t, *J* = 7 Hz; 2H; COO*CH_2*), 5.5 (s; 1H; *cis-CH_2*=C-CH_3), 6.1 (s; 1H; *trans-CH_2*=C-CH_3), 7.0 (d, *J* = 9 Hz; 4H; *CH* in aromatic), 7.8 (d, *J* = 9 Hz; 4H; *CH* in aromatic).

Poly[6-[4-(4-cyanophenylazo)phenoxy]hexyl acrylate] (PA6ABCN). This polymer was prepared from **6-3** (0.50 g, 1.3 mmol) and AIBN (3.0 mg, 13 μmol) in DMF (5 mL) similarly to **PA6AB2** described in Chapter 2. The polymer was purified by repeated reprecipitation from chloroform into a large excess of methanol and dried under vacuum for 48 h. Conversion: 20 % (0.10 g).

Poly[6-[4-(4-cyanophenylazo)phenoxy]hexyl methacrylate] (PM6ABCN). In a similar manner, **PM6ABCN** was obtained from **6-4** (0.50 g, 1.2 mmol) and AIBN (2.8 mg, 12 μmol) in DMF (5 mL). The polymer obtained was purified by repeated reprecipitation from chloroform into a large excess of methanol and dried under vacuum for 48 h. Conversion: 38 % (0.19 g).

Poly[6-[4-(4-ethoxyphenylazo)phenoxy]hexyl methacrylate] (PM6AB2). This polymer was obtained from **6-5** (0.50 g, 1.2 mmol) and AIBN (2.8 mg, 12 μmol) in DMF (5 mL) similarly to **PA6AB2** (Chapter 2). The polymer was purified by repeated reprecipitation from chloroform into a large excess of methanol and dried under vacuum for 48 h. Conversion: 70 % (0.35 g).

2. Characterization of LCs.

Molecular weight of the polymers was determined by GPC and thermotropic properties of the LCs were determined with DSC as described in Chapter 2. The thermodynamic properties and molecular weight of the polymer LCs are given in Table 6-1.

3. Photochemical Phase Transition.

The photochemical phase transition behavior of the polymer LCs was investigated by means of the apparatus described in Chapter 2. Sample films were prepared in the same manner as described in the preceding chapter.

4. Thermal *cis-trans* Isomerization Behavior of Azobenzenes.

To examine the thermal *cis-trans* isomerization behavior of the azobenzene moieties, change in absorbance at absorption maximum of the *trans*-azobenzenes in the LC phase was observed. The azobenzene LC film was placed in an absorption spectrometer (Shimadzu UV-200S) and thermostated. The film was irradiated at 366 nm (5 mW/cm^2) for 10 min

in the LC phase, and then absorbance at absorption maximum of the *trans*-form (at 360 nm) was measured as a function of time.

RESULTS AND DISCUSSION

1. Characterization of Polymers.

All polymers used in this chapter showed the N phase. The phase transition temperature and Tg were summarized in Table 6-1. Annealing of the azobenzene LC films at temperature just below their T_{NI} gave a well-aligned monodomain of the LC phase. It was observed with polarizing microscope that the films became dark when viewed with the rubbing direction parallel to the one of the crossed polarizes and the transmitted light intensity was highest when the rubbing direction was 45 ° with respect to the polarizers. This result indicates that all mesogens of the polymer LCs are aligned into one direction to form a monodomain of LC phase.

Table 6-1. Phase Transition Temperature and Molecular Weight of Polymer LCs Used in This Chapter[a]

polymer	main chain	X	*Mn*	*Mw / Mn*	phase transition temperature (°C)
PA6AB2	acrylate	OEt	9,100	1.3	G 45 N 155 I
PM6AB2	methacrylate	OEt	58,000	2.3	G 68 N 150 I
PA6ABCN	acrylate	CN	5,300	1.2	G 29 N 135 I
PM6ABCN	methacrylate	CN	17,000	1.4	G 49 N 163 I

[a] Abbreviations: G, glass; N, nematic; I, isotropic; *Mn*, number-average molecular weight; *Mw*, weight-average molecular weight.

trans-Azobenzenes exhibit the absorption maxima at around 350 nm due to a π–π^* transition and at around 450 nm due to an n-π^* transition. The absorbance at around 350 nm was reduced by photoirradiation at 366 nm due to the *trans-cis* photoisomerization of the azobenzene moieties. After irradiation with visible light (> 420 nm), the absorbance was restored owing to *cis-trans* photochemical back-isomerization. This indicates that the photoisomerization of the azobenzene moieties took place reversibly by photoirradiation. In addition, when the polymers irradiated at 366 nm were kept in the dark, the *cis-trans* back-isomerization also occurred thermally.

2. Photochemical Phase Transition and Thermal Phase Transition Behavior of Polymer Azobenzene LCs. Effect of Substituents of Azobenzene Moieties.

As shown in Figure 6-2 for **PA6ABCN**, transmittance of the probe light at 633 nm decayed immediately upon irradiation at 366 nm in the N phase. This was caused by the photochemical N-I phase transition of the azobenzene LCs due to the *trans-cis* photoisomerization of the azobenzene. When photoirradiation was ceased, the transmittance of the probe light recovered. Since the mesogenic *trans*-azobenzene restored thermally, the initial N phase recovered when the irradiated film was kept in the dark. In all samples, the photochemical phase transition was induced repeatedly.

Figure 6-3 shows the time-resolved measurements of the photochemical N-I and the thermal I-N phase transition in **PA6ABCN**. The photochemical N-I phase transition in **PA6ABCN** was induced in 200 ~ 300 μs (Figure 6-3(A)). As described in Chapter 2, this response is similar to that observed in **PA6AB2**. On the other hand, the thermal recovery of the N phase in **PA6ABCN** occurred faster than that in **PA6AB2**: it took 800 ms in **PA6ABCN** at 135 °C while it took 7 ~ 8 s in **PA6AB2** at 140 °C.

It is worth noting here that the photochemical phase transition was also induced in 200 ~ 300 μs at room temperature (23 °C) in all polymer azobenzene LCs. These polymers show the Tg at 29 ~ 68 °C, so that the N-I phase transition could be induced even below Tg. Furthermore, when the polymer films were irradiated with a laser pulse at 355 nm at room temperature and kept at the same temperature in the dark, the I phase induced at irradiated site was very stable.

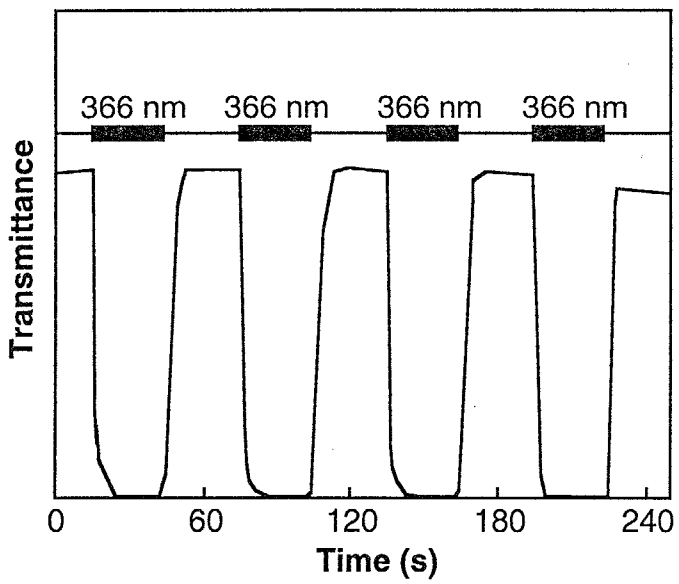

Figure 6-2. Photochemical N-I and thermal I-N phase transition of **PA6ABCN**.
Photoirradiation at 366 nm was performed at 130 °C.

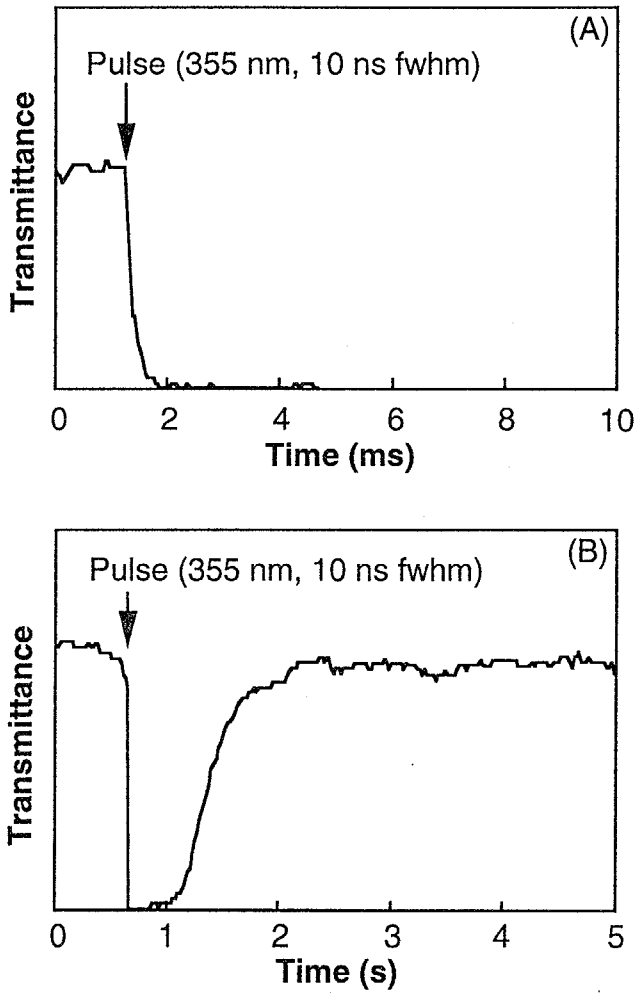

Figure 6-3. Time-resolved measurements of the photochemical N-I and thermal I-N phase transition of **PA6ABCN**: (A) photochemical N-I phase transition at 127 °C; (B) thermal I-N phase transition at 135 °C.

3. Fatigue Resistance of Polymer Azobenzene LC.

Fatigue resistance of the polymer azobenzene LC was evaluated with **PA6ABCN** in detail. Figure 6-4 shows the time-resolved measurements of the photochemical phase transition in **PA6ABCN** before (A) and after irradiation with some laser pulses ((B) and (C)). As shown in Figure 6-4, the initial transmittance of the probe light decreased with repeating the photochemical phase transition. After the sample film was irradiated with 600 pulses of laser, the transmittance of the probe light in the N phase decreased to about 30 % of the level in the virgin sample. This decrease of the transmittance may be due to by-products produced by the photochemical side-reactions of the azobenzenes. Because the by-products destabilized the LC phase, the order parameter of the LC was lowered and the transmittance of the probe light decreased. Although the photochemical phase transition took place after 800 pulses irradiation, the transmittance in the N phase decreased to 15 % of the level in the virgin sample. After pulse irradiation was repeated more than 1000 times, the transmitted light in the N phase could not be detected under the present experimental setup. In conclusion, the photochemical phase transition in **PA6ABCN** can be repeated about 1000 times by irradiation with laser pulses.

4. Effect of Visible-Light Irradiation on I-N Phase Transition.

The *cis-trans* back-isomerization of the azobenzene moiety was also induced photochemically by visible-light irradiation. The *cis-trans* photoisomerization is faster than the thermal isomerization. When the *cis-trans* photoisomerization of the azobenzene is induced with visible light, therefore, one can expect that the N phase recovers more quickly. Thus, the effect of the *cis-trans* photoisomerization of the azobenzene moieties

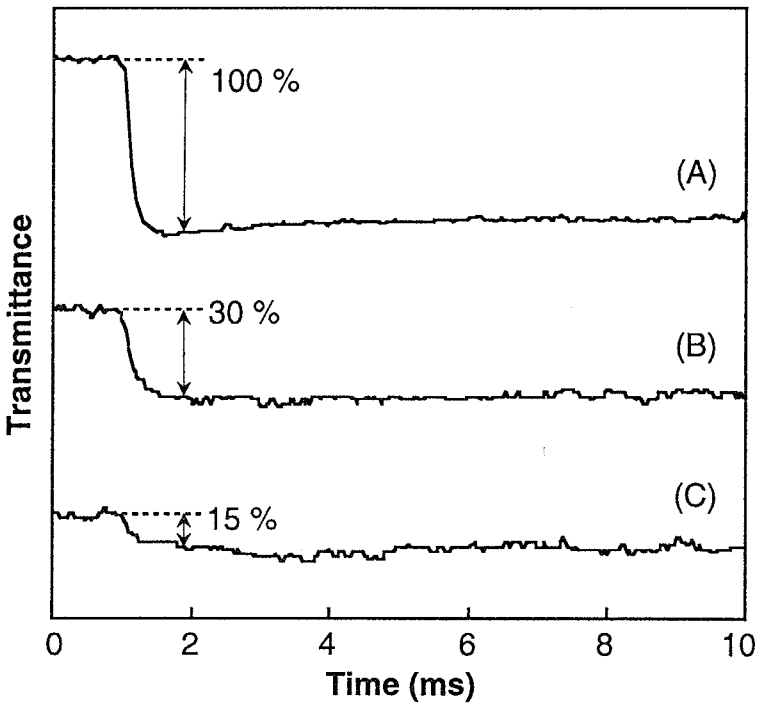

Figure 6-4. Time-resolved measurements of the photochemical phase transition of **PA6ABCN**: (A) in virgin sample; (B) after 600 pulses irradiation; (C) after 800 pulses irradiation.
Laser pulse irradiation at 355 nm (30 mJ/cm2) was performed at 102 °C. Repetition rate of the pulse irradiation was 0.1 Hz.

on the I-N phase transition was investigated for **PA6ABCN**. The LC film was irradiated at 366 nm for 10 s at 76 °C, then the photochemical N-I phase transition took place. At this temperature, the N phase recovered thermally in 43 s when irradiated film was kept in the dark. However, when the film was irradiated with visible light at > 420 nm for 5 s after N-I phase transition to bring about the *cis-trans* photoisomerization, the I-N phase transition was caused in 26 s (Figure 6-5). Since the *cis-trans* isomerization of the azobenzene proceeded effectively by visible-light irradiation, the I-N phase transition occurred quickly. These results suggest that one can further accelerate the I-N phase transition by visible-light irradiation.

5. Effect of Main Chain of Polymers.

A similar photochemical N-I phase transition behavior was also observed in the methacrylate polymers (**PM6AB2** and **PM6ABCN**). However, the methacrylate polymers were different from the acrylate polymers in the thermal I-N phase transition behavior. Figure 6-6 shows the response time for the I-N phase transition of the polymer LCs as a function of temperature. In all polymers, the response time decreased with increasing temperature. At all temperatures, the thermal I-N phase transition of the methacrylate polymers was slower than that of the corresponding acrylate polymers. From these results, it can be assumed that the structure of the main chain of the polymers affects the *cis-trans* thermal isomerization process of the azobenzene moiety or the reorientation process of the mesogenic *trans*-azobenzene.

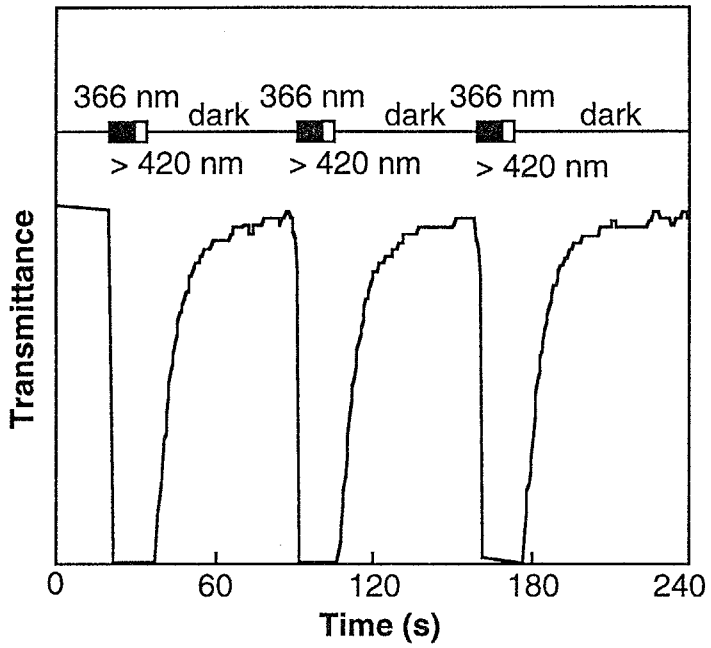

Figure 6-5. Effect of visible-light irradiation on photochemical phase transition of **PA6ABCN**. Photoirradiation at 366 nm and > 420 nm was carried out at 78 °C.

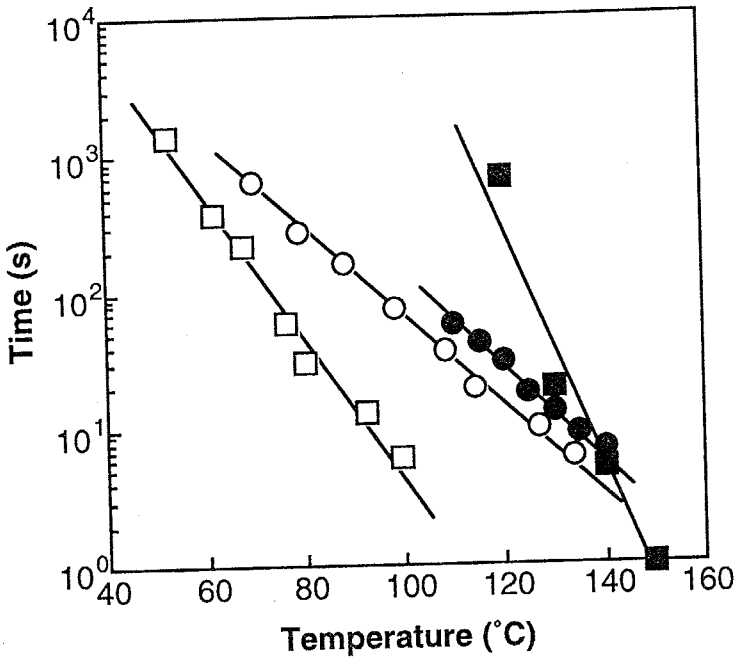

Figure 6-6. Response time for thermal I-N phase transition of polymer azobenzene LCs as a function of temperature: ○, **PA6AB2**; ●, **PM6AB2**; □, **PA6ABCN**; ■, **PM6ABCN**.

6. Thermal *cis-trans* Isomerization Behavior of Azobenzenes.

The thermal I-N phase transition consists of two processes: the *cis-trans* thermal isomerization and the reorientation of the mesogenic *trans*-azobenzenes. To explore the difference in the thermal I-N phase transition behavior between these polymers, the author studied the thermal *cis-trans* isomerization process in detail. The thermal isomerization behavior was observed by absorption spectroscopy. For the *cis-trans* isomerization, the first-order rate constant (k_{c-t}) was determined by fitting the experimental data to eq 2-4. Typical examples of the first-order plots according to eq 2-4 for the *cis-trans* isomerization of the azobenzene films at various temperatures were shown in Figure 6-7. As shown in Figure 6-7, eq 2-4 gives a good fit to the thermal *cis-trans* isomerization. From the slope of the first-order plots, the k_{c-t} values were obtained at each temperature.

The values of k_{c-t} of the donor-acceptor azobenzenes were larger than that of the corresponding non-donor-acceptor azobenzenes at any temperatures. In other words, the thermal *cis-trans* isomerization of the donor-acceptor azobenzenes proceeds more effectively than that of the non-donor-acceptor azobenzenes as described in Chapter 4. Note that the rate-determining step of the thermal recovery of the N phase is the *cis-trans* isomerization process (Chapter 2). Since the rate-determining step was accelerated with the donor-acceptor pair, the thermal I-N phase transition of **PA6ABCN** occurred more quickly than that of **PA6AB2**.

Figure 6-8 shows the Arrhenius plots for the *cis-trans* isomerization. The values of an activation energy were obtained from the slope of these plots. Figure 6-8 also shows the Arrhenius plots for the thermal I-N phase transition of the polymer LC films. The rate constant of the I-N phase transition was defined as a reciprocal of the response time. In the acrylate polymers, the slope of the Arrhenius plots for the phase transition was the same as that for the *cis-trans* isomerization. This means that the activation

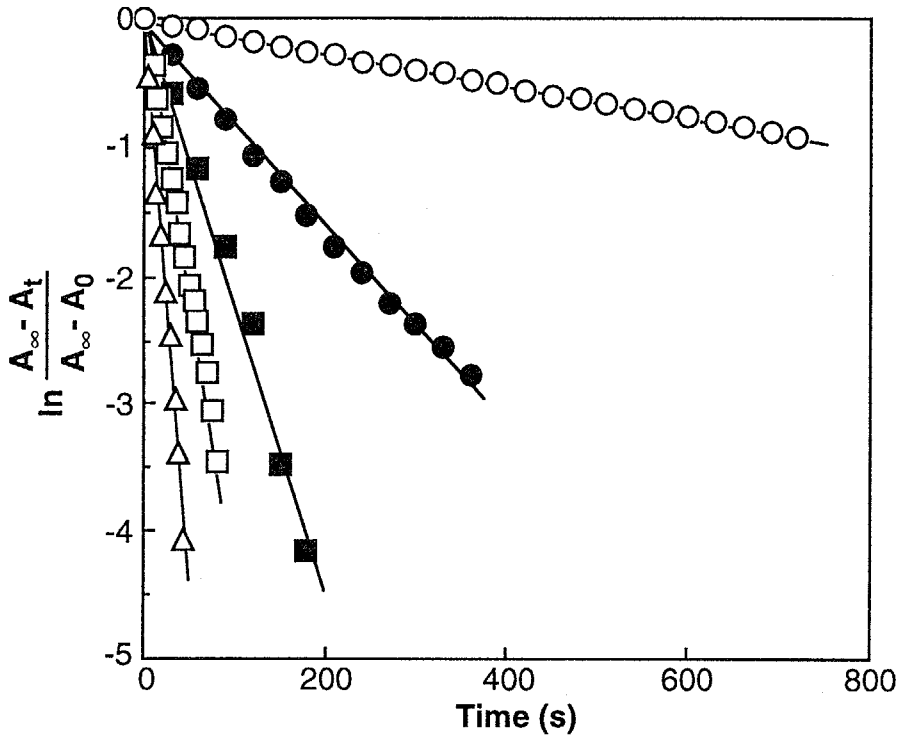

Figure 6-7. First-order plots for *cis-trans* thermal isomerization in **PM6AB2**: ○, at 50 °C; ●, at 70 °C; ■, at 80 °C; □, at 90 °C; △, at 100 °C.

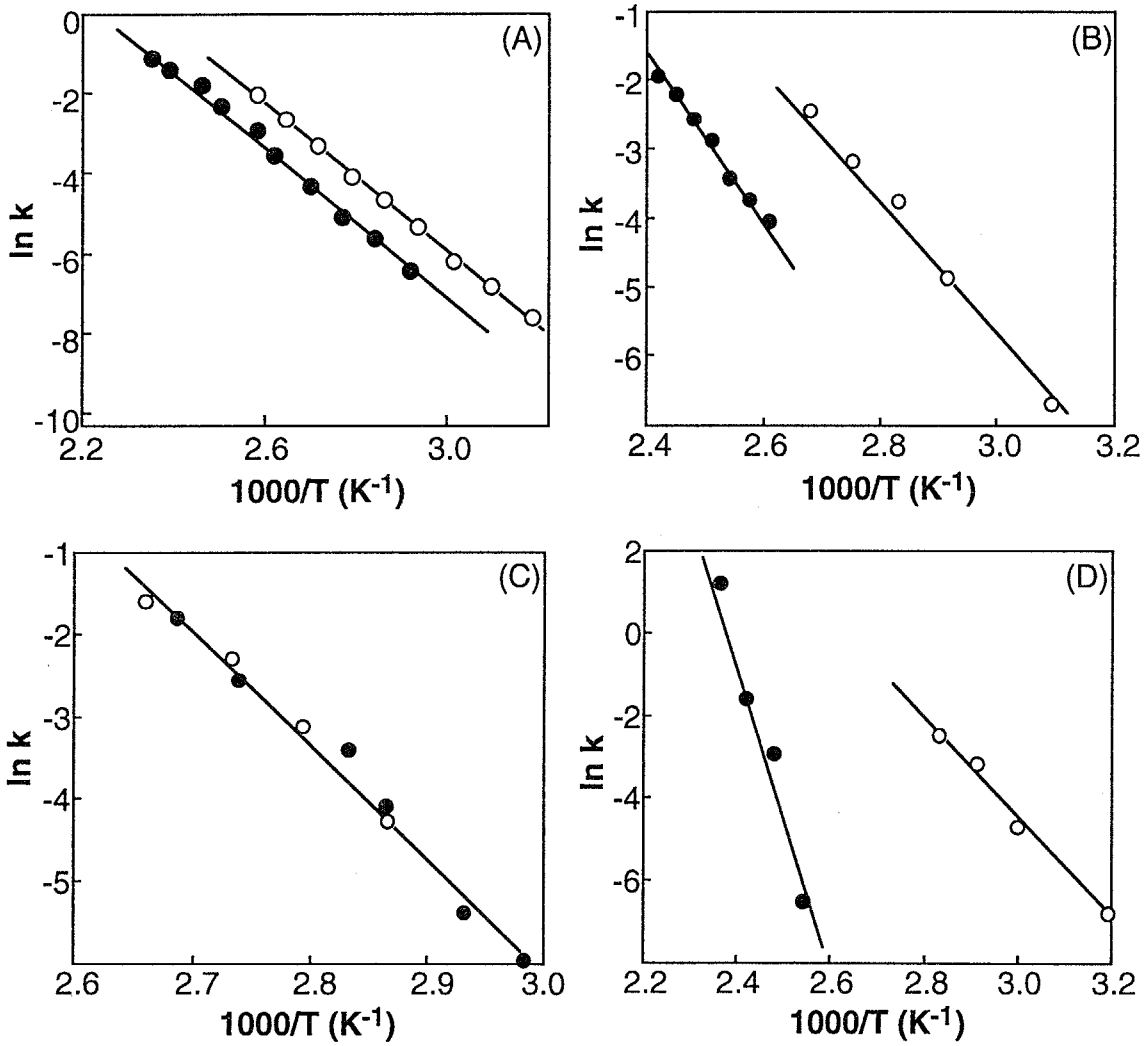

Figure 6-8. Arrhenius plots for the thermal *cis-trans* isomerization of azobenzene moiety and thermal I-N phase transition in polymer LCs. (A), **PA6AB2**; (B), **PM6AB2**; (C), **PA6ABCN**; (D), **PM6ABCN**: ○, for *cis-trans* isomerization; ●, for I-N phase transition.

energy for the I-N phase transition was identical with that of the *cis-trans* isomerization in the acrylate polymers. For example, in **PA6ABCN**, the values of the activation energy were 26 kcal/mol for the *cis-trans* isomerization and 28 kcal/mol for the I-N phase transition (Figure 6-8 (C)). Namely, as described in Chapter 2, the rate-determining step of the I-N phase transition is the *cis-trans* isomerization process in the acrylate polymers. In the methacrylate polymers, however, the activation energy for the I-N phase transition was different from that for the isomerization process: it was 24 kcal/mol for the *cis-trans* isomerization and 81 kcal/mol for the I-N phase transition in **PM6ABCN** (Figure 6-8 (D)). The same tendency was observed in **PA6AB2** and **PM6AB2** (Figure 6-8 (A) and (B)). The activation energy for the thermal isomerization showed almost the same values between acrylate and methacrylate polymers. This result suggests that the *cis-trans* isomerization process was not affected by the structure of the main chain of the polymer. Therefore, the difference in the thermal I-N phase transition between these polymers may be interpreted as the reorientation process of the mesogenic *trans*-azobenzene plays an important role in the phenomena. It is known that flexibility of the polymer main chain influences the temperature range of the LC phase and Tc of polymer LCs, because the mobility of the segments of the polymers affects the LC behavior.[2-4] The methacrylate main chain is more rigid than the acrylate main chain, thus the segmental motion of the main chain of the methacrylate polymers may be restrained. For this reason, the reorientation process of the methacrylate polymers was slower than that of the acrylate polymers.

CONCLUSION

The photochemical N-I phase transition of the polymer azobenzene LCs with a donor-acceptor pair was induced in 200 μs by irradiation with a laser pulse to bring about the *trans-cis* photoisomerization of azobenzenes. When the photoirradiation was ceased, the initial N phase was recovered thermally. In the photochemical N-I phase transition, effect of substituents at 4,4'-positions of the azobenzene moiety and structure of the main chain of the polymer was not observed. On the other hand, the thermal recovery of the N phase depended strongly on the substituents and the main-chain structure. The electron-donating and accepting substituents at 4,4'-positions of the azobenzenes accelerated the thermal I-N phase transition, because the thermal *cis-trans* isomerization of the azobenzene with donor-acceptor took place effectively. Furthermore, the I-N phase transition was also accelerated by visible-light irradiation. These results suggest that the polymer azobenzene LCs with electron donor and acceptor is potential quick-responsive photonic materials (such as all-optical switching and real-time holography materials).

The thermal I-N phase transition of the methacrylate polymers was slower than that of the acrylate polymers, since the segmental motion of the main chain of the polymer was restrained. In general, methacrylate polymers show high Tg and low flexibility of the main chain. These features of the methacrylate polymers would be disadvantageous to optical switching materials. One can, however, expect the methacrylate polymers for optical image storage materials, because the stored image may be very stable due to their high Tg and low flexibility of the main chain.

References and Notes

(1) Ringsdorf, H.; Schmidt, H.W. *Makromol. Chem.* **1984,** *185*, 1327.

(2) Shibaev, V.P.; Platé, N.A. *Adv. Polym. Sci.* **1984**, *60/61*, 173.

(3) Gemmell, P.; Gray, G.; Lacey, D. *Mol. Cryst. Liq. Cryst.* **1985**, *108*, 324.

(4) Shibaev, V.P. In *Liquid-Crystal Polymers,* Platé, N.A. Ed.; Plenum Press: New York, USA, 1993; pp 193-249.

Chapter 7

Photochemical Phase Transition Behavior of Polymer Liquid Crystals with Hydroxyazobenzene Moieties

INTRODUCTION

As described in the preceding chapters, the photochemical phase transition of the azobenzene LCs can be induced by photoirradiation. This phase transition is due to the *trans-cis* photoisomerization of the azobenzene moieties. It has not been clarified, however, if heat generated by the non-radiative relaxation of the excited azobenzenes affects the photochemical phase transition. If the local temperature of the LCs rises above their Tc with the heat generated by the non-radiative relaxation, the "heat-mode" phase transition may be induced by photoirradiation. In this chapter, therefore, the effect of the heat on the photochemical phase transition of LCs was discussed.

It is known that the quantum yield (Φ) for the *trans-cis* photoisomerization of hydroxyazobenzene is lower by one order of magnitude than that of its *O*-alkyl derivatives: $\Phi = \sim 10^{-2}$ in the former and $\Phi = \sim 10^{-1}$ in the latter.[1,2] In hydroxyazobenzenes, consequently, the relaxation of the excited state occurs mainly through non-radiative

process with generation of the heat. When the photochemical phase transition behavior of the hydroxyazobenzene system is compared with that of the alkoxyazobenzene system, therefore, one can evaluate the influence of the heat. Thus, in this chapter the hydroxyazobenzene derivative was used as the chromophore.

EXPERIMENTAL

1. Materials.

Structures of the polymer LCs used in this chapter are shown in Figure 7-1. **PM6ABOH** and **P7-2** have 4'-hydroxyazobenzene moieties as a photosensitive chromophore: the former is a homopolymer and the latter is a copolymer with cyanobiphenyl monomer. **PM6AB2** and **P7-1** are analogous polymers with 4'-ethoxyazobenzene moieties. Polymers with hydroxyazobenzene moiety were synthesized according to Scheme 7-1. Preparation of **PM6AB2** was described in Chapter 6.

General Method of Preparation. THF, DMF and dichloromethane were distilled over calcium hydride. Unless otherwise noted, all materials and other solvents were commercially available and used as received. The products were characterized by ^{1}H-NMR and ^{13}C-NMR spectroscopy as described in Chapter 2. IR spectra were recorded on a JASCO FT/IR-610 spectrometer.

***p*-(6-Hydroxyhexyloxy)nitrobenzene (7-1).** *p*-Nitrophenol (25 g, 180 mmol) was dissolved in DMF (50 mL), and the resulting

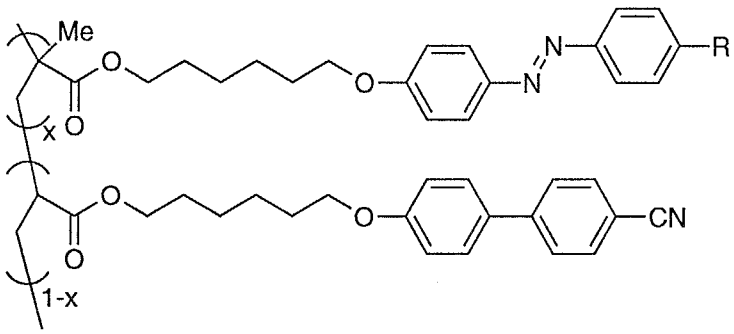

P7-1: R = OEt; x = 0.1
PM6AB2: R = OEt; x = 1.0
P7-2: R = OH; x = 0.1
PM6ABOH: R = OH; x = 1.0

Figure 7-1. Structures of polymer LCs used in this chapter.

Schem 7-1. Synthetic route for polymers with 4'-hydroxyazobenzene moiety.

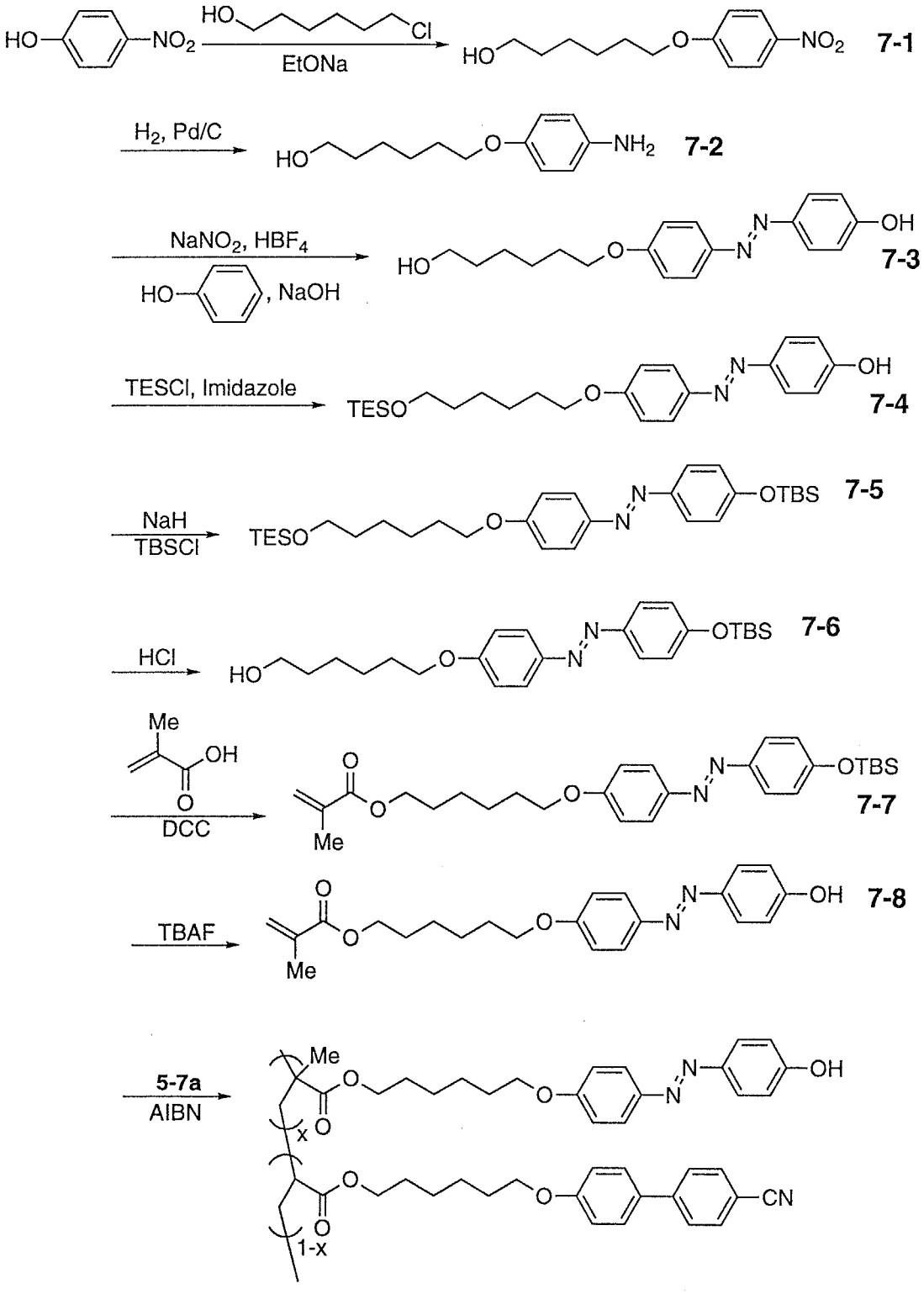

solution was added slowly to a suspension of sodium hydride (60 %, in oil; 7.2 g, 180 mmol) in 30 mL of DMF at room temperature. After stirring for 2 h, 6-chloro-1-hexanol (25 g, 180 mmol) was added to the mixture at room temperature, and the reaction mixture was stirred at 120 °C for 48 h. The solution was cooled to room temperature and poured into 300 mL of water. The white precipitate produced was collected and dried under vacuum. The crude product was purified by column chromatography on silica gel (chloroform/ethyl acetate = 2/1) to obtain 28 g of white powder (**7-2**, 120 mmol) in 67 % yield. ^{1}H-NMR ($CDCl_3$): δ 1.5-1.8 (m; 8H; CH_2), 3.7 (t, J = 6 Hz; 2H; CH_2OH), 4.1 (t, J = 6 Hz; 2H; OCH_2), 6.9 (d, J = 8 Hz; 2H; *CH* in aromatic), 8.2 (d, J = 8 Hz; 2H; *CH* in aromatic).

***p*-(6-Hydroxyhexyloxy)aniline (7-2).** A mixture of **7-1** (25 g, 100 mmol) and Pd/C (1.2 g) was added to 50 mL of THF, and the resulting suspension was stirred vigorously at room temperature. The suspension was bubbled with hydrogen gas at room temperature for 4 h. The precipitate was removed and the solvent was evaporated, and 20 g (96 mmol) of **7-2** was obtained in 96 % yield. ^{1}H-NMR ($CDCl_3$): δ 1.5-1.8 (m; 8H; CH_2), 3.6 (t, J = 6 Hz; 2H; CH_2OH), 3.9 (t, J = 6 Hz; 2H; OCH_2), 6.6 (d, J = 8 Hz; 2H; *CH* in aromatic), 6.7 (d, J = 8 Hz; 2H; *CH* in aromatic).

4-(6-Hydroxyhexyloxy)-4'-hydroxyazobenzene (7-3). Fluoboric acid (48 wt%; 27 g, 144 mmol) and **7-2** (15 g, 72 mmol) were dissolved in 100 mL of water, and the resulting solution was cooled at 0 °C. With stirring, 5.0 g (73 mmol) of sodium nitrite in water (30 mL) was added dropwise to the solution to produce diazonium salt. A mixture of phenol (6.8 g, 72 mmol) and sodium hydroxide (8.6 g, 216 mmol) in

water (100 mL) was added slowly at 0 °C, and the reaction mixture was stirred at room temperature for 2 h. After the reaction mixture was neutralized with acetic acid, the precipitated solid was collected and washed with water and recrystallized from chloroform to obtain 13 g (40 mmol) of yellow crystal (**7-3**) in 56 % yield. ^{1}H-NMR ($CDCl_3$): δ 1.5-1.8 (m; 8H; CH_2), 3.7 (t, J = 6 Hz; 2H; CH_2OH), 4.0 (t, J = 6 Hz; 2H; OCH_2), 6.8 (d, J = 8 Hz; 2H; *CH* in aromatic), 7.0 (d, J = 8 Hz; 2H; *CH* in aromatic), 7.8 (d, J = 8 Hz; 2H; *CH* in aromatic), 7.9 (d, J = 8 Hz; 2H; *CH* in aromatic).

4-(6-Hydroxyhexyloxy)-4'-(*tert*-butyldimethylsilyloxy)azobenzene (7-6). Imidazole (1.6 g, 23 mmol) and **7-3** (6.0 g, 19 mmol) were dissolved in DMF (50 mL), and 1.6 g (23 mmol) of chlorotriethylsilane (TESCl) was added to the resulting solution at 0 °C with stirring. The reaction mixture was warmed to room temperature and stirred for 24 h. After DMF was removed under reduced pressure, the orange solid obtained was dissolved in ethyl acetate and the solution was washed with an aqueous ammonium chloride. After the solution was dried with sodium sulfate, the solvent was removed under vacuum. The red powder obtained was dissolved again in 20 mL of THF, and the resulting solution was added slowly to a suspension of sodium hydride (60 %, in oil; 1.6 g, 40 mmol) in THF (20 mL) at room temperature. Chloro-*tert*-butyldimethylsilane (TBSCl) (6.0 g, 40 mmol) in THF (10 mL) was added to the resulting suspension. After the mixture was stirred at room temperature for 12 h, 100 mL of hydrochloric acid (1 M) was added, and the reaction mixture was stirred at room temperature for 2 h. The product was extracted with ether and washed with a saturated aqueous sodium hydrogen carbonate. The crude product was purified by column chromatography on silica gel (ethyl acetate/*n*-hexane = 2/1) to

obtain 4.4 g of orange crystal in 53 % yield. ^{1}H-NMR ($CDCl_3$, δ): 0.24 (s; 6H; $Si(CH_3)_2$), 1.0 (s; 9H; $SiC(CH_3)_3$), 1.5-1.8 (m; 8H; CH_2), 3.7 (t, J = 6 Hz; 2H; CH_2OH), 4.0 (t, J = 6 Hz; 2H; OCH_2), 6.9 (d, J = 10 Hz; 2H; *CH* in aromatic), 7.0 (d, J = 8 Hz; 2H; *CH* in aromatic), 7.8 (d, J = 10 Hz; 2H; *CH* in aromatic), 7.9 (d, J = 8 Hz; 2H; *CH* in aromatic).

6-[4-(4-Hydroxyphenylazo)phenoxy]hexyl methacrylate (7-8). Methacrylic acid (2.5 g, 30 mmol), **7-6** (4.4 g, 10 mmol) and DMAP (1.2 g, 10 mmol) were dissolved in 30 mL of dichloromethane. With stirring, a solution of DCC (4.1 g, 20 mmol) in dichloromethane (10 mL) was added slowly to the resulting solution at 0 °C. After stirring at room temperature for 20 h, the precipitate was removed, and the solution was washed with hydrochloric acid (2 M) and a saturated aqueous sodium hydrogen carbonate. The solution was dried with sodium sulfate and the solvent was removed. The red solid obtained and tetra-*tert*-butylammonium fluoride (TBAF) (5.0 g, 19 mmol) were dissolved again in 20 mL of THF and the resulting solution was stirred at room temperature for 3 days. Water (50 mL) was added to the reaction mixture, and the product was extracted with ether. The crude product was purified by column chromatography on silica gel (ethyl acetate/*n*-hexane = 1/1) and recrystallized from ethanol to obtain 1.2 g (3.1 mmol) of (**7-8**) in 31 % yield. mp: 99 - 100 °C. ^{1}H-NMR ($CDCl_3$): δ 1.7-1.8 (m; 8H; CH_2), 1.9 (s; 3H; $CH_2=C(CH_3)$), 4.0 (t, J = 6.0 Hz; 2H; $COOCH_2$), 4.2 (t, J = 6 Hz; 2H; OCH_2), 5.3 (s; 1H; *OH*), 5.5 (s; 1H; *trans*-$CH_2=C(CH_3)$), 6.1 (s; 1H; *cis*-$CH_2=C(CH_3)$), 6.9 (d, J = 8 Hz; 2H; *CH* in aromatic), 7.0 (d, J = 8 Hz; 2H; *CH* in aromatic), 7.8 (d, J = 8 Hz; 2H; *CH* in aromatic), 7.9 (d, J = 8 Hz; 2H; *CH* in aromatic). ^{13}C-NMR ($CDCl_3$): δ 18.3, 25.7, 25.8, 28.5, 29.1, 64.8, 68.1, 114.7, 115.8, 124.3,

124.5, 125.5, 136.4, 146.9, 147.1, 158.1, 161.1, 167.8. IR (KBr, cm^{-1}): 3232, 2940, 2865, 1691, 1636, 1606, 1590, 1330, 1257, 1233, 844.

Polymerization. Polymers were prepared from the corresponding azobenzene monomers and cyanobiphenyl monomers (**5-7a**). Polymerization was conducted in DMF with AIBN as an initiator similarly to **PA6AB2** described in Chapter 2 (see Table 7-1). Each polymer was purified by reprecipitation of a THF solution into a large excess of methanol.

Table 7-1. Conditions for Polymerization[a]

polymer	azobenzene monomer, g	cyanobiphenyl monomer, g	initiator, mg	solvent, mL	conversion, %
P7-1	0.094	0.80	7.0	3	62
P7-2	0.10	0.90	7.0	3	55
PM6AB2	1.0	-	7.0	5	68
PM6ABOH	0.30	-	1.3	0.8	42

[a] Polymerization was carried out at 60 °C for 48 h.

2. Characterization of Polymer LCs.

Molecular weight of the polymers was determined by GPC (JASCO, CO-966, PU-980, and UV-970; eluent: chloroform or THF; column: K-802, K-803, K-804, and K-805 (for chloroform) or KF-806M and KF-806L (for THF)) calibrated with standard polystyrenes. LC

behavior was examined by polarizing microscopy, and thermodynamic properties of LCs was determined by DSC as described in Chapter 2. Molecular weight and the thermodynamic properties are given in Table 7-2. Mole fraction of the azobenzenes introduced into the copolymers was determined by the same method described in Chapter 5.

3. Photochemical Phase Transition.

The photochemical phase transition behavior of the polymer LCs was investigated by means of the apparatus described in Chapter 2. Sample films were prepared in the same manner as described in the preceding chapter.

4. Isomerization Behavior of Azobenzenes.

Isomerization behavior of the azobenzenes in the LC phase was evaluated by transient absorption spectroscopy as described in Chapter 4. The film of the polymer LCs was excited with the laser pulse at 355 nm under exposure to the analyzing light from the Xe flash-lamp. The analyzing light passed through the LC film was collimated on the monochromator, and its intensity was measured with the SMA (gate width: 800 ns) synchronized with the analyzing light.

For slower decays, the isomerization behavior was evaluated with a JASCO V-550 absorption spectrometer.

RESULTS AND DISCUSSION

1. LC Behavior of Polymers.

It was observed with a polarizing microscope that all polymers used in this chapter showed LC phase. Phase structures and phase transition temperatures are summarized in Table 7-2. The copolymers (**P7-1** and **P7-2**) exhibited the N phase, and their temperature ranges of the N phase and Tc were almost the same. On the other hand, the homopolymer with hydroxyazobenzene (**PM6ABOH**) showed the Sm phase, while its *O*-ethyl derivative (**PM6AB2**) exhibited the N phase. Annealing of the LC films at temperature just below their Tc gave a well-aligned monodomain of the LC phase.

Table 7-2. Phase Transition Temperature and Molecular Weight of Polymer LCs Used in This Chapter[a]

Polymer	Mole fraction of azobenzenes	*Mn*	*Mw / Mn*	Phase Transition Temperature, °C
P7-1	0.11	28,000	1.9	G 35 N 130 I
P7-2	0.13	12,000	1.4	G 38 N 127 I
PM6AB2	1.0	41,000	6.7	G 88 N 151 I
PM6ABOH	1.0	50,000[b]	3.8[b]	G 112 Sm 148 I

[a] Abbreviations: G, glass; N, nematic; Sm, smectic; I, isotropic; *Mn*, number-average molecular weight; *Mw*, weight-average molecular weight.

[b] THF was used as an eluent.

2. Isomerization Behavior of Azobenzenes.

Figure 7-2 shows the time-resolved absorption spectra of the copolymer films in the LC phase (at 120 °C). In both polymers, absorption band appeared at around 360 nm in the absorption spectra due to a π-π* transition of the *trans*-azobenzenes. The absorbance at the π-π* band was reduced by irradiation with a laser pulse at 355 nm (30 mJ/cm^2) in the LC phase owing to the *trans-cis* photoisomerization of the azobenzene moieties. The degree of the change in the absorbance in **P7-2** was smaller than that in **P7-1**. This means that the concentration of the *cis* isomer of **P7-2** produced by laser pulse irradiation was lower than that of **P7-1**. After pulse irradiation, the absorbance in **P7-2** recovered almost completely in 30 ms at 120 °C because of the *cis-trans* thermal back-isomerization of azobenzene. In **P7-1**, however, the *cis* isomer showed much longer lifetime: the lifetime of its *cis* isomer was about 2 s at 120 °C as described in Chapter 6. A similar photoisomerization behavior was also observed in the homopolymers (**PM6AB2** and **PM6ABOH**).

3. Photochemical Phase Transition Behavior of Copolymers.

In the polymer LC with the ethoxyazobenzene moiety (**P7-1**), transmittance of the probe light decayed immediately upon irradiation at 366 nm at 100 °C as shown in Figure 7-3 (A). This was caused by the photochemical N-I phase transition of the polymer LCs due to the *trans-cis* photoisomerization of the azobenzene moiety. When photoirradiation was ceased, the transmittance of the probe light recovered thermally. Since the *cis-trans* thermal isomerization took place, the initial N phase recovered when the irradiated film was kept in the dark. At 100 °C, the photochemical phase transition of **P7-1** was induced repeatedly. In **P7-**

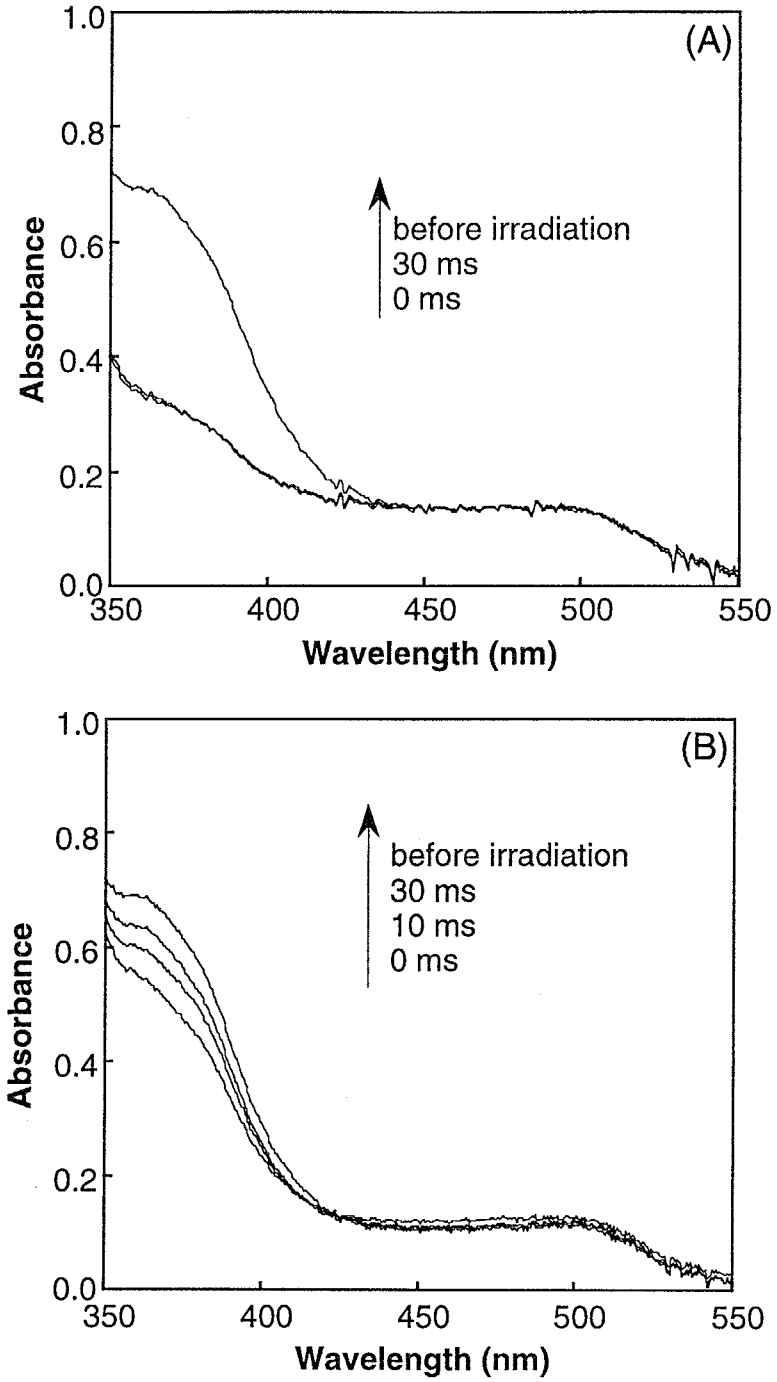

Figure 7-2. Time-resolved absorption spectra of polymer LC films in the N phase at 120 °C. Delay times after pulse irradiation (at 355 nm, 30 mJ/cm^2) were indicated in the figure.
(A), **P7-1**; (B), **P7-2**.

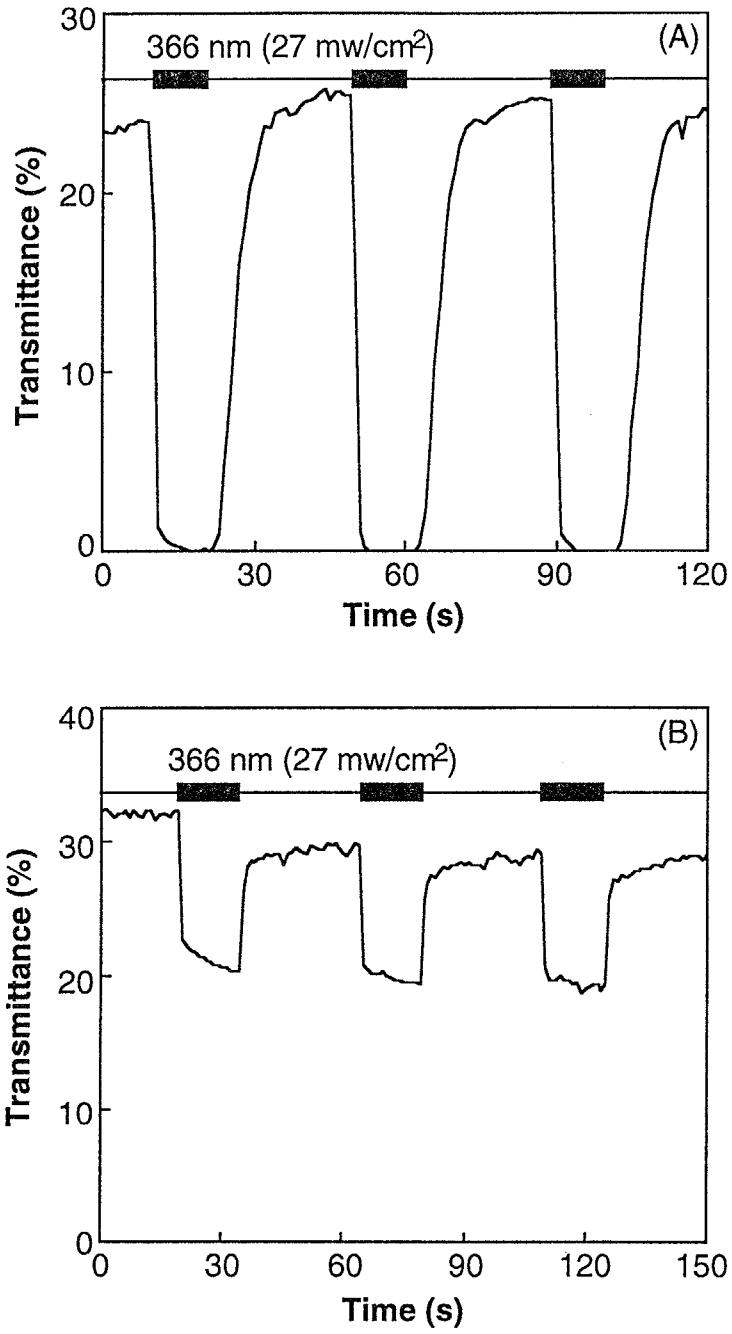

Figure 7-3. Photochemical N-I and thermal I-N phase transition of copolymers. (A), **P7-1** at 100 °C; (B), **P7-2** at 110 °C.

1, the photochemical phase transition depended on temperature: it could be induced completely at temperature above 100 °C, while it did not take place below 100 °C.

In the polymer LC with the hydroxyazobenzene moiety (**P7-2**), however, the photochemical phase transition did not occur completely at any temperature by irradiation at 366 nm (Figure 7-3 (B)). As mentioned above, the hydroxyazobenzene shows a lower value of Φ for the *trans-cis* photoisomerization than that in its *O*-alkyl derivatives,[1,2] and the *cis* isomer of the hydroxyazobenzene vanishes quickly.[1-4] In the photostationary state, therefore, the concentration of the *cis* isomer of the hydroxyazobenzene was lower than that of ethoxyazobenzene. As described in Chapter 5, there is a threshold concentration of the *cis* isomers in the photochemical phase transition of the polymer LCs. In **P7-2**, the concentration of the *cis* isomer may be insufficient for the photochemical N-I phase transition in the photostationary state.

Figure 7-4 shows the time-resolved measurements of the photochemical N-I phase transition in the copolymers with a laser pulse at 355 nm of 10 mJ/cm^2. Irradiation with the laser pulse caused the photochemical phase transition in **P7-1**. The N-I phase transition was induced in 300 μs. As described in the preceding chapter, this response is similar to that observed in the other systems. Below 110 °C, however, the N-I phase transition in **P7-1** did not occur completely by laser pulse irradiation. On the other hand, the photochemical phase transition in **P7-2** was not observed under this experimental condition (Figure 7-4 (B)). In the hydroxyazobenzenes, the Φ of the *trans-cis* photoisomerization is lower than in the ethoxyazobenzenes, and most molecules excited with the laser pulse is relaxed through the non-radiative pass.[5] Thus, in **P7-2**, the concentration of the *cis* isomer was lower and the heat generated by laser pulse irradiation may be larger

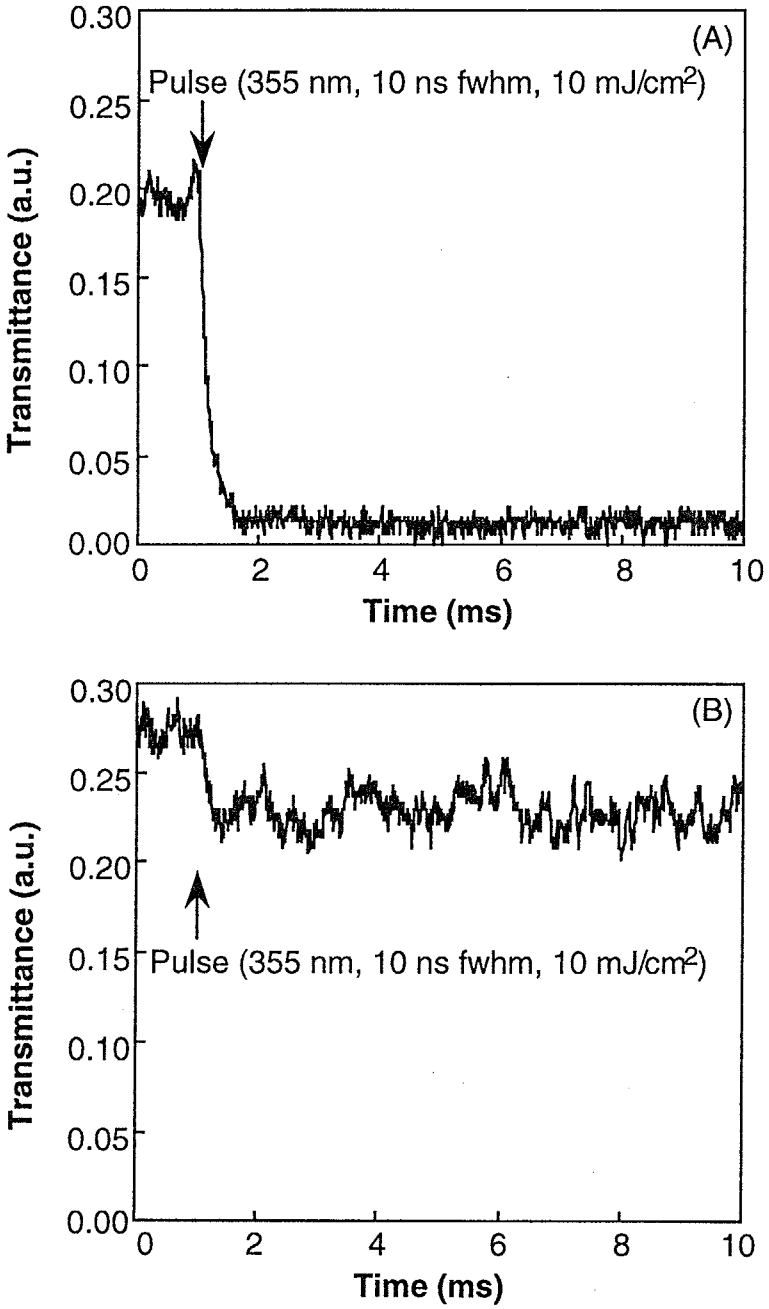

Figure 7-4. Time-resolved measurements of the photochemical N-I phase transition of copolymers at 115 °C: (A), **P7-1**; (B), **P7-2**.

than that in **P7-1**. The different behavior in the photochemical phase transition, therefore, is interpreted as a large change in the structure of the azobenzene moieties plays a crucial role in the phenomena. The result obtained in **P7-2** suggests that the effect of the heat generated by photoirradiation is not important in the photochemical phase transition of LCs.

When the LC film was irradiated with a laser pulse of 30 mJ/cm^2, the photochemical N-I phase transition was induced in 300 μs even in **P7-2**. Although the Φ is very low in **P7-2**, the *cis* form may be produced more than the threshold concentration with a relatively high-power laser pulse. Figure 7-5 shows the time-resolved measurements of the thermal I-N phase transition of the copolymers. The response time of the I-N phase transition was 1.5 s in **P7-1**, while it was 300 ms in **P7-2**, namely the thermal recovery of the N phase in **P7-2** was faster by one order of magnitude than that in **P7-1**. It is known that the *cis-trans* isomerization of the hydroxyazobenzene derivatives proceeds through an intermediate (hydrazone form) (Scheme 7-2).[3,4] The hydrazone form was produced by proton transfer from the hydroxyl group to the azo group, and this tautomer is converted into the *trans* form of azobenzenes. In the thermal *cis-trans* isomerization, hydroxyazobenzenes prefer this two-step mechanism to the one-step mechanism because the activation energy of this mechanism is lower than that of the one-step mechanism: the activation energy is ~ 10 kcal/mol in the former and ~ 20 kcal/mol in the later as described in Chapter 6 (Figure 7-6).[1-4] Owing to the low activation energy, the thermal back-isomerization of hydroxyazobenzene is quicker than that of ethoxyazobenzene. In **P7-2**, therefore, the thermal recovery of the N phase took place quickly. As described in Chapters 4 ~ 6, the thermal recovery of the N phase was accelerated with donor-acceptor pairs. In the donor-acceptor azobenzenes, the activation

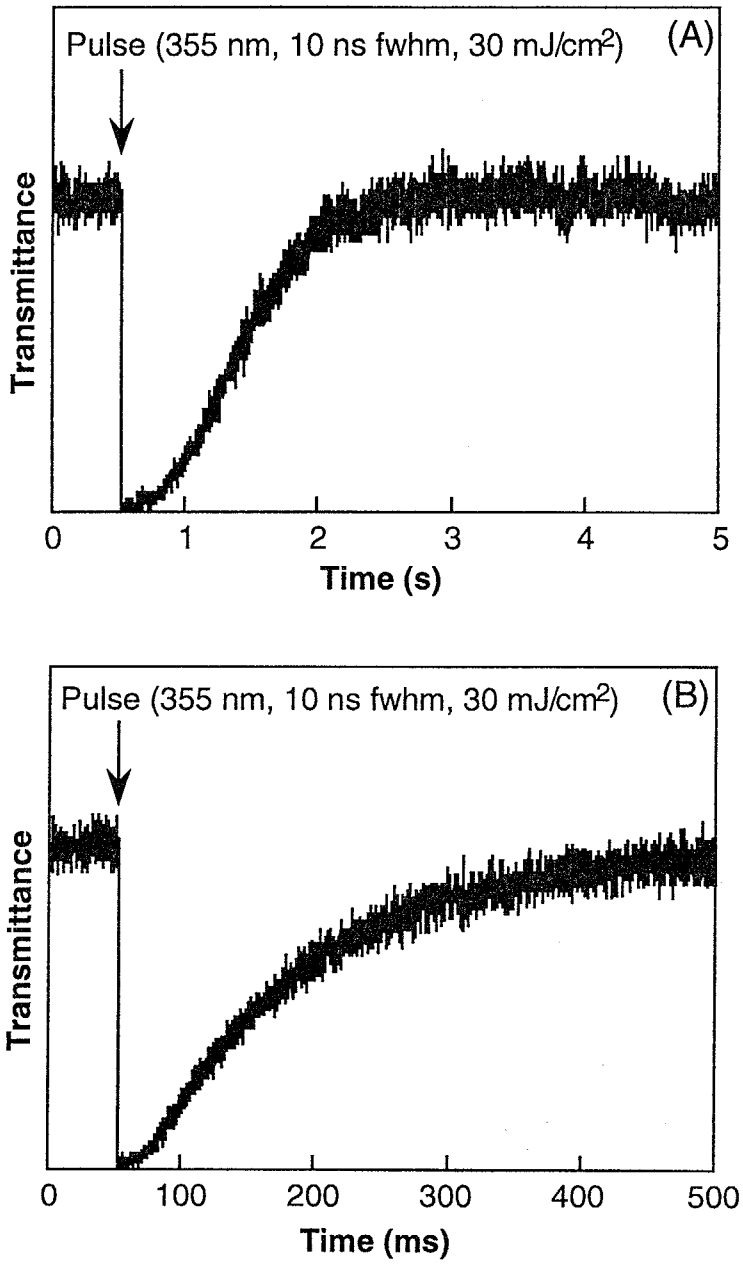

Figure 7-5. Time-resolved measurements of the thermal I-N phase transition of copolymers. Irradiatiom with a laser pulse at 355 nm (30 mJ/cm^2) was performed at 120 °C.
(A), **P7-1**; (B), **P7-2**.

Scheme 7-2. Mechanism of *cis-trans* thermal back-isomerization.

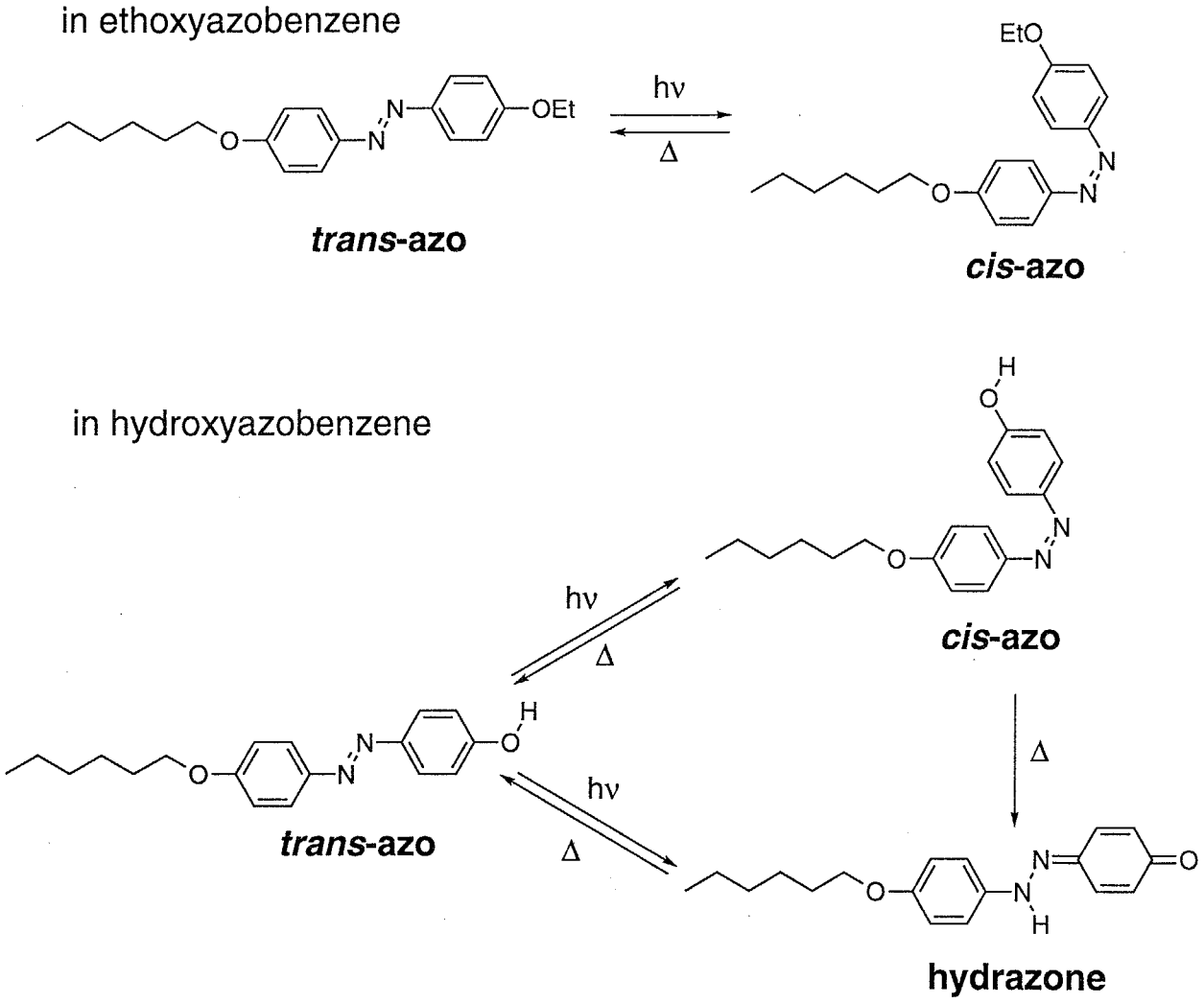

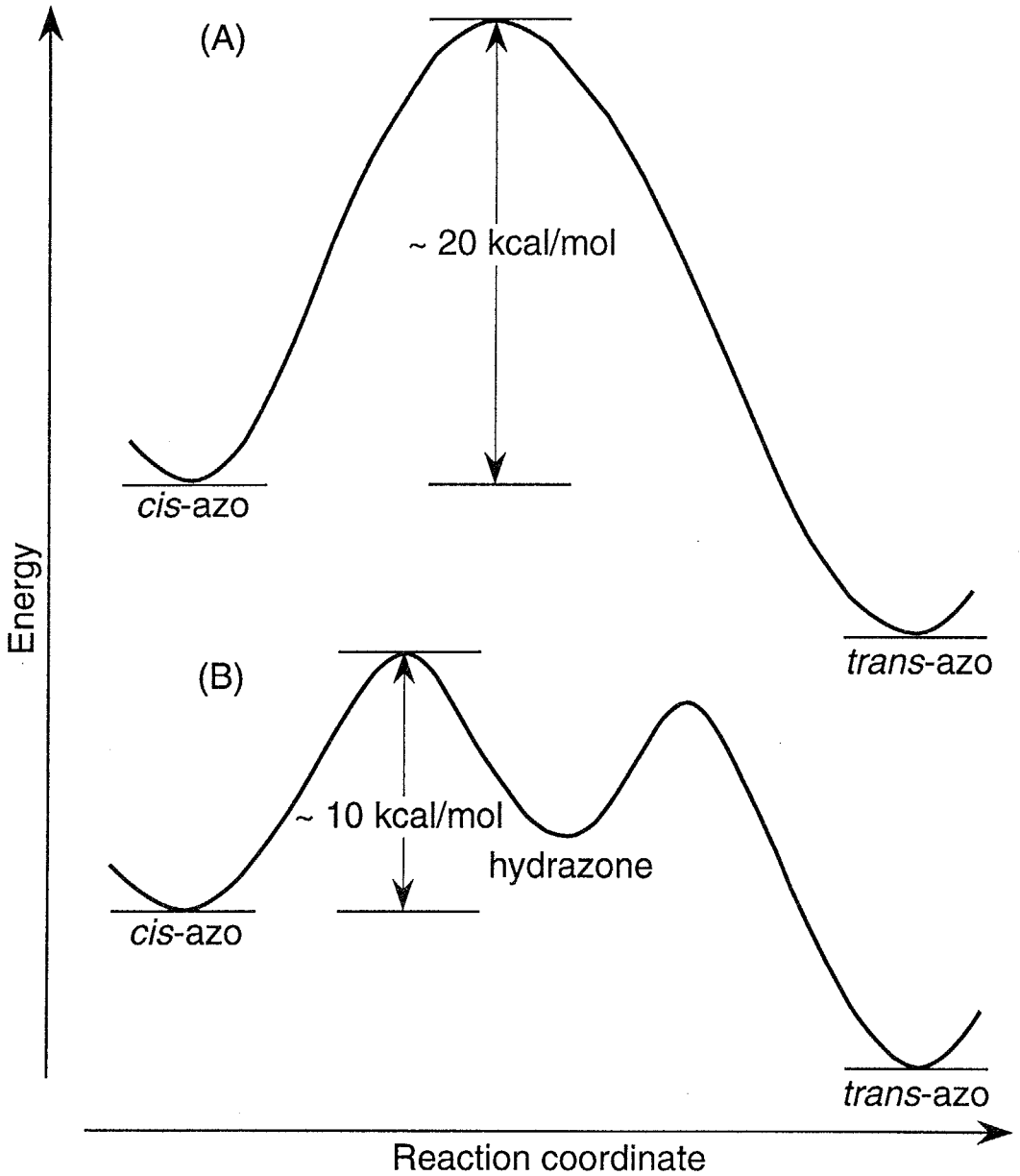

Figure 7-6. Energy surface diagram:
(A), for ethoxyazobenzene;
(B), for hydroxyazobenzene.

energy of the *cis-trans* isomerization was decreased by changing the electronic structures of the molecules. On the other hand, in the present system the activation energy was reduced by the intermediate (Figure 7-6). In both azobenzenes, the transition state of the reaction was stabilized with distinct manners. The result obtained in **P7-2** suggests that another approach is possible to accelerate the thermal recovery of the N phase.

4. Photochemical Phase Transition Behavior of Homopolymers.

As described in Chapter 6, the photochemical phase transition of **PM6AB2** was induced completely in 200 μs in the temperature range between Tc and room temperature (below Tg).

On the other hand, **PM6ABOH** showed quite different photochemical phase transition behavior from the other LC systems. As shown in Figure 7-7 (A), at high temperature (> 100°C) the photochemical LC-I phase transition of **PM6ABOH** was not induced by irradiation at 366 nm. At 30 °C, however, the LC-I phase transition took place almost completely. In this polymer, above 100 °C the concentration of the *cis* isomer in the photostationary state may also be lower than the threshold concentration due to the low Φ of photoisomerization and the short lifetime of the *cis* isomer. At low temperature, although the Φ of the *trans-cis* isomerization was low, the *cis* isomer produced by steady light irradiation was accumulated because of the slow thermal back-isomerization. When the concentration of the *cis* isomer became higher than the threshold value by accumulation, the photochemical LC-I phase transition was induced in **PM6ABOH**.

In **PM6ABOH**, the change in the probe light was not observed by irradiation with a laser pulse of 10 mJ/cm^2 at 120 °C and at 40 °C. It is difficult to compare the phase transition behavior between **PM6AB2** and

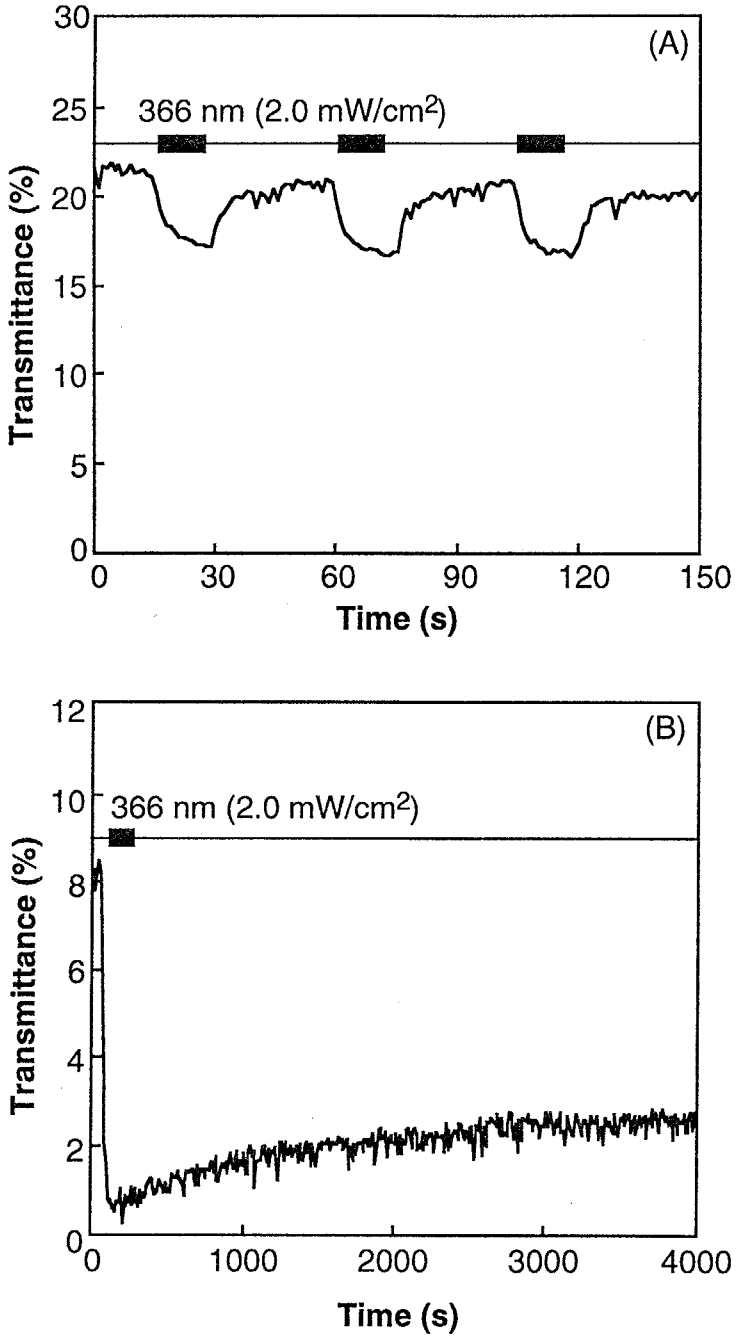

Figure 7-7. Photochemical Sm-I phase transition of **PM6ABOH**: (A), at 110 °C; (B), at 30 °C.

PM6ABOH, because they show a different phase structure. From these results, however, the author considers that the effect of the heat generated by photoirradiation is not important in the photochemical phase transition of photochromic LCs.

In **PM6ABOH**, the photochemical phase transition was also induced in 300 μs with a laser pulse of 30 mJ/cm^2. Figure 7-8 shows the time-resolved measurements of the thermal phase transition of the homopolymers. As described in Chapter 6 the LC phase was restored in 3 s in **PM6AB2**, while it was not restored completely in **PM6ABOH**. Since **PM6ABOH** shows the Sm phase, the thermal recovery of the initial Sm phase may need much longer time than that in the N phase even though the *cis-trans* back-isomerization took place effectively.

CONCLUSION

The influence of the heat generated by photoirradiation was discussed. In the polymer LCs with the hydroxyazobenzene moiety, in which the Φ for the photochemical isomerization is very low and large amount of the heat was generated by photoirradiation, the photochemical phase transition was not induced by irradiation with steady light or laser pulse of 10 mJ/cm^2. Under the same experimental condition, the photochemical phase transition took place completely in the polymer LCs with the ethoxyazobenzene moiety. Hence, it is concluded that the photochemical phase transition occurs mainly by the "photon-mode" process and the heat-mode process dose not play an important role in the phenomena.

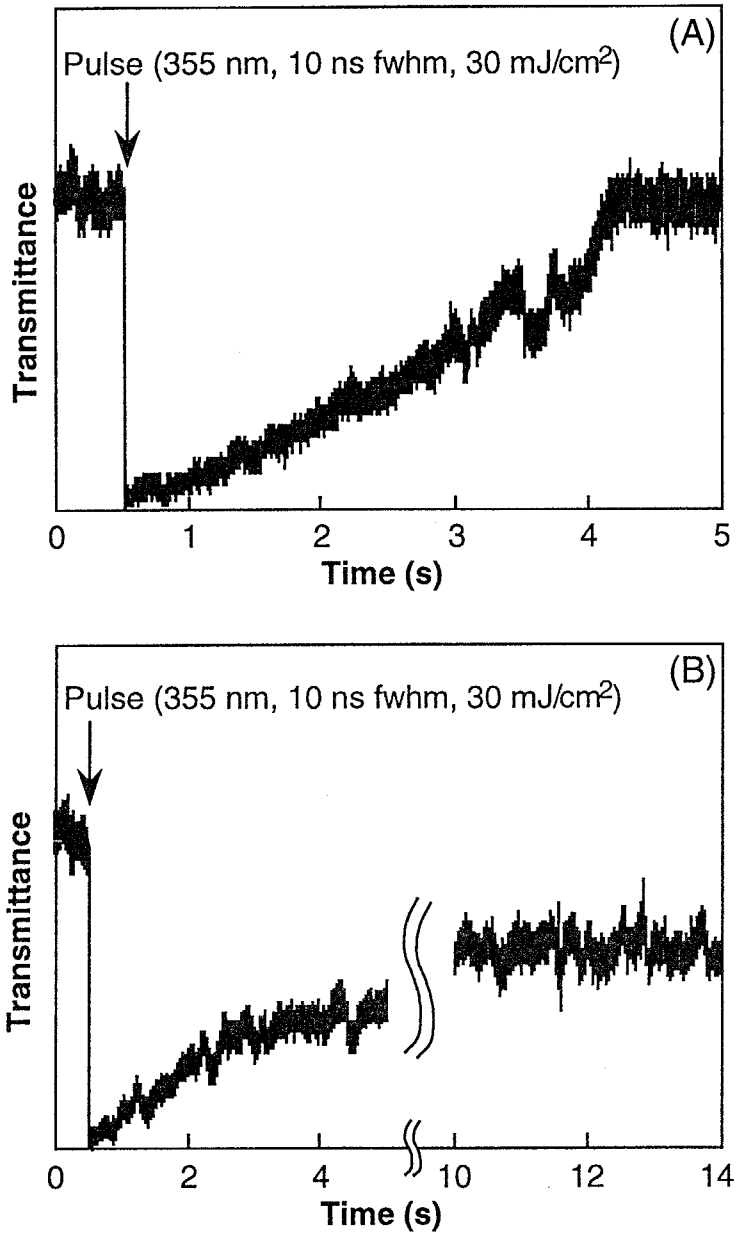

Figure 7-8. Time-resolved measurements of the thermal I-N phase transition of homopolymers. Irradiatiom with a laser pulse at 355 nm (30 mJ/cm^2) was performed at 120 °C. (A), **PM6AB2**; (B), **PM6ABOH**.

When the copolymer with the hydroxyazobenzene moiety was irradiated with a laser pulse of 30 mJ/cm^2, the N-I phase transition was also caused completely. Since the *cis-trans* back-isomerization of the hydroxyazobenzenes took place quickly through the intermediate (hydrazone form), the I phase induced in the copolymer vanished quickly; the N phase recovered in 300 ms at 120 °C. This result suggests that a different approach from the donor-acceptor azobenzenes is possible to accelerate the thermal recovery of the N phase.

References and Notes

(1) Gabor, G.; Fischer, E. *J. Phys. Chem.* **1962**, *66*, 2478.

(2) Margerum, J.D.; Miller, L.J. in *Photochromism*; Brown. G.H., Ed.; John Wiley & Sons: New York, USA, 1971; pp 557-632.

(3) Fischer, E.; Frei, Y.F. *J. Chem. Soc.* **1959**, 3159.

(4) Wettermark, G.; Langmuir, M.E.; Anderson, D.G. *J. Am. Chem. Soc.* **1965**, *87*, 476.

(5) A part of the excited molecules which did not isomerize to the *cis* form tautomerized to the hydrazone form with a low Φ (Scheme 7-2). The formation of the hydrazone structure may involve a rehybridization from sp^2 (coplanar structure) to sp^3 (tetrahedral structure). This tetrahedral structure would destabilize the LC phase. However, the influence of the hydrazone on photochemical phase transition may not be important, because the molecular shape of the hydrazone form is similar to that of *trans*-azobenzene and its lifetime is very short.

Chapter 8

SUMMARY

In this thesis, various azobenzene derivatives were prepared as photochromic LCs, and their photochemical phase transition behavior was investigated. In Chapter 2, the photochemical phase transition behavior of the low-molecular-weight and polymer azobenzene LCs was described, in which emphasis was placed on the comparison between the low-molecular-weight and polymer LCs. The effect of the position of core units in side chains on the photochemical phase transition of the polymer azobenzene LCs was investigated in Chapter 3. In Chapters 4 and 5, the photochemical and thermal phase transition behavior of LCs with donor-acceptor azobenzenes was discussed in the guest/host system. Acceleration of the thermal recovery in the polymer azobenzene LCs was studied in Chapter 6. In Chapter 7, the effect of the heat generated by photoirradiation on the photochemical phase transition was described.

Photochemical Phase Transition Behavior of Azobenzene Liquid Crystals

In Chapter 2, the author described the phase transition behavior of low-molecular-weight and polymer azobenzene LCs. In the films of the azobenzene LCs, the photochemical N-I phase transition was induced in 200 μs in the whole temperature range of the N phase by irradiation with a short laser pulse to cause the isomerization. No difference in the response time of the photochemical phase transition was observed between low-molecular-weight and polymer azobenzene LCs. In the polymer azobenzene LCs, the photochemical phase transition took place in the same time even below Tg.

The origin of the photochemical phase transition in the azobenzene LCs is the disappearance of the LC nature of the system. The photochromic LCs are considered to contain a molecular switch attached to each mesogen. In other words, they are a *supramolecular assembly of the molecular switches* driven by photon. With light, mesogenic molecules (*trans*-azobenzenes) are converted into non-mesogenic molecules (*cis*-azobenzenes), and the structure of the LC phase is disorganized by the *trans-cis* isomerization. In this system, since each molecule organizing the supramolecular assembly is switched with photon directly, the disorganization of the assembly occurred very effectively and the LC nature of the system vanished completely even below Tg of the polymer. The photochemical phase transition, therefore, is induced in the polymer azobenzene LCs below Tg.

It was found that the photochemical phase transition is not affected by the structure of the main chain of the polymer (Chapter 6) but it is influenced by the position of the azobenzene moiety in the side chain of the polymer (Chapter 3). In addition, the heat generated by

photoirradiation did not play any crucial role in the photochemical phase transition of the LCs (Chapter 7).

Thermal Recovery of the LC Phase: Effect of Electron Donor and Acceptor

At temperatures above Tg, the I phase induced at the irradiated site disappeared after some time, depending on the temperature; at high temperatures the I phase disappeared quickly because of effective thermal *cis-trans* back-isomerization, and at temperatures just above Tg, it disappeared very slowly. The thermal recovery of the N phase consisted of two processes: the *cis-trans* thermal back-isomerization of the azobenzene moieties and the reorientation of the mesogenic *trans*-azobenzenes, and the rate-determining step of the recovery was the isomerization process.

In Chapters 4 ~ 6, the effect of the donor-acceptor pair of the azobenzene on the thermal I-N phase transition was discussed. The I-N phase transition was induced rapidly with the donor-acceptor azobenzenes. In these azobenzenes, the *cis-trans* thermal back-isomerization occurred quickly, thus the thermal recovery of the N phase occurred quickly in the low-molecular-weight and polymer LCs with the donor-acceptor azobenzenes. Furthermore, it was found that the time required for the I-N phase transition decreased with increasing the strength of the donor and the acceptor (Chapter 4).

The recovery of the N phase was affected by the structure of the donor-acceptor azobenzene moiety. When the azobenzene with a strong donor-acceptor pair stabilized the N phase, the *cis-trans* back-

isomerization and the reorientation of the mesogen proceeded effectively (Chapter 5). Therefore, the thermal I-N phase transition occurred very quickly.

In the polymer azobenzene LCs, the I-N phase transition was also accelerated with donor-acceptor pairs (Chapter 6). It became apparent that the thermal recovery was affected by flexibility of the polymer main chain. Furthermore, the recovery of the N phase in the azobenzene LCs was also accelerated by visible-light irradiation. These results suggest that the polymer azobenzene LCs with electron donor and acceptor is potential quick-responsive all-optical switching materials and real-time holography materials.

Polymer Azobenzene Liquid Crystals as Candidate for Optical Image Storage Materials

In the polymer azobenzene LCs, the photochemical N-I phase transition was induced even below Tg, and the I glass induced at the irradiated site remained very stable (more than 2 years) even though the *trans* form was restored thermally. This high stability of the I glass arises from the fact that after the *trans-cis-trans* cycles the orientation of the *trans* form became random and this random orientation was frozen without segmental motion of main chain of the polymer below Tg. When the polymer azobenzene LC films were irradiated through photomask below Tg, the image was stored into the film with spatial resolution of 2 μm, which corresponds to a storage capability of 25 Mbit/cm^2.

List of Publications

Chapter 2 Optical Switching and Image Storage by Means of Azobenzene Liquid-Crystal Films.
Tomiki Ikeda and Osamu Tsutsumi.
Science **1995**, *268*, 1873.

Photochemical Phase Transition Behavior of Nematic Liquid Crystals with Azobenzene Moieties as Both Mesogens and Photosensitive Chromophores.
Osamu Tsutsumi, Takeshi Shiono, Tomiki Ikeda, and Giancarlo Galli.
J. Phys. Chem. B **1997**, *101*, 1332.

Chapter 3 Photochemical Phase Transition Behavior of Polymer Azobenzene Liquid Crystals with a Rigid Core Introduced at a Different Position in a Flexible Side Chain.
Osamu Tsutsumi, Yasuo Miyashita, Shigenobu Hirano, Atsushi Shishido, Akihiko Kanazawa, Takeshi Shiono, and Tomiki Ikeda.
Mol. Cryst. Liq. Cryst., in press.

Chapter 4 Rapid Photochemical Manipulation of Liquid Crystal by the Use of Donor-Acceptor Azobenzenes as Photoresponsive Chromophores.
Osamu Tsutsumi, Akihiko Kanazawa, Takeshi Shiono, Tomiki Ikeda, and Lee-Soon Park.

J. Chem. Phys., to be submitted.

Chapter 5 Photochemical Phase Transition Behavior of Polymer Liquid Crystals Induced by Photochemical Reaction of Azobenzenes with Strong Donor-Acceptor Pairs.
Osamu Tsutsumi, Yasuyuki Demachi, Akihiko Kanazawa, Takeshi Shiono, Tomiki Ikeda, and Yu Nagase.
J. Phys. Chem., in press.

Chapter 6 Photochemical Phase Transition Behavior of Polymer Azobenzene Liquid Crystals with Electron-Donating and Accepting Substituents at 4,4'-Positions.
Osamu Tsutsumi, Takashi Kitsunai, Akihiko Kanazawa, Takeshi Shiono, and Tomiki Ikeda.
Macromolecules **1998**, *31*, 355.

Charge Transfer Interaction in Liquid-Crystalline Materials and Their Application to Photonics.
Osamu Tsutsumi, Akihiko Kanazawa, Takeshi Shiono, and Tomiki Ikeda.
Macromol. Symp. **1997**, *116*, 117.

Chapter 7 Photochemical Phase Transition Behavior of Polymer Liquid Crystals with Hydroxyazobenzene Moieties.
Osamu Tsutsumi, Akihiko Kanazawa, Takeshi Shiono, and Tomiki Ikeda.
J. Phys. Chem., to be submitted.

Other publications not described in this thesis

I. Original papers

1) Photochemical Switching of Ferroelectric Liquid Crystals Using a Photoswitchable Chiral Dopant.
Makoto Negishi, Osamu Tsutsumi, Tomiki Ikeda, Tamejiro Hiyama, Joji Kawamura, Masao Aizawa, and Sadao Takehara.
Chem. Lett. **1996**, 319.

2) Liquid Crystal Photonics: Optical Switching and Image Storage by Means of Nematic Liquid Crystals and Ferroelectric Liquid Crystals.
Tomiki Ikeda, Osamu Tsutsumi, and Takeo Sasaki.
Synthetic Metals **1996**, *81*, 289.

3) Liquid Crystal Photonics: Optical Switching and Image Storage by Means of Azobenzene Liquid-Crystal Films.
Atsushi Shishido, Osamu Tsutsumi, and Tomiki Ikeda.
Mat. Res. Soc. Symp. Proc. **1996**, *425*, 213.

4) Distinct Photochemical Phase Transition Behavior of Azobenzene Liquid Crystals Evaluated by Reflection-Mode Analysis.
Atsushi Shishido, Osamu Tsutsumi, Akihiko Kanazawa, Takeshi Shiono, Tomiki Ikeda, and Naoto Tamai.
J. Phys. Chem. B **1997**, *101*, 2806.

5) Photochemical Phase Transition Behavior of Polymer Azobenzene Liquid Crystals with Flexible Siloxane Unit as a Side-Chain Spacer.
Akihiko Kanazawa, Shigenobu Hirano, Atsushi Shishido, Makoto

Hasegawa, Osamu Tsutsumi, Takeshi Shiono, Tomiki Ikeda, Yu Nagase, Eiichi Akiyama, and Yuriko Takamura.
Liq. Cryst. **1997**, *23*, 293.

6) Novel Thermotropic Liquid Crystals without a Rigid Core Formed by Amphiphiles Having Phosphonium Ions.
Akihiko Kanazawa, Osamu Tsutsumi, Tomiki Ikeda, and Yu Nagase.
J. Am. Chem. Soc. **1997**, *119*, 7670.

7) Rapid Optical Switching by Means of Photoinduced Change in Refractive Index of Azobenzene Liquid Crystals Detected by Reflection-Mode Analysis.
Atsushi Shishido, Osamu Tsutsumi, Akihiko Kanazawa, Takeshi Shiono, Tomiki Ikeda, and Naoto Tamai.
J. Am. Chem. Soc. **1997**, *119*, 7791.

8) Liquid Crystal Photonics: Optical Switching and Image Storage by Means of Nematic Liquid Crystals and Ferroelectric Liquid Crystals.
Atsushi Shishido, Osamu Tsutsumi, Akihiko Kanazawa, Takeshi Shiono, and Tomiki Ikeda.
Proceedings of SPIE **1997**, *3143*, 81.

9) Effect of Siloxane Spacer on Photochemical Phase Transition Behavior of Polymer Liquid Crystals with Azobenzene Moieties in the Side Chain.
Akihiko Kanazawa, Atsushi Shishido, Makoto Hasegawa, Osamu Tsutsumi, Takeshi Shiono, Tomiki Ikeda, Yu Nagase, Eiichi Akiyama, and Yuriko Takamura.
Mol. Cryst. Liq. Cryst. **1997**, *300*, 201.

10) Photoinduced Alignment of Polymer Liquid Crystals Containing Azobenzene Moieties in the Side Chain. I. The effect of Light Intensity on Alignment Behavior.
Yiliang Wu, Yasuyuki Demachi, Osamu Tsutsumi, Akihiko Kanazawa, Takeshi Shiono, and Tomiki Ikeda.
Macromolecules **1998**, *31*, 349.

11) Photoinduced Alignment of Polymer Liquid Crystals Containing Azobenzene Moieties in the Side Chain. II. The Effect of Spacer Length of Azobenzene Unit on Alignment Behavior.
Yiliang Wu, Yasuyuki Demachi, Osamu Tsutsumi, Akihiko Kanazawa, Takeshi Shiono, and Tomiki Ikeda.
Macromolecules, in press.

12) Reflection-Mode Optical Switching of Polymer Azobenzene Liquid Crystal.
Atsushi Shishido, Osamu Tsutsumi, Akihiko Kanazawa, Takeshi Shiono, and Tomiki Ikeda.
Mol. Cryst. Liq. Cryst., in press.

II. Review articles

1) 液晶フォトニクス材料
池田 富樹, 堤 治, 榎本 信太郎
表面 **1994**, *32*, 446.

2) 液晶フォトニクス材料：ネマチック液晶と強誘電性液晶を用いたスイッチング

池田 富樹, 堤 治, 榎本 信太郎
有機分子・バイオエレクトロニクス分科会会誌 **1994**, *5*, 241.

3) 液晶フォトニクス材料：光スイッチングと光記録
池田 富樹, 堤 治, 榎本 信太郎
高分子加工 **1995**, *44*, 2.

4) 液晶フォトニクス
池田 富樹, 堤 治
光化学 **1995**, *19*, 34.

5) 液晶光駆動
堤 治, 宍戸 厚, 池田 富樹
光技術コンタクト **1995**, *33*, 475.

6) 液晶フォトニクス
宍戸 厚, 堤 治, 池田 富樹
化学工業 **1995**, *46*, 817.

7) 分子配向の光制御
堤 治, 池田 富樹
化学 **1996**, *51*, 270.

III. Publication at international conference

1) Liquid-Crystalline Materials for Photonics: Optical Switching by Means of Photochemical Phase Transition of Liquid-Crystalline Azobenzene Films.

Tomiki Ikeda and Osamu Tsutsumi.
Spectral Hole-burning and Spectroscopies: Science and Applications (Tokyo, Japan) **1994**, 265.

2) Liquid Crystal Photonics: Optical Switching and Image Storage by Means of Azobenzene Liquid-Crystal Films.
Tomiki Ikeda and Osamu Tsutsumi.
China-Japan Bilateral Symposium on Polymer Materials Science (Yellow Mountain, China) **1995**, 244.

3) Charge Transfer Interaction in Liquid-Crystalline Materials and Their Application to Photonics.
Tomiki Ikeda and Osamu Tsutsumi.
211th ACS National Meeting (New Orleans, USA) **1996**, Poly 189.

4) Liquid Crystal Photonics: Optical Switching and Image Storage by Means of Azobenzene Liquid-Crystal Films.
Tomiki Ikeda, Osamu Tsutsumi, and Atsushi Shishido.
Material Research Society, Spring 1996 Meeting (San Francisco, USA) **1996**.

5) Liquid Crystal Photonics: Photochemical Phase Transition Behavior of Polymer Azobenzene Liquid Crystals.
Osamu Tsutsumi, Akihiko Kanazawa, Takeshi Shiono, and Tomiki Ikeda.
36th IUPAC International Symposium on Macromolecules (Seoul, Korea) **1996**, 455.

6) Liquid Crystal Photonics: Optical Switching in Reflection Mode by

Means of Photoinduced Change in Refractive Index of Azobenzene Liquid Crystals.
Atsushi Shishido, Osamu Tsutsumi, Akihiko Kanazawa, Takeshi Shiono, and Tomiki Ikeda.
36th IUPAC International Symposium on Macromolecules (Seoul, Korea) **1996**, 454.

7) Novel Thermotropic Liquid Crystals without a Rigid Core Formed by Amphiphiles Having Phosphonium Ions and Their Characterizations by Second-Order Nonlinear Optics.
Akihiko Kanazawa, Makoto Hasegawa, Osamu Tsutsumi, Tomiki Ikeda, Yu Nagase, and Jiro Abe.
The 4th IUMRS International Conference in Asia (Makuhari, Japan) **1997**, 206.

8) Liquid Crystal Photonics: Optical Switching Behavior of Azobenzene Liquid Crystals by the Use of Reflection-Mode Analysis.
Atsushi Shishido, Osamu Tsutsumi, Akihiko Kanazawa, Takeshi Shiono, and Tomiki Ikeda.
The 4th IUMRS International Conference in Asia (Makuhari, Japan) **1997**, 208.

9) Liquid Crystal Photonics: Optical Switching and Image Storage by Means of Polymer Azobenzene Liquid Crystals.
Osamu Tsutsumi, Akihiko Kanazawa, Takeshi Shiono, and Tomiki Ikeda.
6th SPSJ International Polymer Conference (Kusatsu, Japan) **1997**, 91.

ACKNOWLEDGMENTS

I would like to express my sincere gratitude to Professor Tomiki Ikeda for his constant guidance and helpful discussion throughout the duration of this work. This study could never have been continued without his guidance.

I wish to express my grateful appreciation to Associate Professor Takeshi Shiono for his helpful advice and discussion.

I grateful acknowledge to Professor Tamejiro Hiyama for his considerable support and hearty encouragement.

I am deeply indebted to Dr. Akihiko Kanazawa for his valuable suggestions and stimulating discussion.

I wish to thank Mr. Shigenobu Hirano, Mr. Takashi Kitsunai, and Mr. Yasuo Miyashita for their collaboration in experiments.

Grateful acknowledgment is made to all members of Ikeda-Shiono laboratory for their kind assistance and cooperation. In addition, thanks are also due to colleagues in Hiyama-Mori laboratory for their assistance and encouragement.

The support of the JSPS Research Fellowships for Young Scientists is acknowledged.

Finally, I heartily express my appreciation to my parents and my lovely wife for their encouragement and support during this study.

December 22, 1997

Osamu Tsutsumi